COORDINATION OF POWER SYSTEM STABILIZER AND FACTS SUPPLEMENTARY CONTROLLER PARAMETERS IN A MULTIMACHINE SYSTEM

A Thesis Submitted
in Partial Fulfillment of the requirements
for the Degree of

MASTER OF TECHNOLOGY

by

BODDETI KALYAN KUMAR

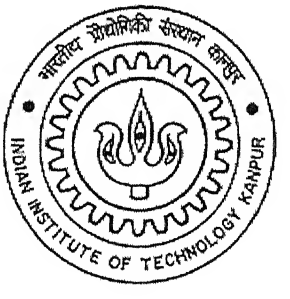

to the

DEPARTMENT OF ELECTRICAL ENGINEERING
INDIAN INSTITUTE OF TECHNOLOGY, KANPUR

FEBURARY 2003

CERTIFICATE

This is to certify that the work contained in this thesis entitled **"Coordination of Power System Stabilizer and FACTS Supplementary Controller Parameters in a Multimachine System"**, has been carried out by B. Kalyan Kumar (Y110425) under my supervision and that this work has not been submitted elsewhere for a degree.

February, 2003

Dr. S. C. Srivastava
Professor
Department of Electrical Engineering
Indian Institute of Technology,
Kanpur-208016

Acknowledgement

I express my deep sense of gratitude towards my thesis supervisor Dr. S. C. Srivastava for his invaluable guidance, moral support and constant encouragement, which helped me, survive through the crests and troughs of my thesis work, and complete successfully. My sincere thanks to him, for taking so much interest in my academic and personal welfare. I also thank Dr. S. N. Singh for his suggestions and encouragement

I also acknowledge the financial support provided by MHRD, government of India, New Delhi under number "MHRD/EE/20010025", for carrying out the present work.

I thank Mr. Ashwani Kumar, Mr. H. K. Singh and Mr. A. Krishna Kumar for their constant encouragement, guidance and excellent company, which was the best part. I thank my best friends satish and vijay for their excellent company and their help, which made my stay in IIT a memorable event.

I thank my parents, brother & sister, and the graceful Lord whose love, concern and blessings enabled me to reach this stage.

Boddeti Kalyan Kumar

CONTENTS

List of Figures

List of Tables

ABSTRACT

Fast exciters having automatic voltage regulator feature have been popularly used to enhance power system transient stability. At high gain settings, it some times introduces a negative damping torque component in the system resulting in small signal instability. The best solution for this is to provide power system stabilizer (PSS) in the exciter control loop. In a multimachine system, the PSS parameters must be coordinated in order to avoid negative interactions. In this thesis, a method based on optimal control strategy with pseudo-decentralization has been proposed for the coordination of the parameters of different PSS in a multimachine system.

Flexible AC Transmission systems (FACTS) are popularly being used in the network to improve the system power transfer capability, provide effective voltage control, offer damping to the power system oscillations and thus, improving the system transient and small signal stability. Among various FACTS controllers, static VAR compensator (SVC) has been extensively used by the power utilities in their network, which employ a supplementary control loop for damping the oscillations. As different PSS in a multimachine system needs coordination to avoid interactions, SVC supplementary controller and PSS needs coordination. The proposed optimal control strategy with pseudo-decentralization method has also been applied for the coordination of SVC supplementary controller and PSS parameters. The proposed method for coordination of PSS as well as PSS and SVC controller has been implemented on WSCC 9-bus and New England 39-bus system. It has been observed that system stability improves considerable with the use of coordinated values of stabilizing controllers.

Chapter 1
Introduction

1.1 General

Power system stability may be broadly defined as that property of a power system that enables it to remain in a state of operating equilibrium under normal operating conditions and to regain an acceptable state of equilibrium after being subjected to a disturbance.

Instability in a power system may be manifested in many different ways depending on the system configuration and operating mode. Traditionally, the stability problem has been one of maintaining synchronous operation. Since power systems rely on synchronous machines for generation of electrical power, a necessary condition for satisfactory system operation is that all synchronous machines remain in synchronism or colloquially "in step". This aspect of stability is influenced by the dynamics of generator rotors and power-angle relationships.

The evaluation of stability mainly concerns with the behavior of the power system when subjected to a transient disturbance. The disturbance may be small or large. Small disturbance in the form of load changes take place continually and the system adjusts itself to the changing conditions. The system must be able to operate satisfactorily under these conditions and successfully supply the maximum amount of load. It must also be capable of surviving numerous disturbances of severe nature such as a short-circuit on a transmission line, loss of a large generator or load, or loss of a tie line between two interconnected systems. The system response to a disturbance involves dynamics of several components. For example, a short-circuit followed by its isolation by protective relays may cause variations in power transfers, machine rotor speeds, and bus voltages. The variations will actuate both generator and transmission system voltage regulators. The speed variations will actuate prime mover governors to act. The change in tie line loading also actuates generation controls. Changes in the bus voltage and system frequency affect loads in varying degrees depending on their individual characteristics. In any given situation, however, the response of only a limited amount of equipment may be significant. Therefore, many assumptions are usually made to simplify the problem and to

focus on factors influencing the specific type of stability problem. The understanding of stability problem is greatly facilitated by the classification of stability in two categories, mainly rotor angle stability and voltage stability.

Voltage stability is the ability of a power system to maintain steady acceptable voltage at all buses in the system under normal operating condition and after being subjected to a disturbance [10]. A system enters a state of voltage instability when a disturbance, increases in load demand, or change in system condition causes a progressive and uncontrollable drop in voltage. The main factor causing instability is the inability of the power system to meet the demand for reactive power. The voltage stability is more pronounced during stressed operations of the system, which gets aggravated, by some form of contingency in the system.

1.2. Rotor angle stability

Rotor angle stability is the ability of synchronous machines in an interconnected power system to remain in synchronism. The stability problem involves the study of the electromechanical oscillations inherent in power systems. A fundamental factor in this problem is the manner in which the power outputs of synchronous machines vary as their rotors oscillate.

Stability is a condition of equilibrium between opposing forces. The mechanism by which interconnected machines maintain synchronism with one another is through restoring forces, which act whenever there are forces tending to accelerate or decelerate one or more machines with respect to other machines. Under steady-state condition, there is equilibrium between the input mechanical torque and the output electrical torque of each machine and the speed remains constant. If the system is perturbed, this equilibrium is upset, resulting in acceleration or deceleration of the rotors of the machine. If one generator temporarily runs faster than the other, the angular position of its rotor relative to that of the slower machine will advance. The resulting angular difference transfers part of the load from the slow machine to the fast machine, depending on the power-angle relationship. This tend to reduce the speed difference and hence the angular separation.

The power angle relationship is highly nonlinear. Beyond a certain limit, an increase in angular separation is accompanied by a decrease in power transfer. This increase the angular separation further leads to instability. In any situation, the stability of the system depends on whether or not the deviations in angular position of the rotor results in sufficient restoring torque.

When a synchronous machine loses synchronism or "falls out of step" with the rest of the system, its rotor runs at a higher or lower speed than that required to generating voltage at system nominal frequency. The "slip' between rotating stator field (corresponding to system frequency) and the rotor field results in large fluctuations in the machine power output, current and voltage. This causes the protection system to isolate the unstable machines from the system. Loss of synchronism can occur between one machine and rest of the system or between groups of machines. In the latter case, synchronism may be maintained within each group after its separation from the others. For convenience in analysis and for gaining useful insight into the nature of stability phenomena, the angular stability has been further classified as small signal stability and transient stability, which are discussed below.

1.2.1. Transient stability

Transient stability is the ability of the power system to maintain synchronism when subjected to a severe transient disturbance. The resulting system response involves large excursion of generator rotor angle and is influenced by the nonlinear power-angle relationship. Stability depends on both the initial operating state of the system and the severity of the disturbance. Usually, the system is altered and the post-disturbance steady-state operation differs from that prior to the disturbance.

Disturbance of widely varying degree of severity and probability of occurrence can occur on the system. The system is, however, designed and operated so as to be stable for a selected set of contingencies. The contingencies usually considered are due to faults of different types such as phase-to-ground, two phase-to-ground, or three-phase faults. These are usually assumed to occur on transmission lines, but occasionally bus or

transformer faults are also considered. The fault is assumed to be cleared by the opening of appropriate breakers to isolate the faulted elements.

In a stable system, the rotor angle may increase to maximum, then decrease or oscillate with decreasing amplitude until it reaches to steady state values. If rotor angle continues to increase steadily until synchronism is lost then this form of instability is referred to as first swing stability. First swing instability is caused by insufficient synchronizing torque. The system may be stable in first swing but may become unstable as a result of growing oscillations as the end state is approached. This form of instability generally occurs when the post fault steady-state condition itself is "small-signal" unstable, and not necessarily as a result of the transient disturbance.

In larger power systems, transient instability may not always occur as first swing instability. It could be the result of the superposition of several modes of oscillations causing large excursions of rotor angle beyond the first swing. In transient stability studies, the study period of interest is usually limited to 3 to 5 seconds following the disturbance, although it may extend to about 10 seconds for very large system with dominant interarea modes of oscillations.

1.2.2. Small signal stability

Small-signal stability is the ability of the power system to maintain synchronism under small disturbances. Such disturbances occur continually on the system because of small variations in loads and generation. The disturbances are considered sufficiently small for linearization of system equations to be permissible for purpose of analysis. Instability that may result can be of two forms

1. Steady increase in rotor oscillations of increasing amplitude due to lack of sufficient damping torque.
2. Rotor oscillations of increasing amplitude due to lack of sufficient damping torque.

The nature of system response to small disturbances depends on a number of factors including the initial operating condition, the transmission system strength, and the type of generator excitation controls used. For a generator connected radially to a larger power system, in the absence of automatic voltage regulators (i.e. with constant field voltage), the instability is due to lack of sufficient synchronizing torque. This results in instability through non-oscillatory modes. With continuously acting voltage regulators, the small disturbance stability problem is one of ensuring sufficient damping of system oscillations. Instability is normally through oscillations of increasing amplitude.

In a practical power system, small-signal stability is largely a problem of insufficient damping of oscillations. The stability of the following types of oscillations is of concern:

1. Local modes or machine-system modes, which are associated with the swinging of units at a generating station with respect to the rest of the power system. The term local is used because the oscillations are localized at one station or a small part of the power system.

2. Interarea modes are associated with the swinging of many machines in one part of the system against machines in the other part. These are caused by two or more groups of closely coupled machines being interconnected by weak ties.

3. Control modes are associated with generating units and other controls. Poorly tuned exciter, speed governors, HVDC converters and static VAR compensators are the usual cause of instability of these modes.

4. Torsional modes are associated with the turbine-generator shaft system rotational components. Instability of torsional modes may be caused by interactions of the shaft oscillations with the excitation controls, speed governors, HVDC controls, and series-capacitor-compensated lines.

For a high value of external system reactance and high generator outputs, the automatic voltage regulator action introduces a positive synchronizing torque component but may produce a negative damping torque component. This effect is more pronounced as the exciter response increases. Even though a high response exciter is beneficial in increasing synchronizing torque but in doing so, it introduces

negative damping. Thus, there is a conflicting requirement with regard to exciter response. One possible alternative is to strike a compromise and set the exciter response so that it results in sufficient synchronizing and damping torque component for the expected range of system operating conditions. This may not always be possible. It may be necessary to use a high response exciter to provide the required synchronizing torque for the transient stability performance. With a very high external system reactance, even with low exciter response, the net damping torque coefficient may be negative. An effective way to meet the conflicting exciter performance required with regard to system stability is to provide a power system stabilizer.

The basic function of a power system stabilizer (PSS) is to add damping to the generator rotor oscillations by controlling its excitation using auxiliary stabilizer signals. To provide damping, the stabilizer must produce a component of electrical torque in phase with rotor speed deviations. A logical signal to be used as input to the stabilizer is the speed deviation. A direct feedback of speed signal would result in a damping torque component. However, in practice both the generator and the exciter (depending on its type) exhibit frequency dependent gains and phase characteristics. Therefore, the PSS transfer function should have appropriate phase compensation circuit to compensate for the phase lag between the exciter input and the electrical torque. In ideal case, with the phase characteristics of PSS being an exact inverse of the exciter and generator phase characteristics to be compensated, the PSS would result in a pure damping torque at all oscillating frequencies. There may be negative interactions between PSS installed at different generators, which may decrease the damping or even make the system unstable. To avoid interactions, the PSS parameters of different generators must be coordinated.

Static VAR compensators, which are basically used to maintain the voltage at the specified value at the bus where it has been placed, can also be used for providing damping to oscillatory modes. A supplementary controller with similar structure as that of the PSS can be utilized for providing damping to oscillatory modes. As different PSS are to be coordinated to avoid interactions, similarly, supplementary controller of SVC and PSS must be coordinated.

1.3. State of the Art

A large percentage of the generating units are equipped with continuously acting voltage regulators. It has already been established that the voltage regulator action had a detrimental impact upon the dynamic stability of the power system. Demello and Concordia [1] have studied the phenomenon of stability as effected by thyristor-type excitation systems and established understanding of stabilizing requirement for such systems.

The power system stabilizer was developed to aid in damping the oscillations via modulation of the generator excitation. In reference [18] the use of accelerating power to provide damping of synchronous machine oscillations through supplementary control of excitation (PSS) has been studied for a single machine infinite bus system. A practical approach of deriving stabilizer action with accelerating power is described using measurement of electrical power and frequency of a voltage synthesized from machine terminal voltage and current.

In ref. [15], a technique for selecting the parameters of stabilizer in multimachine power systems has been presented. The technique enables the selection of the parameters of stabilizers such that specified improvement in the damping ratios of the poorly damped modes of oscillations are approximately realized. In ref. [2,16] the general concepts associated with applying power system stabilizer utilizing shaft speed, A.C. bus frequency, and electrical power inputs are developed. These works lay the foundation for tuning of the stabilizers with respect to practical aspects of stabilizer applications.

The earlier PSS designs were based upon the single machine infinite bus system. These works, however, considered design of PSS for one machine at a time, and did not attempt to coordinate the PSS parameters of all the generators simultaneously. Due to lack of coordination, there may be interaction between the PSS and this may lead to instability of the system. In later work, the coordination of PSS parameters for different generators got due importance. In ref. [21], a method was developed for the coordination of PSS parameters in a multimachine system (the aim of the method was

to provide, through the action of the stabilizer, an electrical damping torque proportional to speed perturbance).

In ref. [4], an integrated method has been proposed for the design of power system stabilizer in multimachine systems. The parameters of all the stabilizers were simultaneously determined, so that the dynamic interactions of various machines are properly taken into account during the design procedure. By imposing output feedback and decentralization as structural constraints on the control problem, the PSS parameters were obtained. While this work did not take different operating conditions in to considerations, ref. [5,9] proposed a design method for damping controllers, which guarantees the system stability for all operating conditions in a prescribed set. The method consists of a multivariable linear inequality optimization procedure, which allows the coordinated design of various PSS in the system. Ref. [28] used the inequality method where the design objective of the PSS parameters was given in terms of inequalities and these were solved using genetic algorithm.

In ref. [25] a fuzzy basis function network (FBFN) based power system stabilizer (PSS) was presented to improve power system dynamic stability. The proposed FBFN based PSS provides a framework for combining numerical and linguistic information in a uniform fashion. The proposed FBFN was trained over a wide range of operating conditions in order to re-tune the PSS parameters in real-time based on machine loading conditions.

Different methods of coordination of PSS in multimachine system were studied in ref. [24]. The classical phase compensation, μ synthesis method and linear matrix inequality methods were studied and the results obtained were compared. It was observed that the decentralized controllers needed gain values more than that of the centralized controllers for same amount of damping enhancement. However, the centralized controller has less disturbance rejection and requires fast communication links for its implementation.

Tie-line power oscillations occur due to excitation of lightly damped inter-area modes of rotor oscillations. Traditionally such modes have been damped using the power system stabilizers. Recently there has been growing interest in use of Flexible AC

Transmission Systems (FACTS) controllers for the purpose of damping low-frequency power swings. For this purpose, supplementary control circuit is provided along with main control circuit. Static VAR compensator (SVC) has been one such FACTS controller, popularly utilized. Ref. [22,26] described the selection of the feedback signal to FACTS controllers for damping the interarea power oscillations to ensure stable and secure operation of the bulk transmission system. The main criterion for selecting the feedback signal is to select a signal that maximizes the controllability and observability of the system and minimizes the interactions resulting in the inter-area modes.

In ref. [6], a new technique has been described using modal analysis for calculating the electrical damping and synchronizing torque coefficients induced on generator through the action of FACTS stabilizers (FDS) in multimachine systems. For a given modal frequency and for an increment in gain values of each stabilizer, it is possible to assess from an array of induced damping and synchronizing torque coefficients, the effect of each stabilizer on the damping of individual generators. Furthermore, using this array, the technique is extended to calculate the contribution of the gain increment.

When both PSS and FACTS controllers are present in the system, there will be interactions between them similar to different PSS in a system. These types of interactions were first studied by Gibbard and Pourbeik [30]. In this work, they studied the interactions of the PSS and FACTS controllers and found that the interactions adversely affect the damping of the inter-area modes of oscillations. In ref. [8], a method was developed by using the concept of induced torque coefficients for the simultaneous coordination of PSS and FDS in order to enhance the damping of the rotor modes of oscillations in a multimachine system.

1.4 Motivation

Limited literature survey presented in the earlier section reveals that most of the tuning methods for power system stabilizers are extensions of the single machine

infinite bus case [1,2,16,18]. The parameters of PSS tuned by single machine infinite bus case may not give satisfactory results in multimachine system. The tuning based on single machine infinite bus system concept does not consider the dynamics of all the generators simultaneously and hence it neglects the important aspect of interactions between the controllers. These interactions may make some modes of oscillations under-damped or unstable and there by affecting the system stability.

Different methods have been used in the literature for the coordination of the controller parameters [4-6], such as, induced damping torque, linear inequality, and decentralized methods. The damping torque method, in which PSS and FACTS controllers utilize induced damping torques on the generator rotors, need high-speed communication network. Even though, there is adequate communication network the calculation of induced torque is laborious. The linear inequality and decentralized methods take different operating conditions into consideration (loss of line, increase of loads etc.). The system parameters have to be calculated every time the operating condition changes. The required characteristics are then represented in the form of inequalities, which are solved to get the desired parameter values. Thus, the computational burden increases drastically, as compared to other methods and becomes impractical for the large systems.

Therefore, there is a need to develop a method, which can coordinate the controllers considering the dynamics of all the generators, simultaneously. In addition, the computational burden is minimal so that it can be easily implemented for large systems. The controllers must be robust so that its parameters need not change with operating condition. The system must remain stable for different operating conditions with the parameters obtained for the controllers. An attempt has been made in this thesis to develop a methodology for coordinating different PSS in the system and also PSS and FDS, satisfying the above objectives.

1.5 Thesis Organization

The thesis has been organized into four chapters.

The present Chapter-1 introduces the general concepts of stability and need for coordination of damping controllers. It presents a state of the art in the area of the research work and sets the motivation behind the present work.

Chapter-2 first presents the mathematical modeling of generators, exciter and power system stabilizers used in this work. A robust coordination procedure of the PSS parameters has been described. The proposed coordination procedure of multiple PSS has been implemented on WSCC 9-bus and New England 39-bus systems and the results have been presented in this chapter.

Chapter-3 has described a coordination procedure of PSS and static VAR compensator supplementary controller. The coordination procedure has been implemented on the two systems and the results are presented, in the chapter.

Chapter-4 concludes the main findings of the research work carried out in this thesis and brings out few areas of further research with respect to coordination of parameters of PSS and FACTS stabilizers.

Chapter 2

Control Coordination of Power System Stabilizers

2.1 Introduction

Power system stabilizers are effectively used in improving the dynamic performance of power systems. The basic function of a power system stabilizer (PSS) is to extend stability limits by modulating generator excitation to provide damping to the oscillations of synchronous machine rotors. These oscillations of concern typically occur in the range of approximately 0.2 to 2.0 Hz, and insufficient damping may limit the ability to transmit power. To enhance damping, the stabilizer must produce a component of electrical torque on the rotor, which is in phase with rotor speed deviation. The implementation details of PSS differ depending upon the stabilizer input signal employed. However, for any input signal, the stabilizer must compensate for the phase lag offered by the excitation system, which collectively determines the transfer function from the stabilizer output to the component of electrical torque, which can be modulated via excitation control.

Several strategies for design of PSS for multimachine power systems have been proposed in the literature during the last two decades. These methods usually employ sequential approach, in a sense that the PSS parameters of each machine are computed one at a time, mostly extending the single machine infinite bus concept [2, 15, 16]. Although they provide satisfactory results most of the time, these techniques lack a more precise representation of the dynamic interactions among the various machines, in the system.

In this context, integrated methods, as opposed to the sequential procedure, became attractive due to their ability to properly take into account all dynamic interactions. New methods and tools for optimal controller design, applicable to large-scale multimachine system, have been developed [4-6]. However, these methods utilize single machine infinite bus modeling for tuning of PSS of each generator, separately. Hence, it involves more number of iterations and also does not promise coordinated optimal settings. In this thesis, power system stabilizers are designed using optimal control strategies [4] with pseudo-decentralization [7] taking dynamics of all the machines at a time. This method

has been implemented on WSCC 9-Bus system and New England 39-bus system. The PSS of both the systems have been tuned using optimal control strategies with pseudo-decentralization.

2.2 Modeling of Power System Components

For designing the power system stabilizers and studying its performance, detailed dynamic model of generator and its excitation system has been used which are described below.

2.2.1 Synchronous Machine

A two-axis model of synchronous generator has been used in this thesis. The model ignores sub transients due to the fast dynamics of the damper windings. The two-axis model of a generator in a m-machine system is shown in fig: 2.1.

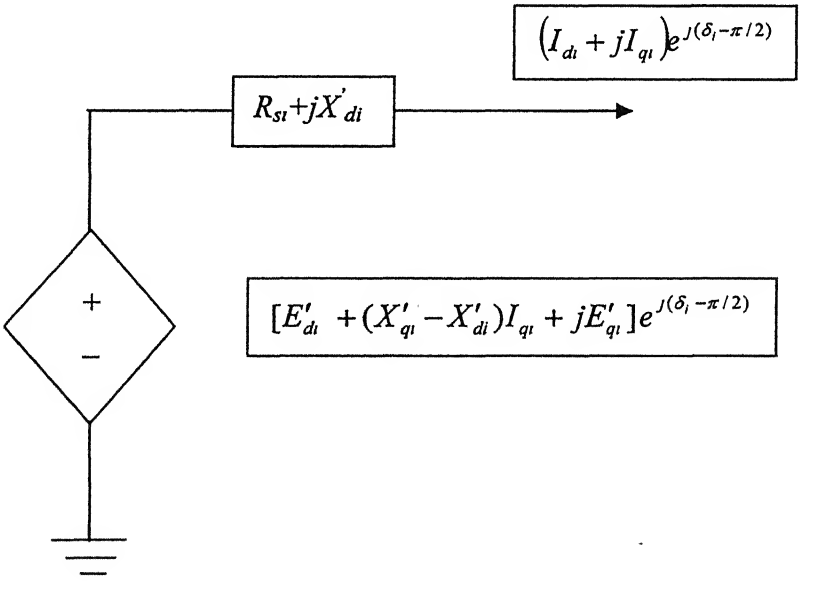

Figure 2.1: Two-axis model of a Synchronous machine

The differential equations describing the fourth order of the generator model can be written as follows:

$$T'_{doi}\frac{dE'_{qi}}{dt} = -E'_{qi} - (X_{di} - X'_{di})I_{di} + E_{fdi} \qquad i = 1,\ldots\ldots\ldots,m \qquad (2.1)$$

$$T'_{qoi}\frac{dE'_{di}}{dt} = -E'_{di} - (X_{qi} - X'_{qi})I_{qi} \qquad i = 1,\ldots\ldots\ldots,m \qquad (2.2)$$

$$\frac{d\delta}{dt} = \omega_i - \omega_s \qquad i = 1,\ldots\ldots\ldots,m \qquad (2.3)$$

$$M_i\frac{d\omega_i}{dt} = T_{mi} - [E'_{qi} - X'_{di}I_{di}]I_{qi} - [E'_{di} - X'_{qi}I_{qi}]I_{di} - D_i(\omega_i - \omega_s) \quad i = 1,\ldots\ldots\ldots,m \qquad (2.4)$$

Where,

δ = Machine rotor angle with respect to a synchronously rotating frame

ω = Rotor speed

M = Machine inertia

T_m = Mechanical input torque

E_q' = Quadrature axis induced voltage behind the transient reactance.

E_d' = Direct axis induced voltage behind the transient reactance.

I_q = Quadrature axis stator current.

I_d = Direct axis stator current.

X_q = Quadrature axis stator steady state reactance.

X_d = Direct axis stator steady state reactance.

X_q' = Quadrature axis stator transient reactance.

X_d' = Direct axis stator transient reactance.

E_{fd} = Voltage induced due to rotor field excitation.

2.2.2 Exciter modeling

The main objective of the excitation system is to control the field current of the synchronous machines. The field current is controlled so as to regulate the terminal voltage of the machine. As the field circuit time constant is high (of the order of few seconds), fast control of the field current requires field forcing. Thus, exciter should have a high ceiling voltage, which enables it to operate transiently with voltage levels that are 4 to 5 times the normal. The rate of change of voltage should also be fast.

There are three distinct types of excitation systems based on the power source utilized:

1. DC excitation system, which utilizes a DC generator with commutator.
2. AC excitation system, which uses alternator and either stationary or rotating rectifier to produce the direct current, needed.
3. Static exciter system in which the power is supplied through transformer and rectifiers.

The first two types of exciters are also called rotating exciters, which are mounted on the same shaft as the generator and driven by the prime mover.

The excitation system used in this thesis is IEEE Type 1[11]. This IEEE Type 1 exciter was first defined in an IEEE committee report in 1968. The IEEE Type 1 system represents a majority of the excitation systems in service. It essentially represents D.C. rotating exciter but with some modifications can also represent static exciters. This is shown in the figure 2.2. Here, V_R is the output of the regulator, which is limited. The regulator time constant has single time constant T_A and a positive gain K_A. The function $S_E=f(E_{fd})$ represents the saturation function of the exciter.

It is to be noted that the limits on V_R also impose limits on E_{fd}. Actually the latter are usually specified, and the former can be found from the equation (in steady state).

$$V_R - (K_E + S_E) E_{fd} = 0 \qquad (2.5)$$

$$E_{fdmin} \leq E_{fd} \leq E_{fdmax} \tag{2.6}$$

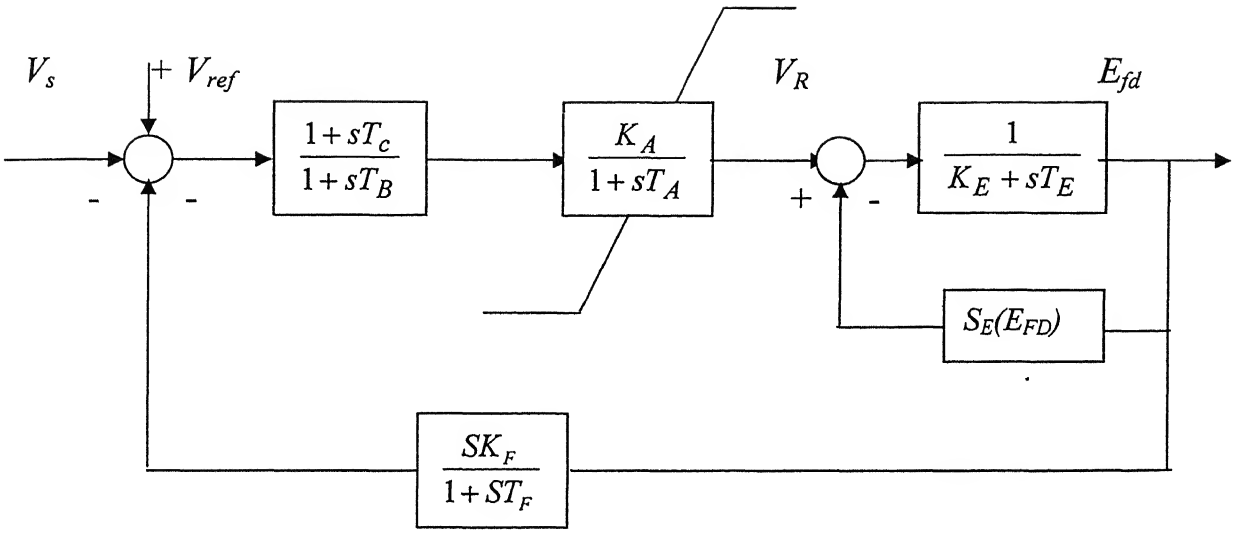

Figure. 2.2 IEEE Type -1 DC Exciter

IEEE Type 1 exciter scheme can also represent the static excitation system by specifying the following parameters.

$K_E = 1$, $T_E = 0$, $S_E = 0$. To simplify further we can specify $T_R = 0$, $T_F = 0$, $K_F = 0$.

In this thesis, a simplified model is taken for the excitation system. The dynamic equation for this model is:

$$T_A \frac{dE_{fd}}{dt} = -E_{fd} + K_A\left(V_{ref} - V_t\right) \tag{2.7}$$

Where,

K_A = Regulator amplifier gain

T_A = Regulator time constant

V_{ref}= Reference voltage setting

V = Generator terminal voltage.

2.2.3 Power Balance Equations

For each machine, two algebraic equations can be written for computing stator quantities. The idea is to express I_{di} and I_{qi} in terms of the state and network variables. These equations are as follows (also shown by a vector diagram in fig: 2.3):

$$E_{di}' - V_i \sin(\delta_i - \theta_i) - R_{si} I_{di} + X_{qi}' I_{qi} = 0 \qquad i = 1,\ldots\ldots,m \qquad (2.8)$$

$$E_{qi}' - V_i \cos(\delta_i - \theta_i) - R_{si} I_{qi} - X_{di}' I_{di} = 0 \qquad i = 1,\ldots\ldots,m \qquad (2.9)$$

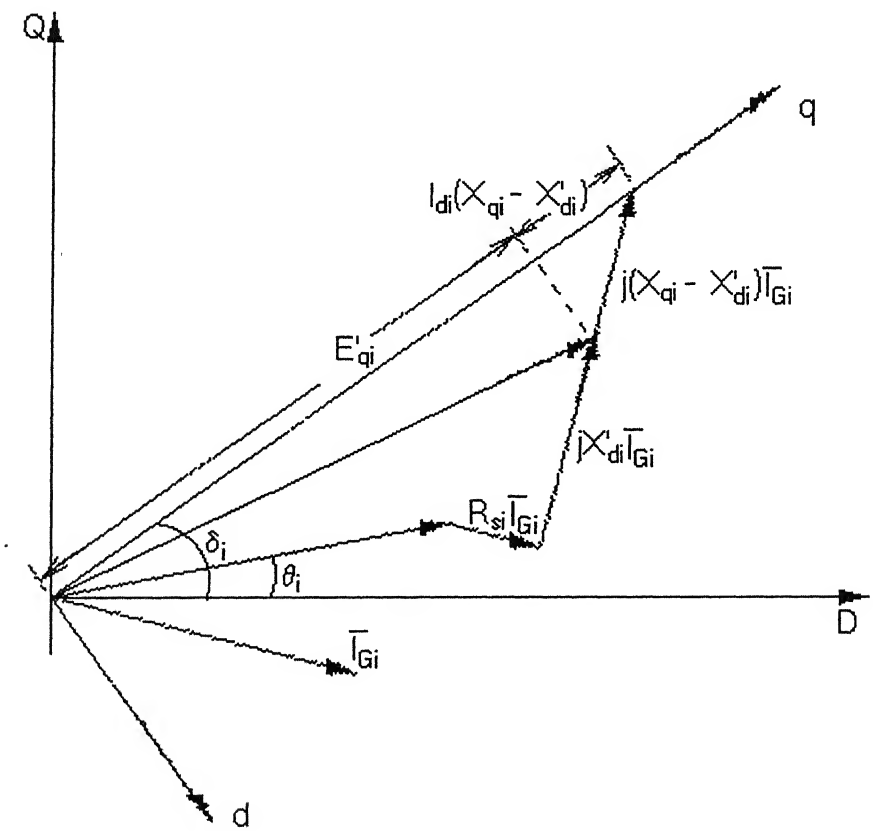

Fig: 2.3 Vector diagram of a synchronous machine showing stator quantities.

The power balance equations at the generator buses (i =1...m) are:

$$I_{di}V_i \sin(\delta_i - \theta_i) + I_{qi}V_i \cos(\delta_i - \theta_i) + P_{Li}(V_i) - \sum_{K=1}^{n} V_i V_k Y_{ik} \cos(\theta_i - \theta_k - \alpha_{ik}) = 0 \quad (2.10)$$

$$I_{di}V_i \cos(\delta_i - \theta_i) - I_{qi}V_i \sin(\delta_i - \theta_i) + Q_{Li}(V_i) - \sum_{K=1}^{n} V_i V_k Y_{ik} \sin(\theta_i - \theta_k - \alpha_{ik}) = 0 \quad (2.11)$$

The usual power flow equations given below describe the power balance at the load buses ($i = m+1,.....,n$)

$$P_{Li}(V_i) - \sum_{k=1}^{n} V_i V_k Y_{ik} \cos(\theta_i - \theta_k - \alpha_{ik}) = 0 \quad (2.12)$$

$$Q_{Li}(V_i) - \sum_{k=1}^{n} V_i V_k Y_{ik} \sin(\theta_i - \theta_k - \alpha_{ik}) = 0 \quad (2.13)$$

Where,

P_{Li} is the real power at the i^{th} load bus

Q_{Li} is the reactive power at the i^{th} load bus

V_i, θ_i are the voltage magnitude and angle at the i^{th} load bus

V_k, θ_k are the voltage magnitude and angle at the k^{th} bus

Y_{ik}, is the admittance between buses i and k

α_{ik} is the angle of Y_{ik}

The set of dynamic equations (2.1-2.4, 2.7) and algebraic equations (2.8-2.13) completely describe the power system, model.

2.2.4 System Linearization:

A Power system is described by a set of nonlinear dynamic and algebraic equations as already described. The complex algebraic equations have to be separated into real and imaginary parts. Symbolically, this Differential Algebraic Equations (DAE) can be denoted in brief as:

$$\dot{X} = f(X,Y) \tag{2.14}$$

$$0 = g(X,Y) \tag{2.15}$$

Where,

X = Vector of dynamic state variables

$$= \left[\delta \quad \omega \quad E_q' \quad E_d' \quad E_{fd}\right]^t \tag{2.16}$$

Y = Vector of algebraic variables

$$= \left[I_q \quad I_d \quad V \quad \theta\right]^t \tag{2.17}$$

Equation (2.14) represents the dynamic equation of the power system. Equation (2.15) represents the algebraic equations, expressed in the real form. The equation represents explicitly the traditional load-flow equations and the other algebraic equations. Defining initial operating point as (X_o, Y_o) and linearizing around this operating point, we get the following equations

$$\Delta\dot{X} = A\Delta X + B\Delta Y \tag{2.18}$$

$$0 = C\Delta X + D\Delta Y \tag{2.19}$$

Where,

$$A = \left[\frac{\partial f}{\partial X}\right]_{(Xo,Yo)} \qquad B = \left[\frac{\partial f}{\partial Y}\right]_{(Xo,Yo)}$$

$$C = \left[\frac{\partial g}{\partial X}\right]_{(Xo,Yo)} \qquad D = \left[\frac{\partial g}{\partial Y}\right]_{(Xo,Yo)} \tag{2.20}$$

Solving for the vector ΔY from eq. (2.19) and substituting it in eq. (2.18) gives.

$$\Delta\dot{X} = \left(A - BD^{-1}C\right)\Delta X \qquad (2.21)$$

Where, $\widetilde{A} = (A - BD^{-1}C)$ is known as the reduced system Jacobian. The Eigen values of the reduced system Jacobian have been used to find out the stability of the system, the damping and frequency of different oscillatory modes.

2.3. Power System Stabilizer (PSS)

It is well established that fast acting exciter with high gain AVR can contribute to oscillatory instability [1]. This type of instability is characterized by low frequency (0.2 to 2.0 Hz) oscillations, which can persist (or even grow in magnitude). This type of instability can endanger system security and limit power transfer. The major factors that contribute to the instability are

1. Loading of the generators or tie line.
2. Maximum power transfer capability of transmission lines
3. Power factor of the loads
4. AVR gain.

An efficient solution to the problem of oscillatory instability is to provide damping to the generator rotor oscillations. This is conveniently done by providing power system stabilizer (PSS), which are supplementary controllers in the excitation systems [16]. The objective of designing PSS is to provide additional damping torque without affecting the synchronizing torque at critical oscillation frequency. The PSS are designed mainly to stabilize local and interarea modes. However, care must be taken to avoid unfavorable interactions with intra-plant modes, which introduces new modes, which may become unstable.

Structure of Power system stabilizer

The block of a PSS used, in general, is shown in the figure 2.4. It consists of a washout circuit, dynamic compensator, and limiter. The function of each of the components of the PSS is given below.

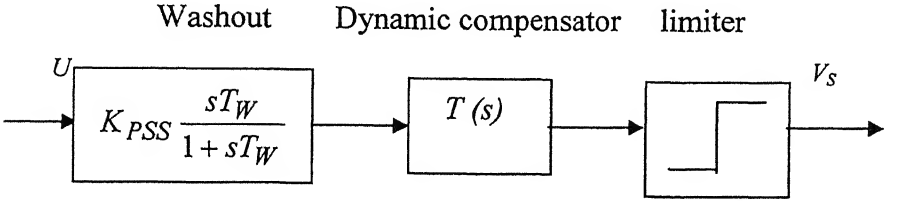

Figure 2.4 basic block diagram of a PSS.

Washout circuit:

The washout circuit is provided to eliminate steady-state bias in the output of PSS, which will modify the generator terminal voltage. The PSS is expected to respond only to transient variations in the input signal (usually rotor speed deviation) and not to the DC offsets in the signal. This is achieved by subtracting from it the low frequency component of the signal obtained by passing the signal through a low pass filter.

The washout circuit acts essentially as a high pass filter and it must pass all frequencies that are of interest. If only the local modes are of interest, the time constant T_w can be chosen in the range of 1 to 2 sec. However, if interarea modes are also to be damped, then T_w must be chosen in the range of 10 to 20 sec. A recent study [16] has shown that a value of T_w is necessary to improve damping of the interarea modes. There is a noticeable improvement in the first swing stability when T_w is increased from 1.5 to 10.

Dynamic compensator:

The dynamic compensator used in practice is made up of multiple stages lead-lag compensators. A two-stage lead-lag has the following transfer function.

$$T(S) = \frac{K_S(1+sT_1)(1+sT_3)}{(1+sT_2)(1+sT_4)} \tag{2.22}$$

Where, K_s is the gain of PSS. The time constants, T_1 to T_4 are chosen to provide a phase lead to the input signal in the range of frequencies that are of interest (0.1 to 3.0 Hz). With static exciters, only one lead-lag stage may be necessary. In general, the dynamic compensator can be chosen with the following transfer function.

$$T(S) = \frac{K_S N(s)}{D(s)} \tag{2.23}$$

Where

$$N(S)=1+a_1 s+a_2 s^2+.....+a_n s^n$$
$$D(S)=1+b_1 s+b_2 s^2+.....+b_p s^p$$

The zeros of *D (s)* should lie in the left half of s-plane. They can be complex or real. Some of the zeros of *N (s)* can lie in the right half s-plane making it a non-minimum phase. For design purpose, PSS transfer function is approximated to *T (s)*, the transfer function of the dynamic compensator. The effect of the washout filter may be neglected in the design, but must be considered in evaluating performance of PSS under various operating conditions.

Limiter

The output of the PSS must be limited to prevent the PSS acting to counter the action of AVR. For example, when load rejection takes place, the AVR acts to reduce the terminal voltage whereas PSS action calls for higher value of the terminal voltage. It may even be desirable to block the PSS action in case of load rejection.

The negative limit of PSS output is of importance during the back swing of the rotor. The AVR action is required to maintain the voltage after the angular separation has increased PSS action in the negative direction must be curtailed more than in the positive direction. Ontario hydro uses a –0.05 p.u. as the low limit and 0.1 to 0.3 as the higher limit [16].

Control signal

The obvious control signal (to be used as input to the PSS) is deviation in the rotor velocity. However, for practical implementation other signals such as bus frequency, electrical power, and acceleration power are also used [2].

The control signals such as rotor speed, frequency, and electrical power are locally available. The speed signal is inherently sensitive to the present torsional oscillations at frequencies in the range of 8 to 20 Hz, which can lead to negative damping of the torsional mode. A practical solution to this problem is to provide a torsional filter tuned to the frequency of the critical mode.

2.3.1 Coordination of Power System Stabilizer Parameters

The PSS transfer function can be represented as

$$G_{PSS} = K_{PSS} \frac{sT_W}{1+sT_W} \frac{(1+sT_1)}{(1+sT_2)} \frac{(1+sT_3)}{(1+sT_4)} \qquad (2.24)$$

Where T_W, T_1, T_2, T_3, T_4 are the wash out and lead-lag time constants respectively. This transfer function can be rewritten as [4],

$$G_{PSS} = d + \frac{\beta_1 s + \beta_0}{s^2 + \alpha_1 s + \alpha_0} \qquad (2.25)$$

Where,

$$d = k_{PSS} T_1 T_3 / T_2 T_4$$

$$\alpha_0 = 1/T_2 T_4$$

$$\alpha_1 = T_2 + T_4 / T_2 T_4$$

$$\beta_0 = (K_{PSS} / T_2 T_4)(1 - T_1 T_3 / T_2 T_4)$$

$$\beta_1 = (K_{PSS} / T_2 T_4)(T_1 + T_3 - (T_1 T_3 / T_2 T_4)(T_2 + T_4))$$

The state space equations of the PSS can be written as,

$$\dot{X} = A_c X_c + B_c U_c \tag{2.26}$$

$$Y_c = C_c X_c + D_c U_c \tag{2.27}$$

Where,

$$A_c = \begin{bmatrix} 0 & -\alpha_0 \\ 1 & -\alpha_1 \end{bmatrix}$$

$$B_c = \begin{bmatrix} \beta_0 \\ \beta_1 \end{bmatrix}$$

$$C_c = [0 \quad 1]$$

$$D_c = d$$

The PSS design problem consists of determining the parameters of the Gpss(s) i.e. the transfer function, so that the eigen values of the compensated system are sufficiently damped. The time constants of the PSS are so chosen that the phase lag introduced by the exciter be exactly compensated by the PSS. The wash out filter constant has been taken as 10s.

Determination of time constants

Larsen and Swann [2] suggested that the frequency response of the generator terminal voltage magnitude is very close to the electrical torque. The response of the terminal voltage magnitude to change in the voltage reference input is straight forward to measure. Therefore, it is a good signal with which to validate the power system model used for the power system stabilizers design. This model suggested by Larsen and Swann has been used to obtain the frequency response of the exciter by representing all the generators as infinite bus other than the generator for whose exciter the frequency plot is to be taken. The inertia of the generator is made high so as to disable the shaft dynamics. Then the transfer function of the exciter from voltage reference to the torque output is found out there by the frequency response. The PSS dynamic compensator time constants are so chosen such that the frequency response of the PSS matches with the inverse of the exciter frequency response [12].

2.3.2 Determination of coordinated gain values

Compensating the system represented by:

$$\dot{X} = AX + BU \tag{2.28}$$

with the controller given by the state equations (2.26)-(2.27) in feedback connection implies that $Uc = Y$ and $U = Y_c$ [4]. The resulting composite system is then represented as

$$\begin{aligned} \dot{X} &= (A + BD_C C)X + BC_C X_C \\ \dot{X}_C &= A_C X_C + B_C CX \end{aligned} \tag{2.29}$$

If we introduce a feedback loop with a gain K to the system represented by the equation (2.28) such that $U = -KX$, then the system with feed back is given by:

$$\dot{X} = (A - BK)X \tag{2.30}$$

Comparing equation [2.29] and [2.30] gives

$$K = -D_C C \tag{2.31}$$

Thus, the problem boils down to finding a feedback gain K so that D_c can be calculated, thereby the coordinated gains of the PSS. To find out K, an optimal control strategy with pseudo-decentralization has been used.

It is concerned with determining a control strategy that minimizes the following quadratic performance index [4]

$$J(X,U) = 1/2 \int_0^\infty (X^T QX + U^T RU)dt \tag{2.32}$$

Where, the semi definite positive matrix Q and the positive definite matrix R are weighting matrices. The Q and R matrices are both diagonal matrices. Q matrix is selected in such a way that the state representing the input signal to PSS (speed deviation) is given higher value than the other states. Final values of Q and R are obtained by an iterative scheme [7]. This is the so-called linear quadratic regulator problem and its well-known solution is given by the state feed back strategy

$$U = -KX \tag{2.33}$$

Where,

$$K = R^{-1} B^T P \tag{2.34}$$

P is the solution of the algebraic Riccati equation

$$A^T P + PA - PBR^{-1} B^T P + Q = 0 \tag{2.35}$$

From equation (2.31)

$$K = -D_c C \tag{2.36}$$

The matrix K has the form:

$$K = \begin{bmatrix} K_{11}\ K_{12} \ldots\ldots\ldots\ldots K_{1m} \\ k_{21}\ K_{22} \ldots\ldots\ldots\ldots K_{2m} \\ K_{m1}\ K_{m2} \ldots\ldots\ldots\ldots K_{mm} \end{bmatrix}$$

According to the pseudo-decentralization [7], only the diagonal elements are considered and the cross gain terms are neglected.

$$K = \begin{bmatrix} K_{11}\ 0\ 0 \ldots\ldots\ldots\ldots 0 \\ 0\ \ K_{22}\ 0 \ldots\ldots\ldots\ldots 0 \\ 0 \qquad\qquad\qquad K_{mm} \end{bmatrix}$$

Thus

$$D_c = KC^T (CC^T)^{-1}$$

Where,

$D_c = (K_{PSS}\ T_1 T_3 / T_2 T_4)$

C is the output of the system.

Since, times constants, the output matrix, and the gain matrix K are known Dc and there by the PSS gain K_{PSS} can be calculated.

2.4 Simulation Results

The proposed optimal control strategy method based on pseudo-decentralization for coordination of PSS has been implemented on WSCC 9-bus and New England 39-bus systems. The line diagram and the system data for two systems are given in appendix A and B respectively. The results obtained on the WSCC-9 bus system and New England systems are as follows.

2.4.1 WSCC 9-Bus System Simulation Results

This system contains three generators. Machine number one is considered as an infinite bus and power system stabilizers have been assumed to be present at machines 2 and 3. The gains and the different time constants of the power system stabilizers for uncoordinated as well as coordinated cases are given below in tables 2.1 and 2.2. In both the cases, time constants values are same, which were obtained as described in the section 2.3.1 and reference [2]. For the uncoordinated case, the gain values have been separately obtained for each of the two machines treating rest of the system as infinite bus and utilizing linearized analysis [2,12]. The coordinated gains are also obtained by the proposed method as described in section 2.3.2.

Table 2.1 PSS parameters for uncoordinated case (9-bus system)

Machine no.	Kpss	T_w	T_1	T_2	T_3	T_4
2	6.5	10.0s	0.4s	0.035s	0.4	0.035
3	7.8	10.0s	0.38s	0.03s	0.4	0.035

Table 2.2 PSS parameters for coordinated case (9-bus system)

Machine no.	Kpss	T_w	T_1	T_2	T_3	T_4
2	6.038	10.0s	0.4s	0.035s	0.4	0.035
3	3.184	10.0s	0.38s	0.03s	0.4	0.035

With the above PSS values, eigen value plots, participation factor analysis and transient response for a three-phase fault were studied. The 3-phase fault was considered at bus 7. Eigen-value analysis for the 9-bus system at the base operating point without any PSS shows that there are two under-damped modes. The fig. 2.5 shows two under-damped eigen-values of the system with out PSS at machine 2 and 3. Here, the eigen-values having damping ratio less than 0.05 are considered as under-damped modes. The fig. 2.6 shows the participation factor of states, significantly contributing in the under-damped modes. The eigen-values of the system with out PSS are shown in fig. 2.7. The eigen-values of the system with the PSS considered at machine 2 and 3, using coordinated gain values are shown in fig. 2.8. The eigen-values of the system with PSS are moved towards the left in the s-plane significantly when compared to the eigen-values of the system with out any PSS. The coordinated PSS gains result in slight improvement in damping of the system, as compared to the uncoordinated case. The damping ratios are shown below in Table 2.3.

Table 2.3. Damping ratios with coordinated and uncoordinated PSS parameters respectively (9-bus system)

1	1	1	0.781	0.781	1	0.971	0.971	0.0625	0.0625	0.1104	0.1104	1	1	1	1
1	1	1	0.784	0.784	1	0.974	0.974	00547	0.0547	00909	0.0909	1	1	1	1

A 3-phase fault is applied to bus number 7, which was assumed to disappear after 30ms. The transient response of the oscillations was obtained first without PSS and then with PSS having coordinated gains. Fig. 2.9 shows the angle-plot of the generators, without the PSS, after the fault is cleared. It can be seen that the oscillations in the angle of the generators 2 and 3 increase with time. Figs. 2.10 and 2.11 show the angle-plot with the uncoordinated and coordinated PSS at generators 2 and 3. The oscillations in both the cases are damped out. Fig. 2.12 shows the oscillations in the speed deviation of the generators without the PSS, whereas fig. 2.13 and fig. 2.14 show the oscillations in the speed deviation with the uncoordinated and coordinated PSS at the generators. The

oscillations in both the cases are damped out. Fig: 2.15 shows oscillations in the tie line power with out PSS, whereas fig: 2.16 and 2.17 show the oscillations in the tie-line power with uncoordinated and coordinated PSS at the generators. The oscillations in tie line power also dies down with uncoordinated and coordinated PSS, where as it becomes unstable without PSS.

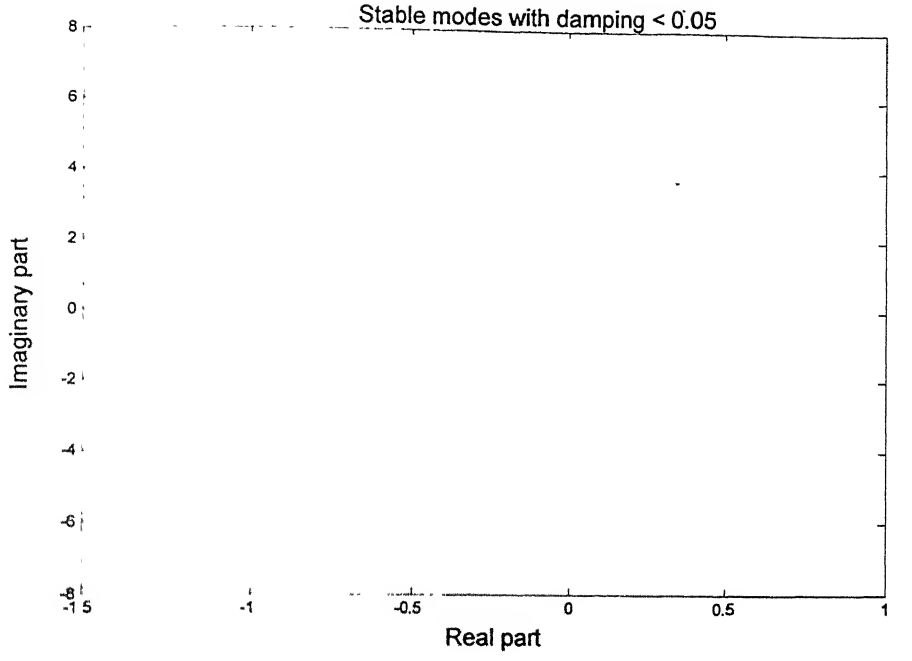

Fig 2.5: Under damped Eigen-values with out PSS (9-bus system)

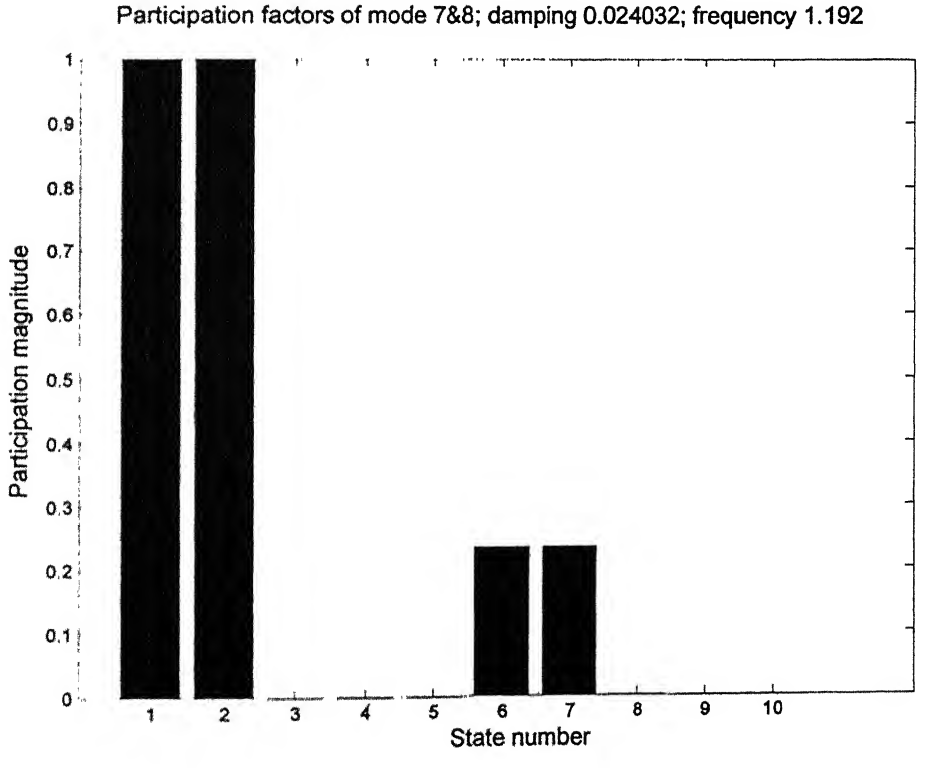

Fig 2.6: Participation factor of under-damped modes (9-bus system)

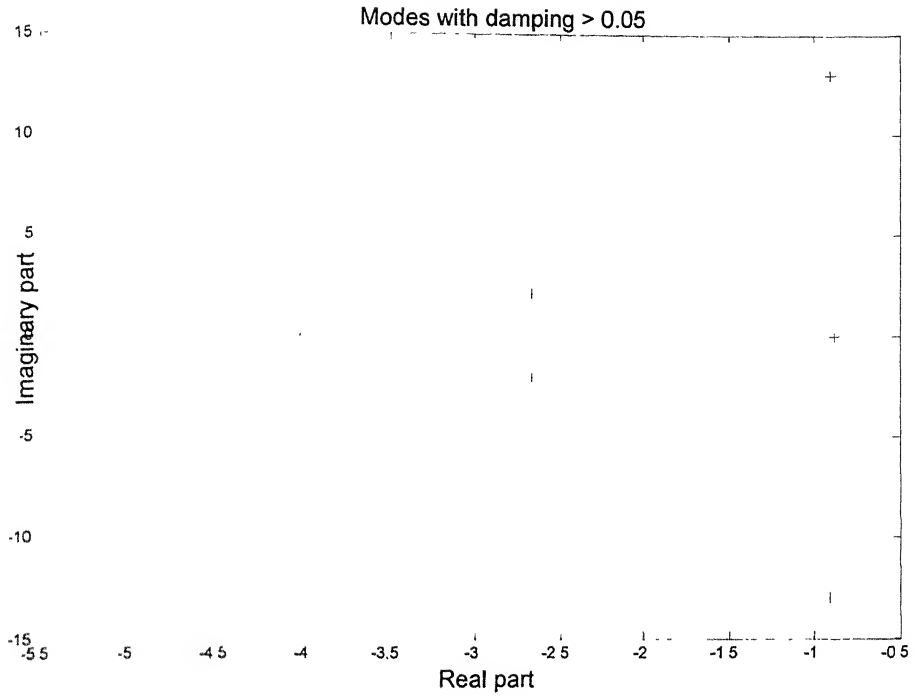

Fig 2.7: Eigen-values with out PSS (9-bus system)

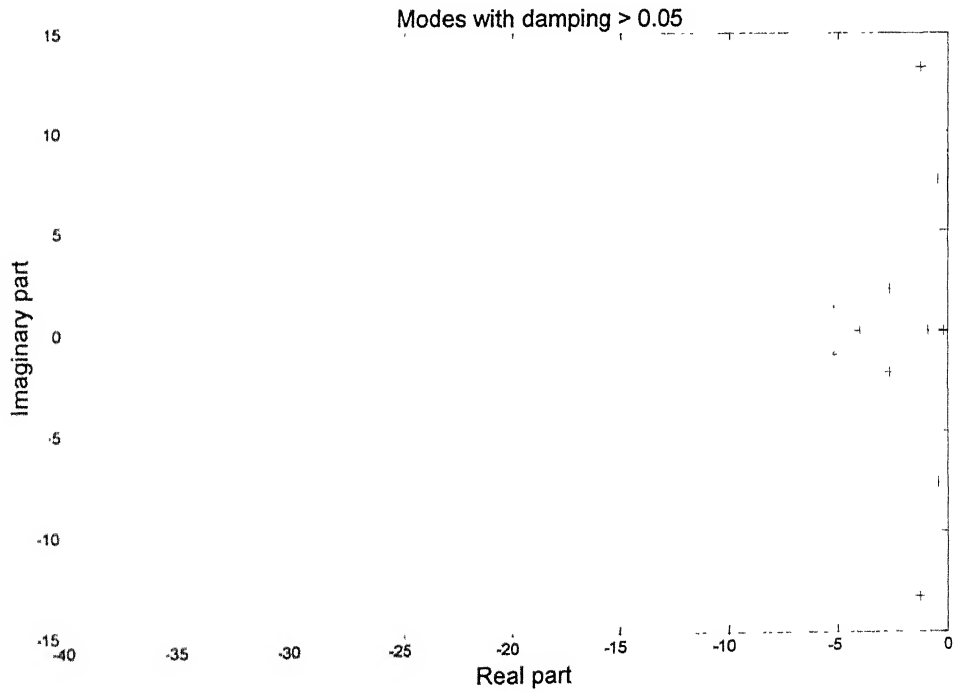

Fig 2.8: Eigen-values with PSS (9-bus system)

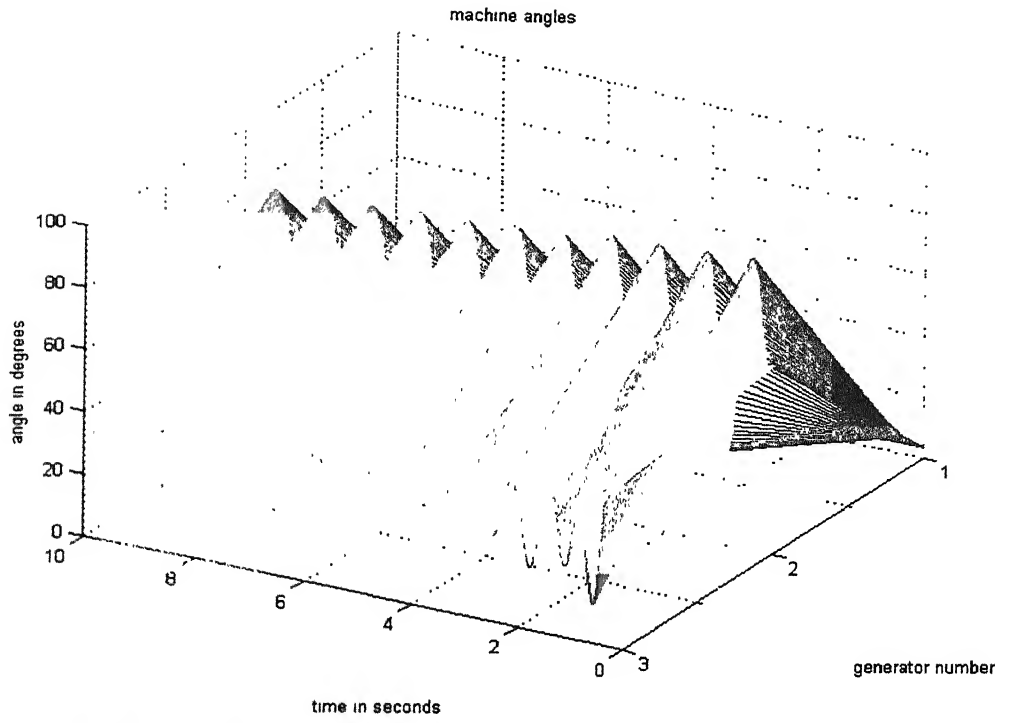

Fig 2.9: Angle-plot of the generators with out PSS (9-bus system).

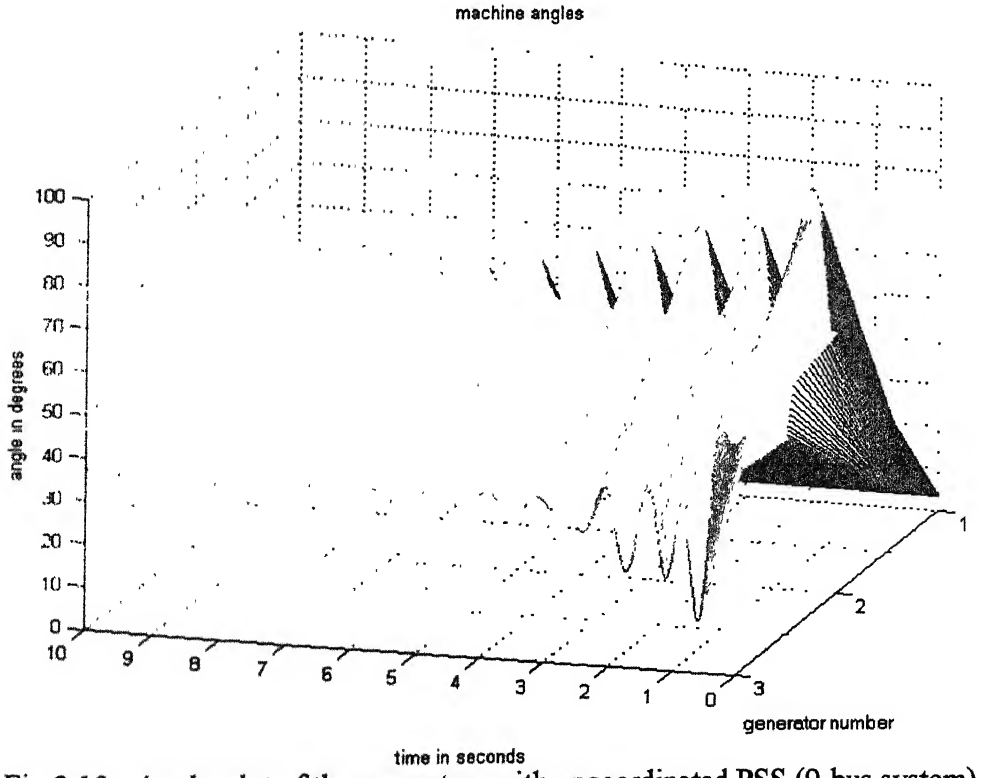

Fig 2.10: Angle-plot of the generators with uncoordinated PSS (9-bus system).

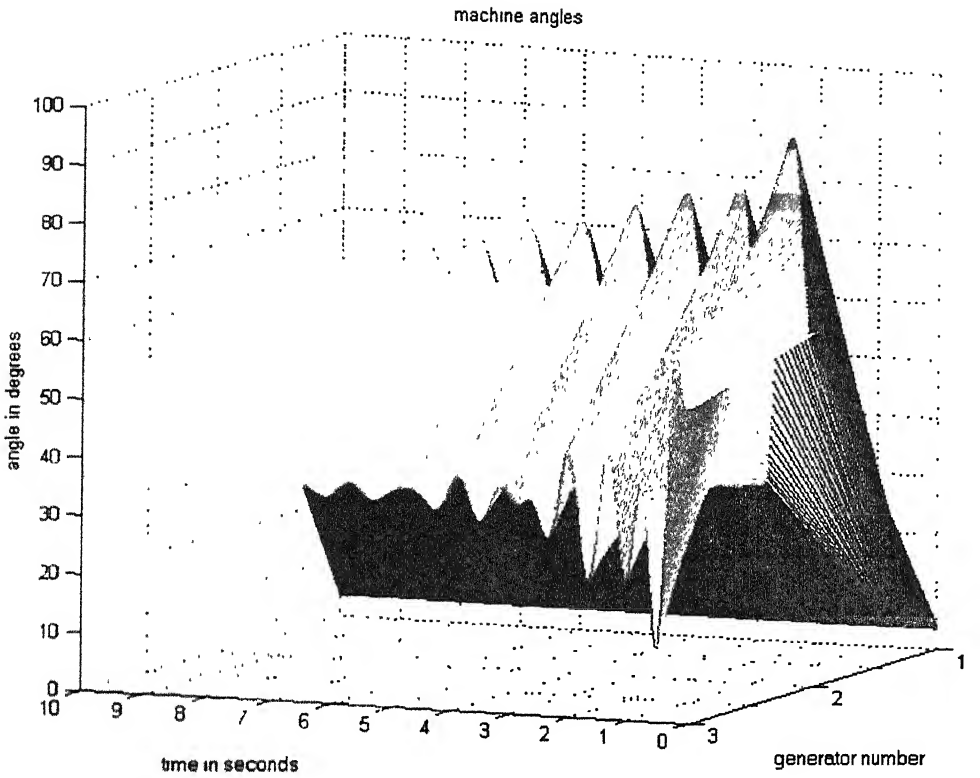

Fig 2.11 Angle-plot with coordinated PSS (9-bus system).

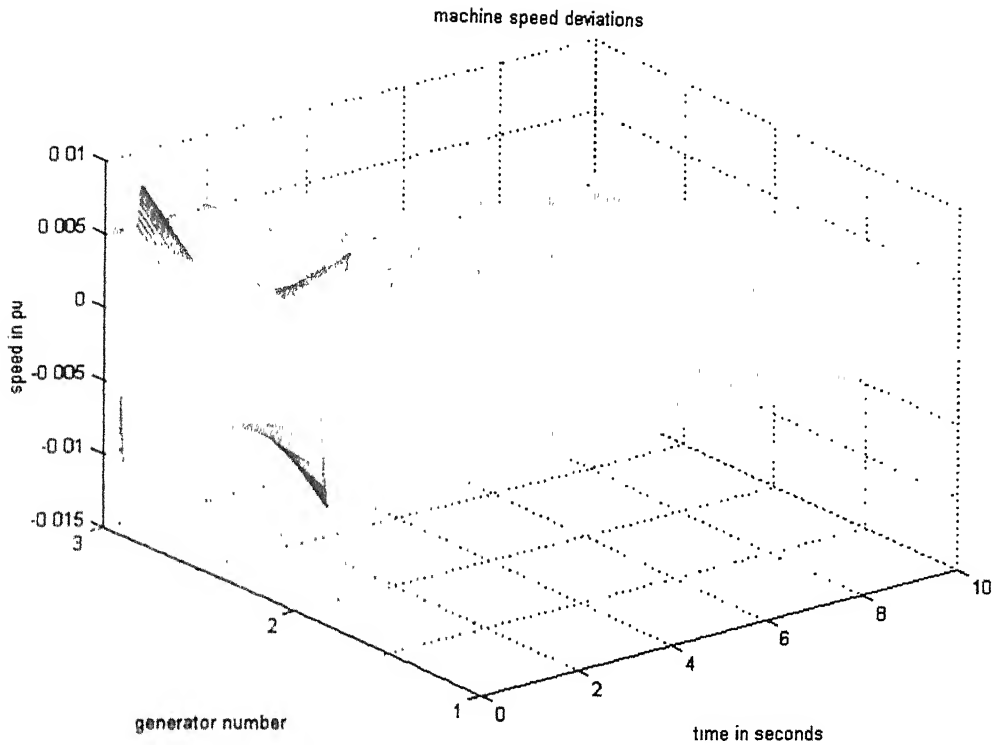

Fig 2.12: Speed deviation plot of the generators with out PSS (9-bus system)

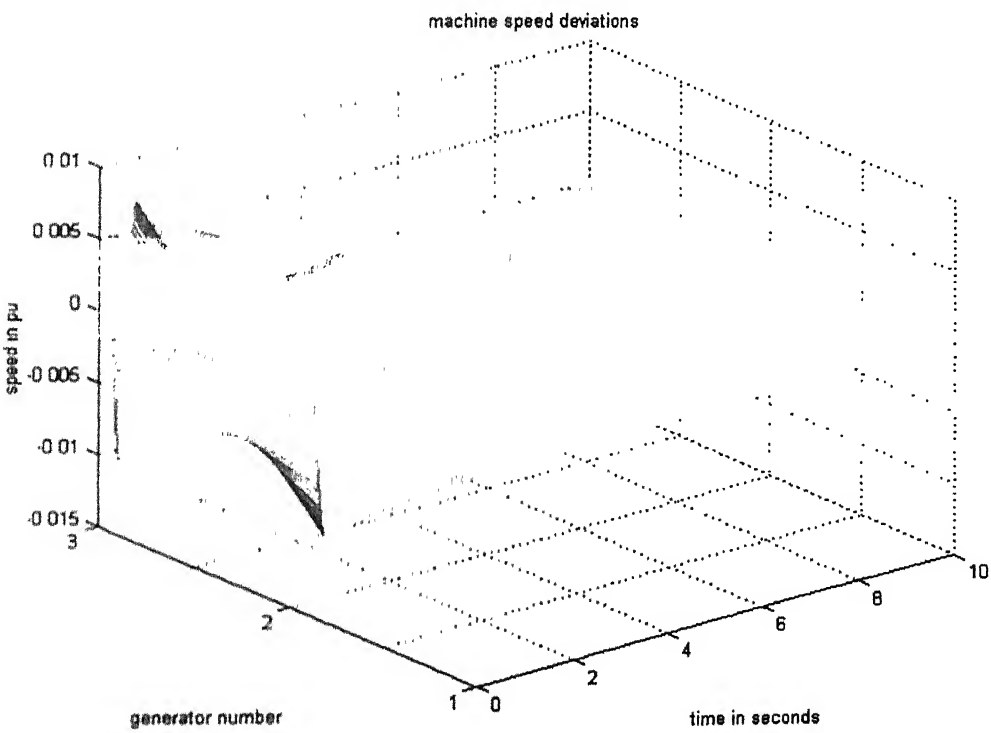

Fig 2.13: Speed deviation plot of the generators with uncoordinated PSS (9-bus system)

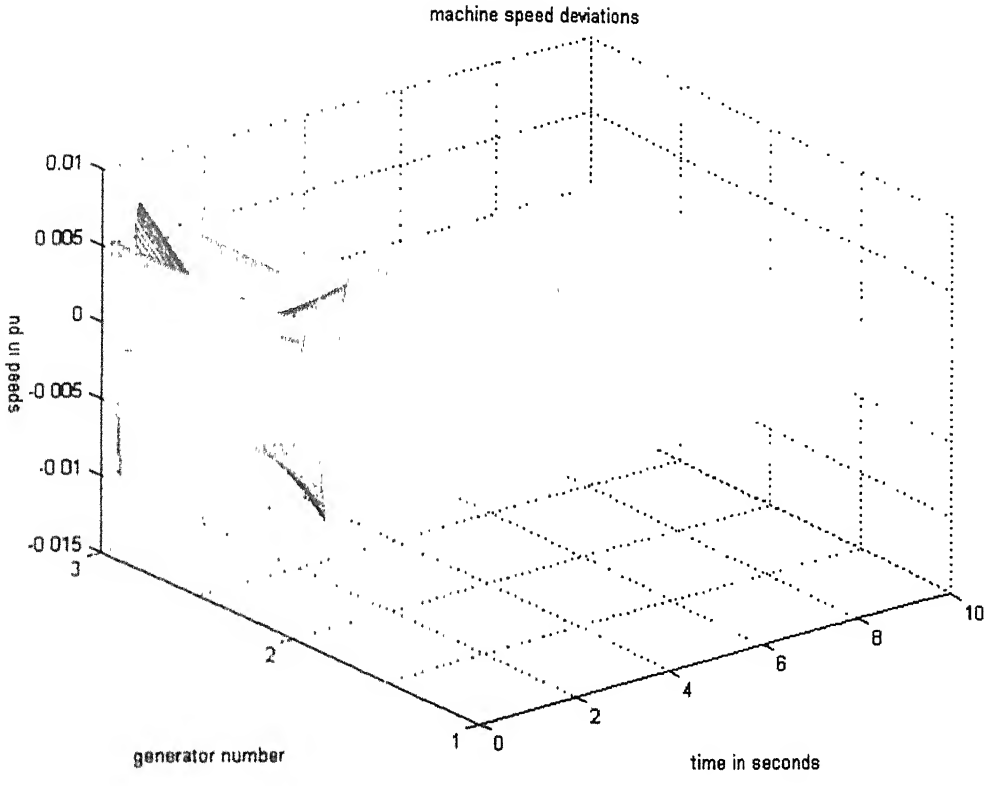

Fig 2.14 Speed-deviation plot with coordinated PSS (9-bus system).

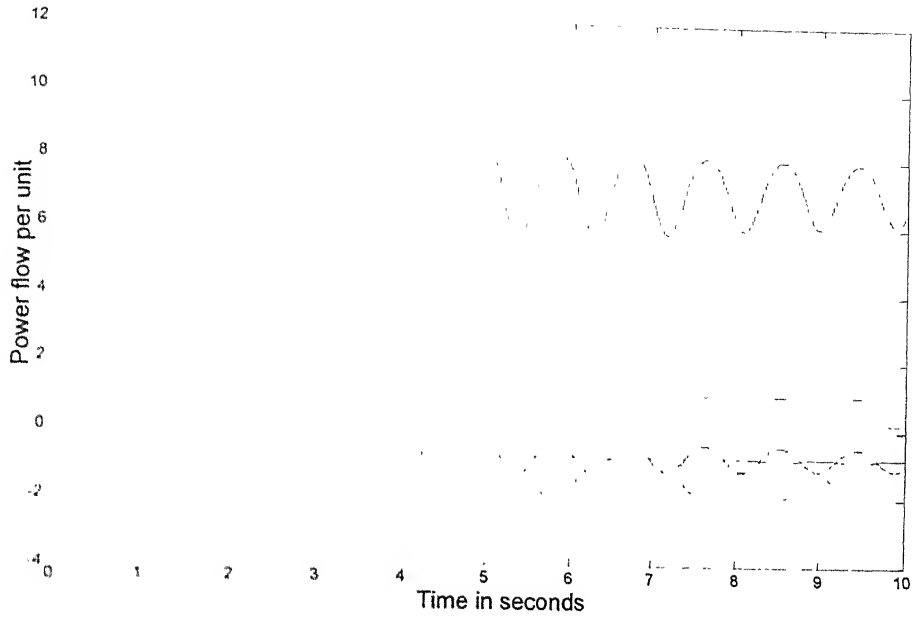

Fig 2.15: Line flow in per units with out the PSS (9-bus system)

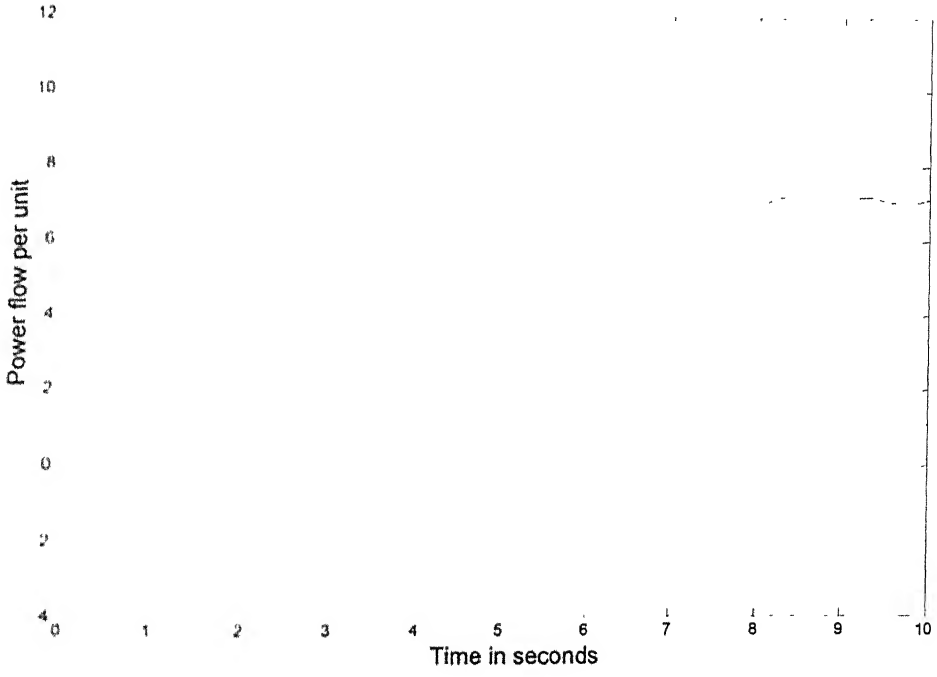

Fig 2.16: Line flow in per units with uncoordinated PSS (9-bus system)

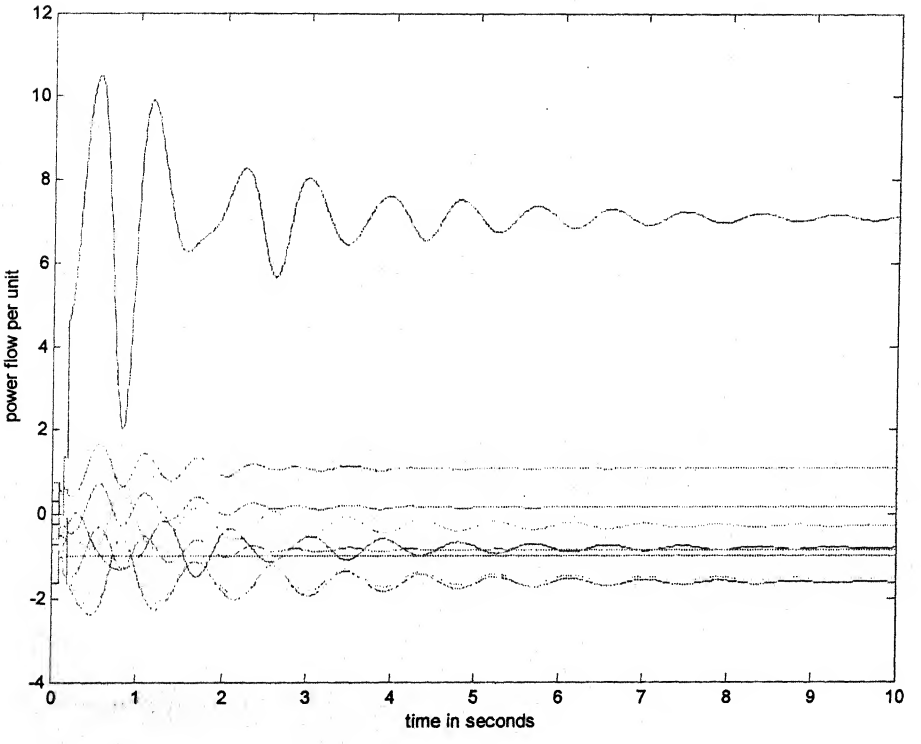

Fig 2.17 Line flow in per units with coordinated PSS (9-bus system)

2.4.2 New England 39-Bus, 10-Generator System Results

The New England system consists of 10 generators and 39 buses. The 10th generator bus is considered as an infinite bus. Machines 3 and 7 are without PSS, as they were found in subsequent studies, because they do not participate significantly in any of the critical modes. Rest of the generators assumed to have PSS. The uncoordinated and coordinated gains, and the dynamic compensator time constants of all the PSS are given below in tables 2.4 and 2.5. In both the cases the lead-lag time constants are same. For uncoordinated case, the gain values have been separately obtained for each of the two machines treating rest of the system as infinite bus and utilizing linearized analysis [2.12]. The coordinated gains are obtained by the proposed method as described in section 2.3.2.

Table 2.4. Uncoordinated PSS parameters (39-bus system)

Gen. No.	PSS gain	T_W sec	T_1 sec	T_2 sec	T_3 sec	T_4 sec
1	98.8	10	0.2	0.01	0.2	0.01
2	32.5	10	0.2	0.01	0.2	0.025
4	15.5	10	0.2	0.025	0.2	0.025
5	17	10	0.2	0.025	0.2	0.025
6	14	10	0.2	0.020	0.2	0.020
8	10.25	10	0.2	0.025	0.2	0.025
9	60.8	10	0.2	0.025	0.2	0.025

Table 2.5. Coordinated PSS parameters (39-bus system)

Gen. No.	PSS gain	T_W sec	T_1 sec	T_2 sec	T_3 sec	T_4 sec
1	47	10	0.2	0.01	0.2	0.01
2	38	10	0.2	0.01	0.2	0.025

4	57.5	10	0.2	0.025	0.2	0.025
5	62	10	0.2	0.025	0.2	0.025
6	68.22	10	0.2	0.020	0.2	0.020
8	35.25	10	0.2	0.025	0.2	0.025
9	110.8	10	0.2	0.025	0.2	0.025

With the above PSS values, eigen-value plots, participation factors analysis and transient response for a three-phase fault were studied. Eigen-value analysis for the 39-bus system at base operating point without any PSS shows that there are 6 unstable modes and 10 under-damped modes. Fig. 2.18 shows the unstable eigen-values of the system without considering PSS at the generators. The unstable eigen-values have positive real part. Fig. 2.19 shows the under-damped eigen-values (damping ratio less than 0.05) with out PSS considered at the generators. It is observed that the system is unstable and under-damped without considering the PSS at the generators. The figures 2.20 to 2.25 show the participation factors of the states of the system, which contribute significantly to the under-damped modes. There are 10 under-damped modes in the system. Figure 2.26 to 2.28 show the participation factors of the states contributing significantly to the unstable modes. There are 6 unstable modes.

A three-phase fault was applied at bus number 17 for 30ms and then the fault was cleared. The oscillations in the system after the fault was cleared were observed without PSS and with uncoordinated and coordinated PSS. Fig. 2.29 shows the angle plot of all the generators, without PSS, after the fault is cleared. It can be seen that oscillations are not damped out but the magnitude of oscillations increase with time. Fig. 2.30 shows the angle-plot of all the generators with uncoordinated PSS. The oscillations in this case are under-damped and the oscillations increase with time. Fig. 2.31 shows the oscillation of the angle with coordinated PSS. It can be seen that the oscillations are damped out in this case. Fig. 2.32 shows speed deviation of rotor with out PSS. Similar to the angle plot, in the speed deviation also the oscillations increase with time, with out PSS. Fig: 2.33 and 2.34 show the oscillations of the speed deviation of the rotor with uncoordinated and

coordinated PSS. Figs. 2.35, 2.36 and 2.37 show the oscillation in the tie line power without and with uncoordinated and coordinated PSS at the generators. The oscillations of the tie line power are under-damped with uncoordinated PSS and are damped out with coordinated PSS

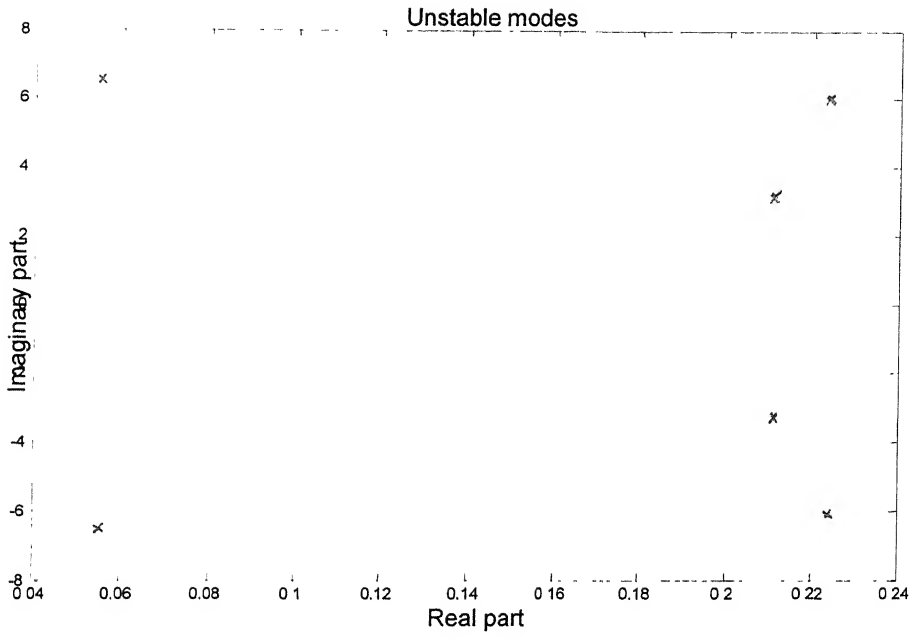

Fig 2.18: Unstable eigen value plot without PSS (39-bus system).

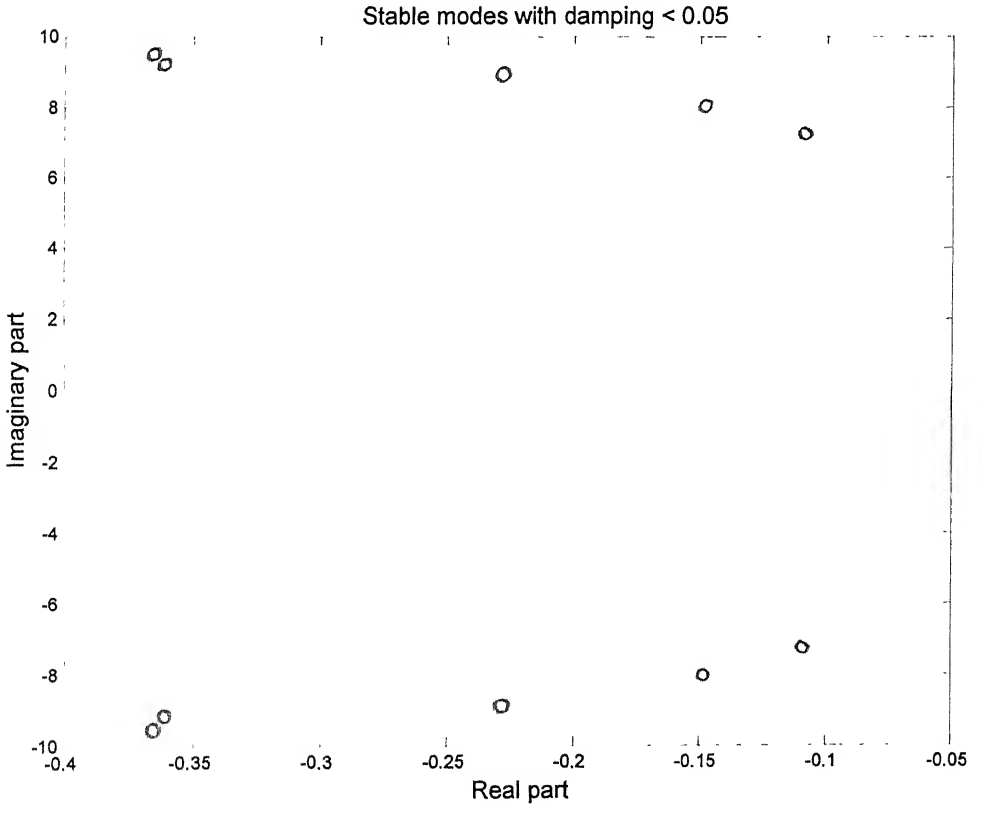

Fig 2.19: Under damped eigen values plot without PSS (39-bus system).

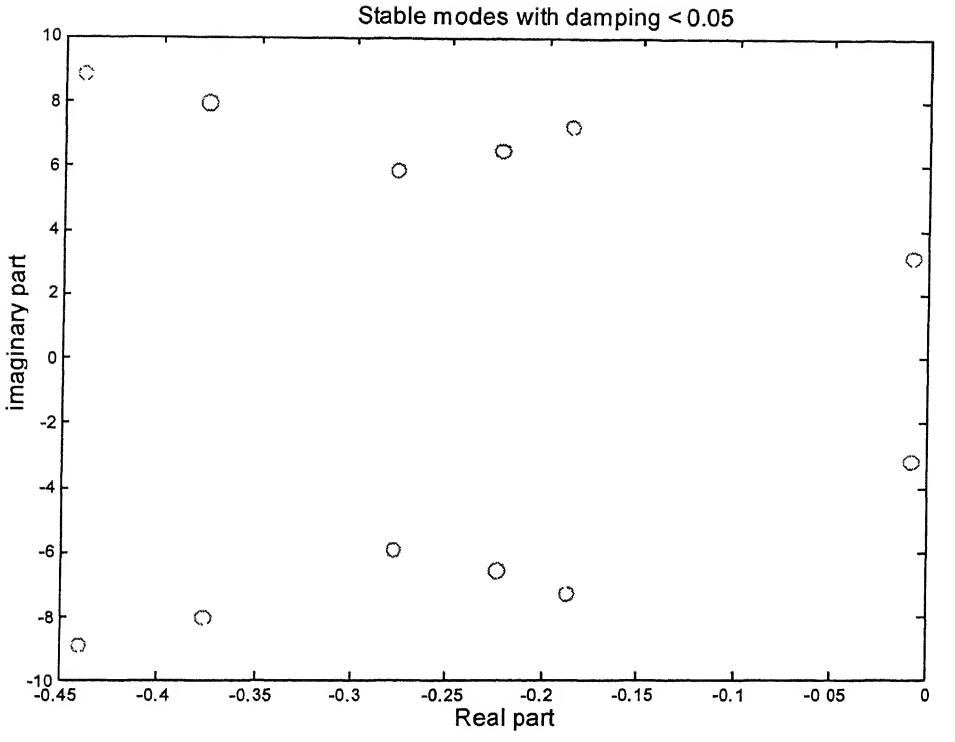

Fig 2.20 Under damped eigen values with uncoordinated PSS (39-bus system)

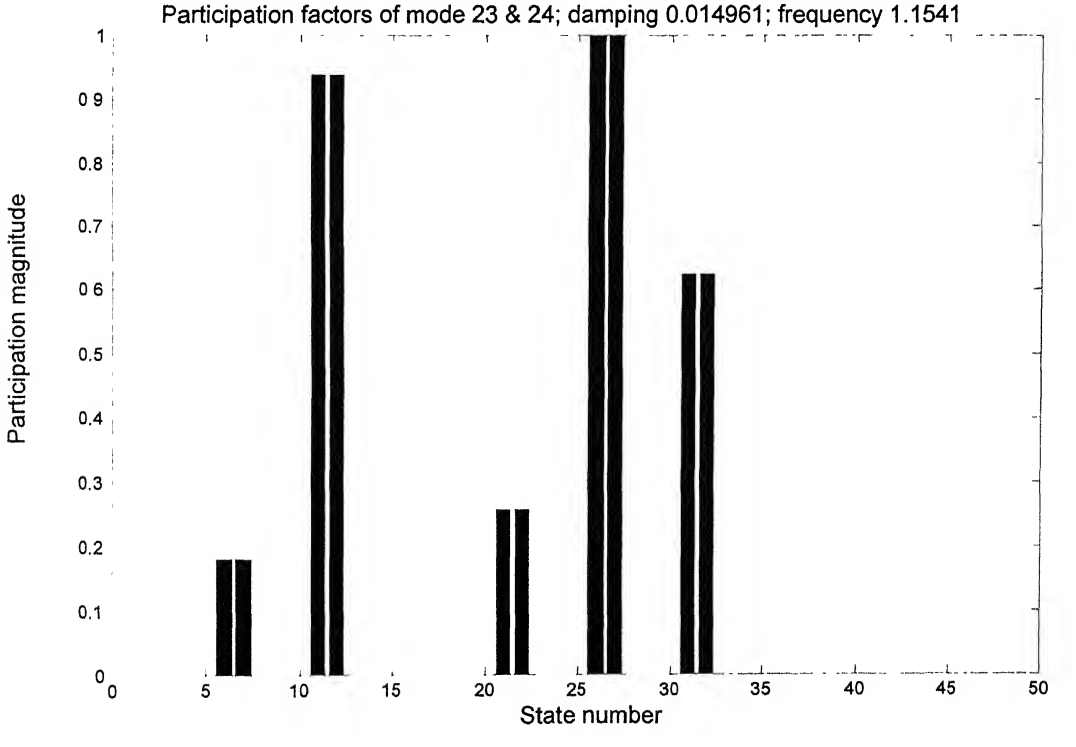

Fig 2.21: Participation factor of mode 23 & 24 (under-damped) (39-bus system)

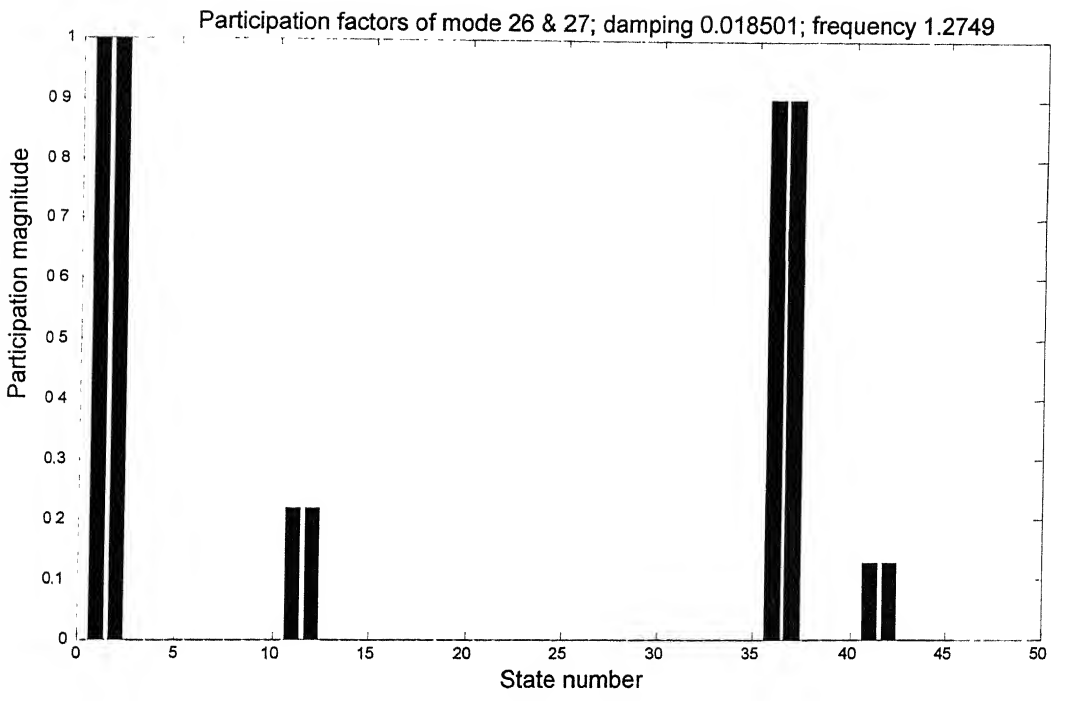

Fig 2.22: Participation factor of mode 26 & 27 (under-damped) (39-bus system)

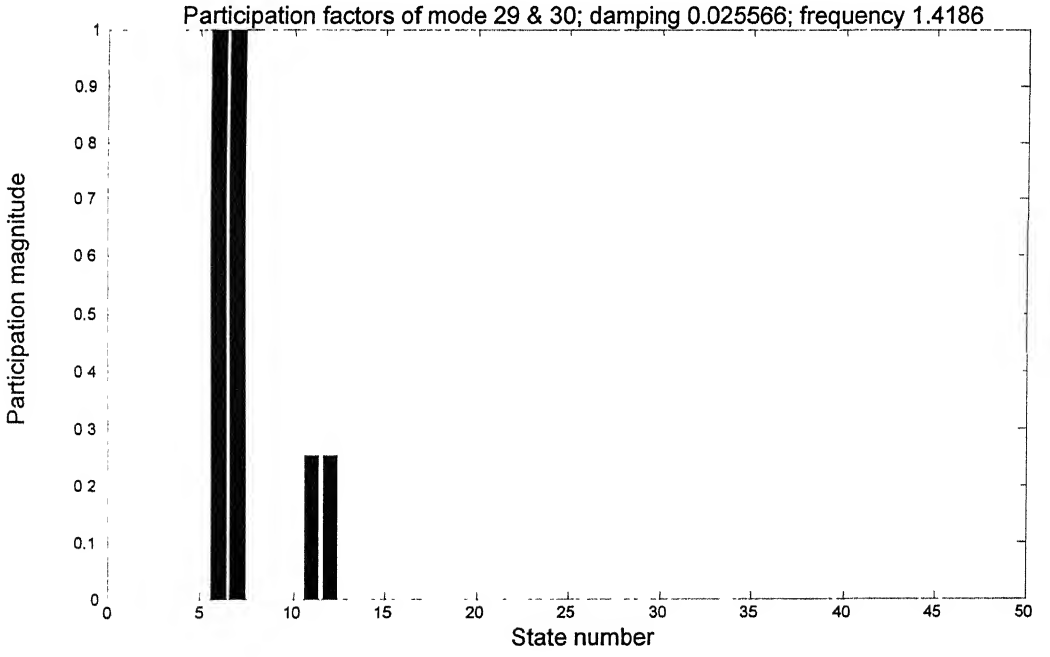

Fig 2.23: Participation factor for mode 29 & 30 (under-damped) (39-bus system)

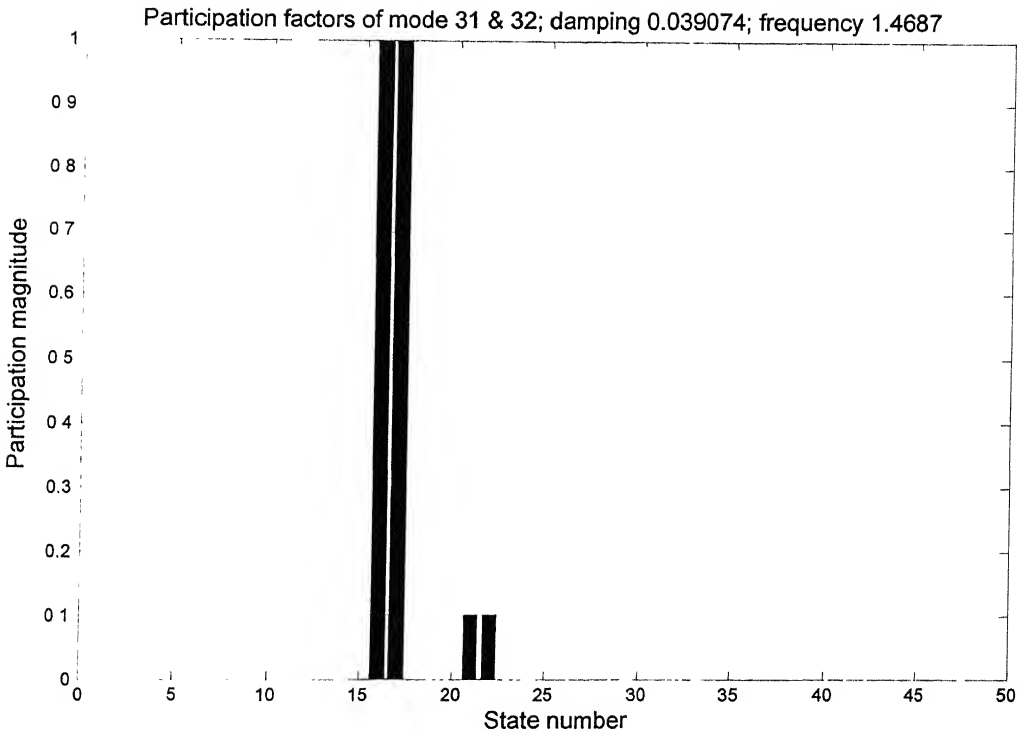

Fig 2.24: Participation factor for mode 31 & 32 (under-damped) (39-bus system)

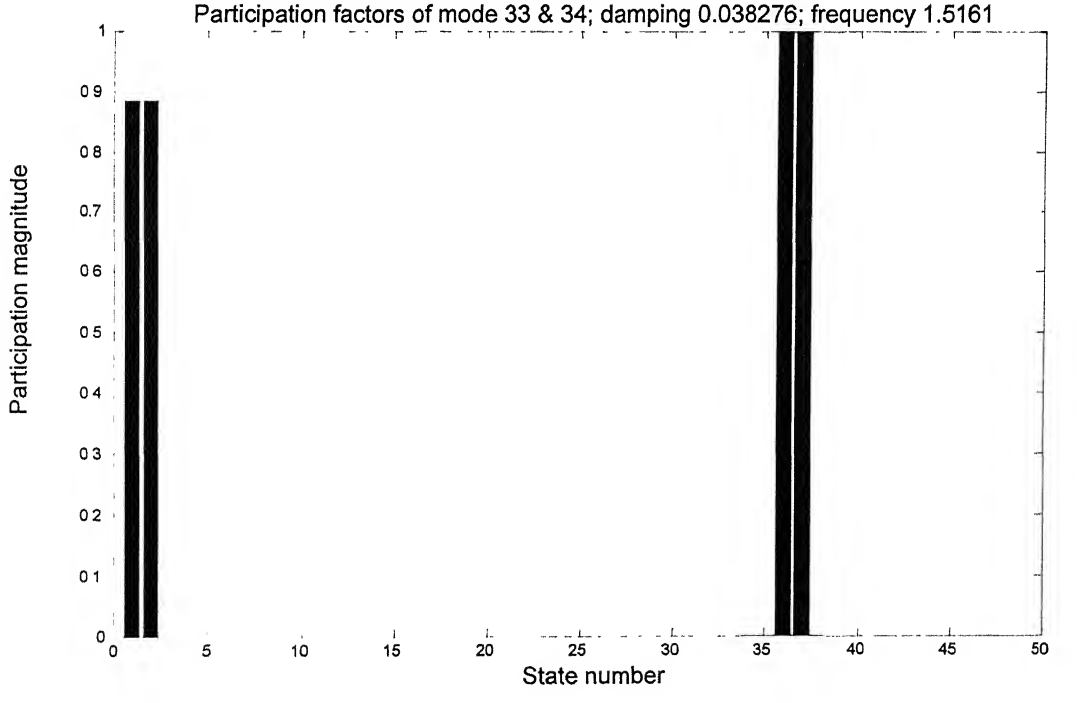

Fig 2.25: Participation factor for mode 33 & 34 (under-damped) (39-bus system)

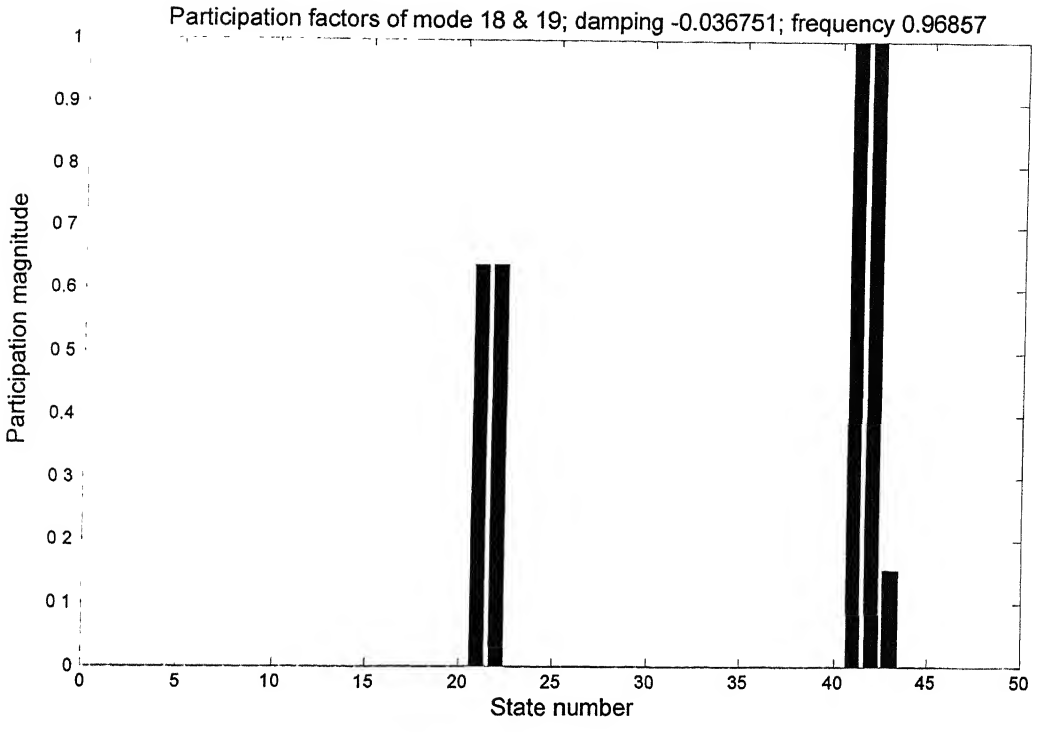

Fig 2.26: Participation f actor for mode 18 & 19 (unstable modes) (39-bus system)

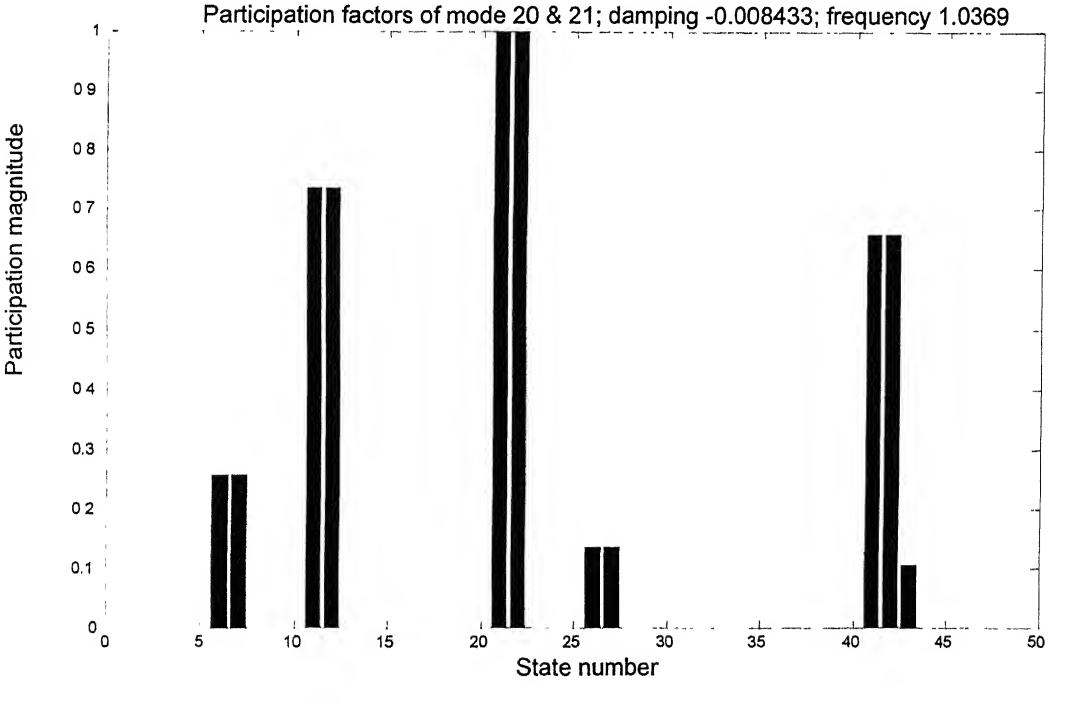

Fig 2.27: Participation factor for mode 20 & 21 (unstable modes) (39-bus system)

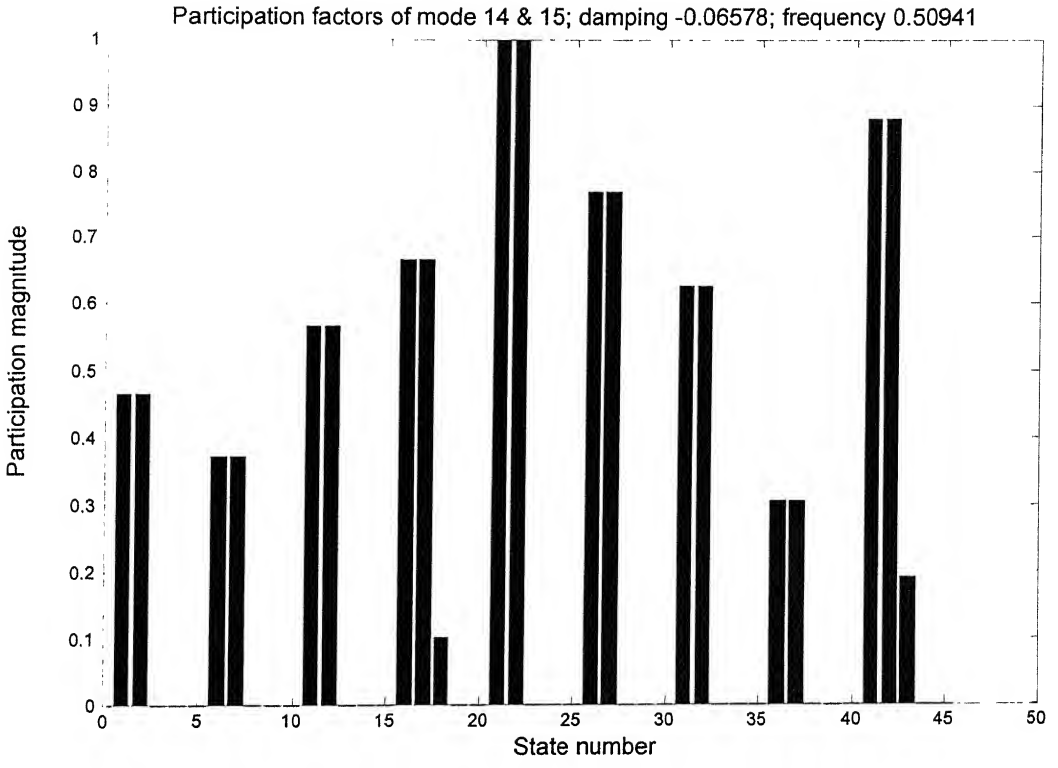

Fig 2.28: Participation factor for mode 14 & 15 (unstable modes) (39-bus system)

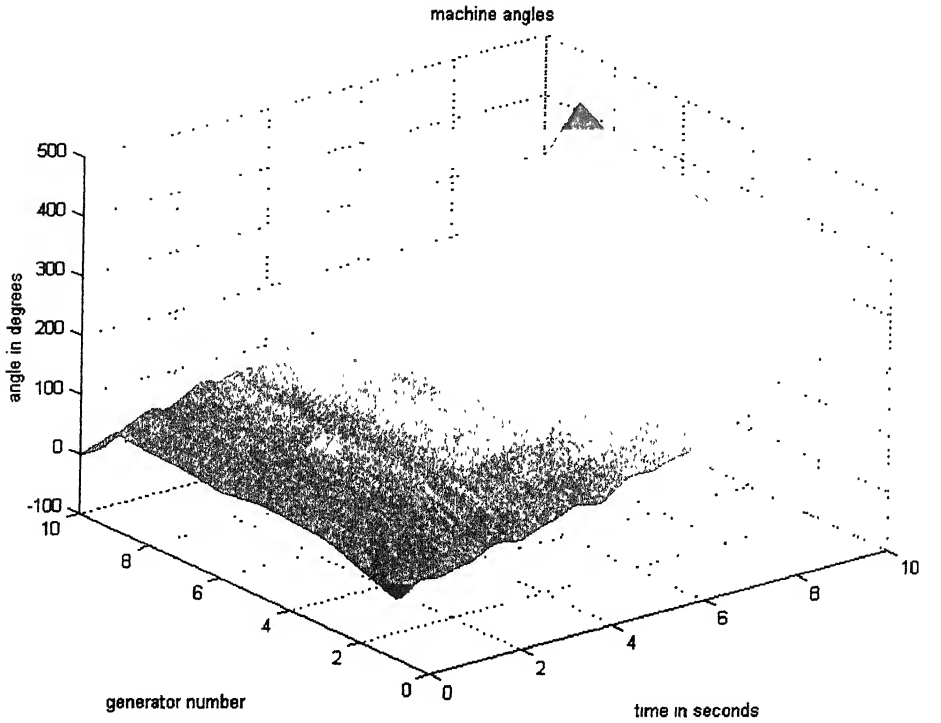

Fig 2.29: Angle-plot of the generators with out PSS (39-bus system)

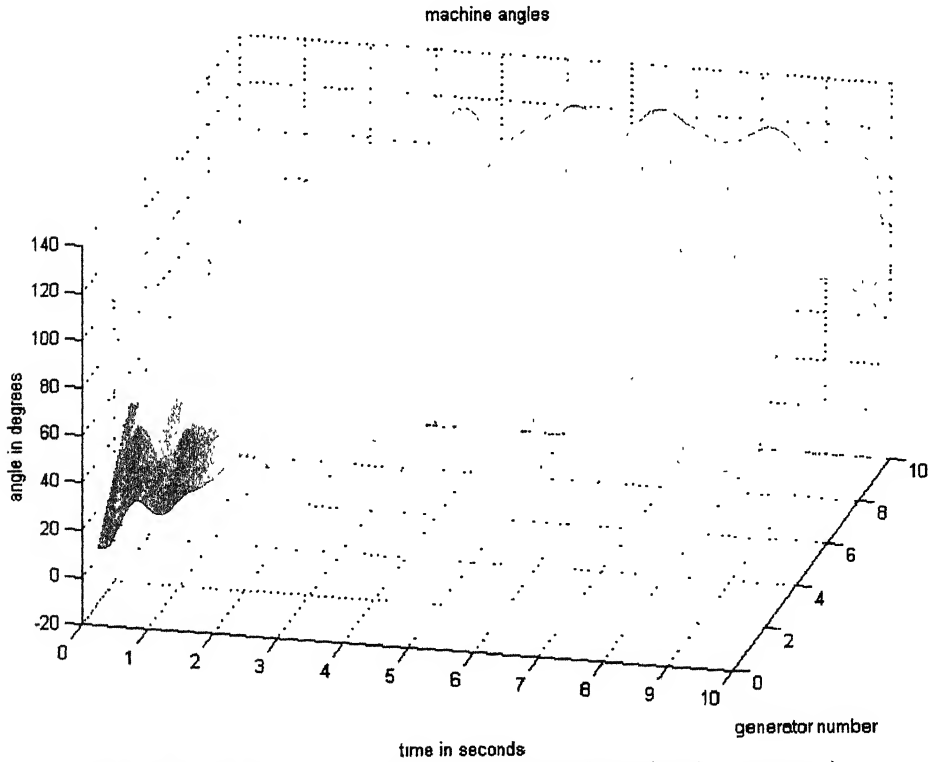

Fig 2.30 Angle-plot with uncoordinated PSS (39-bus system).

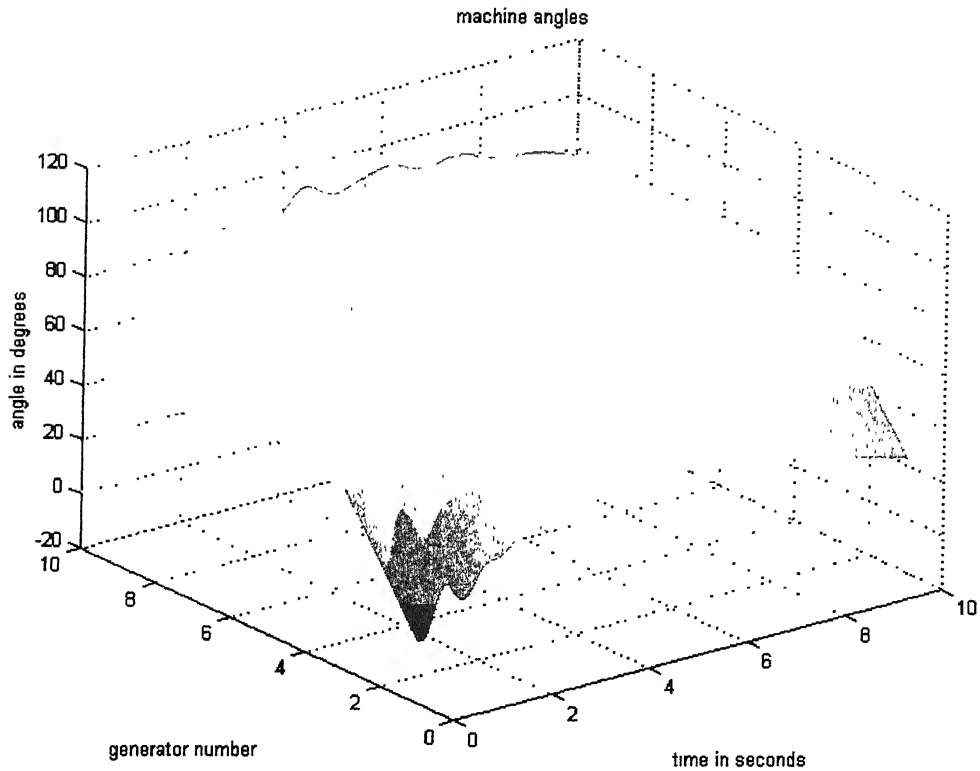

Fig 2.31: Angle-plot of the generators with coordinated PSS (39-bus system)

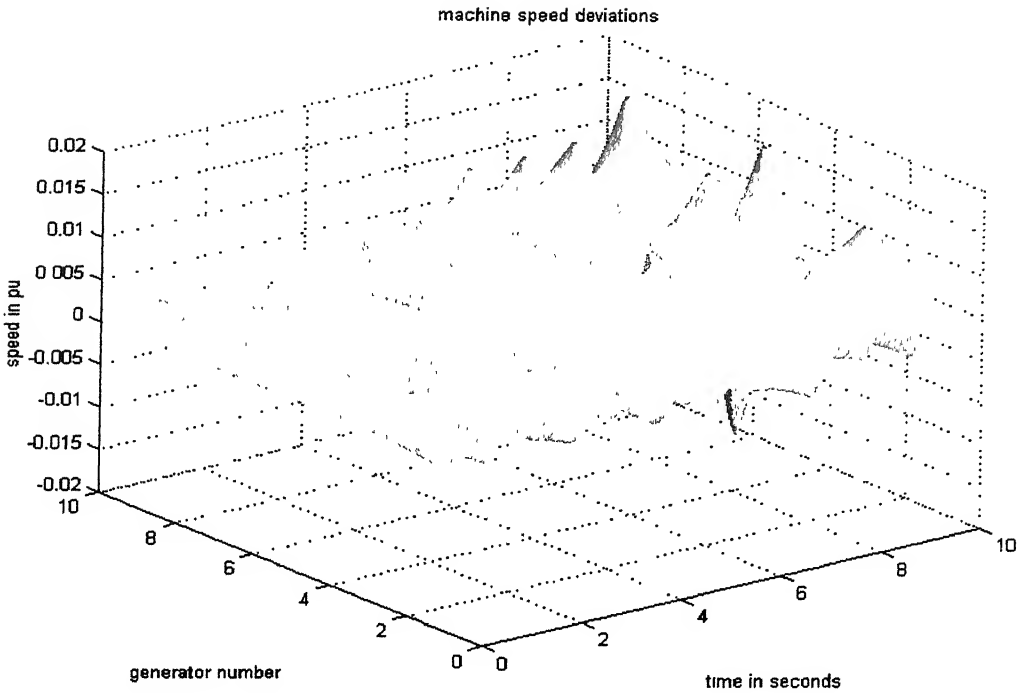

Fig 2.32: Speed deviation plot with out PSS (39-bus system)

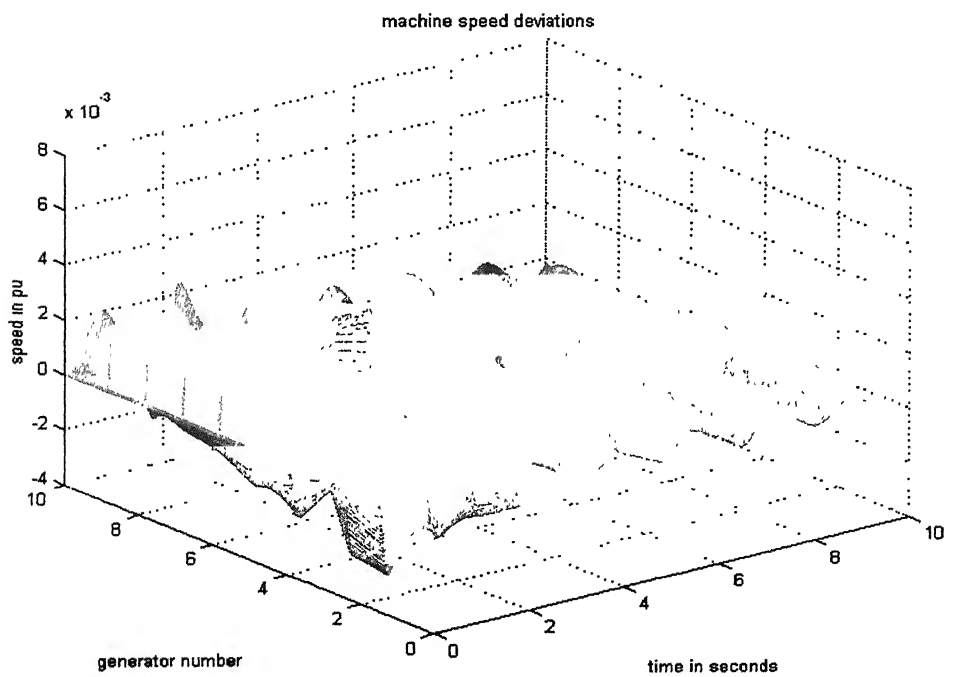

Fig 2.33 Speed-deviation plot with uncoordinated PSS (39-bus system)

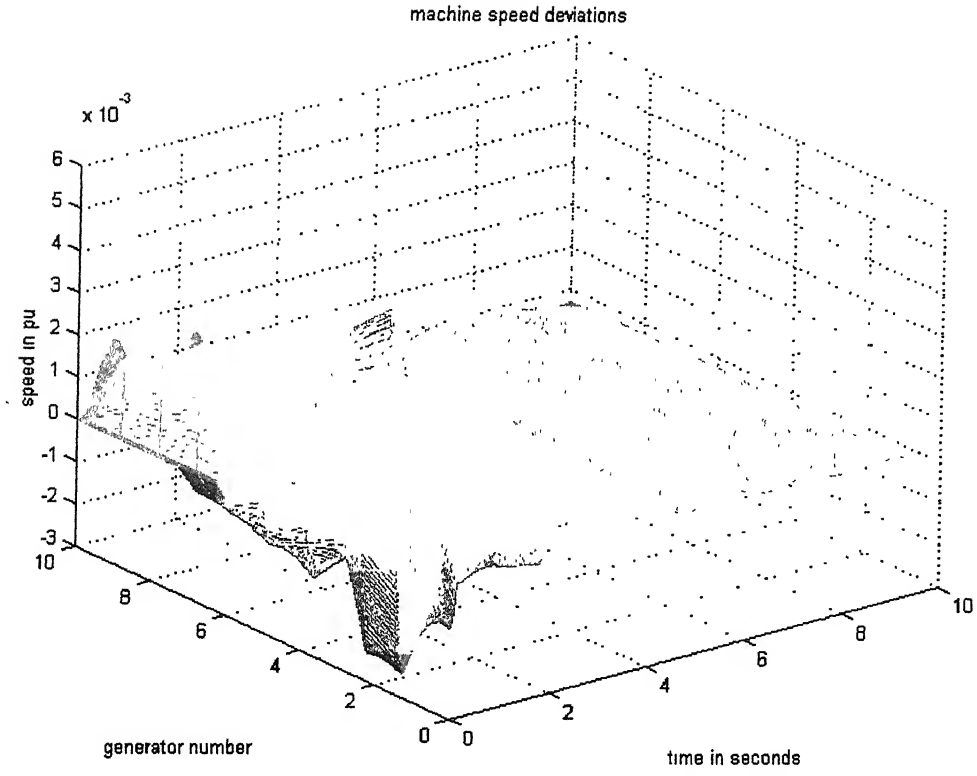

Fig 2.34: Speed deviation plot with coordinated PSS (39-bus system)

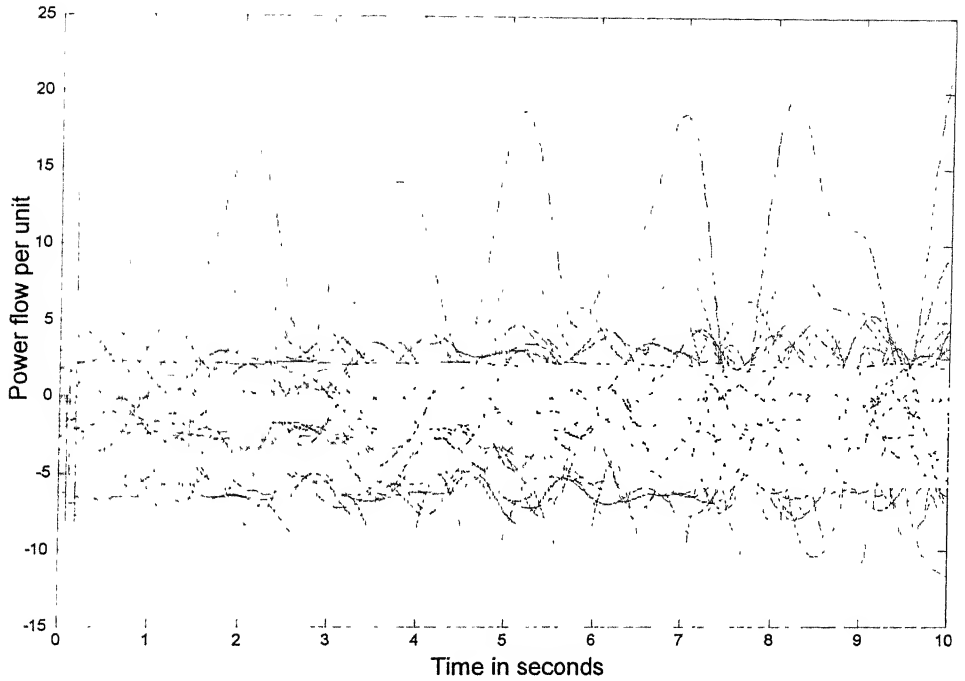

Fig 2.35: Line flows with out PSS (39-bus system).

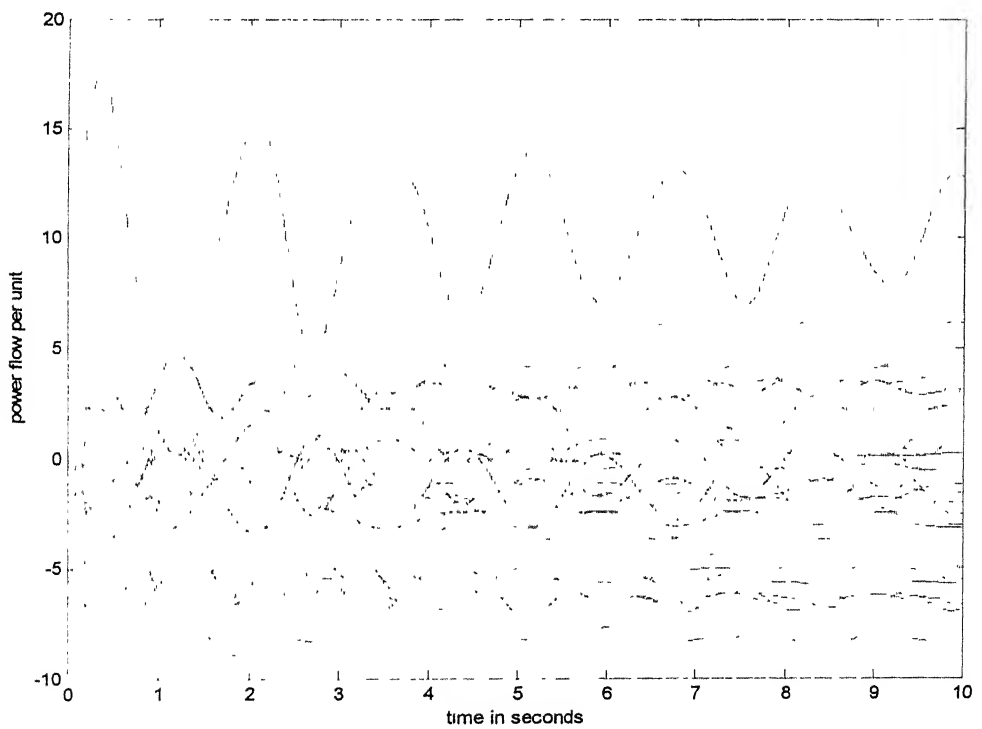

Fig 2.36 Line flows plot with uncoordinated PSS (39-bus system)

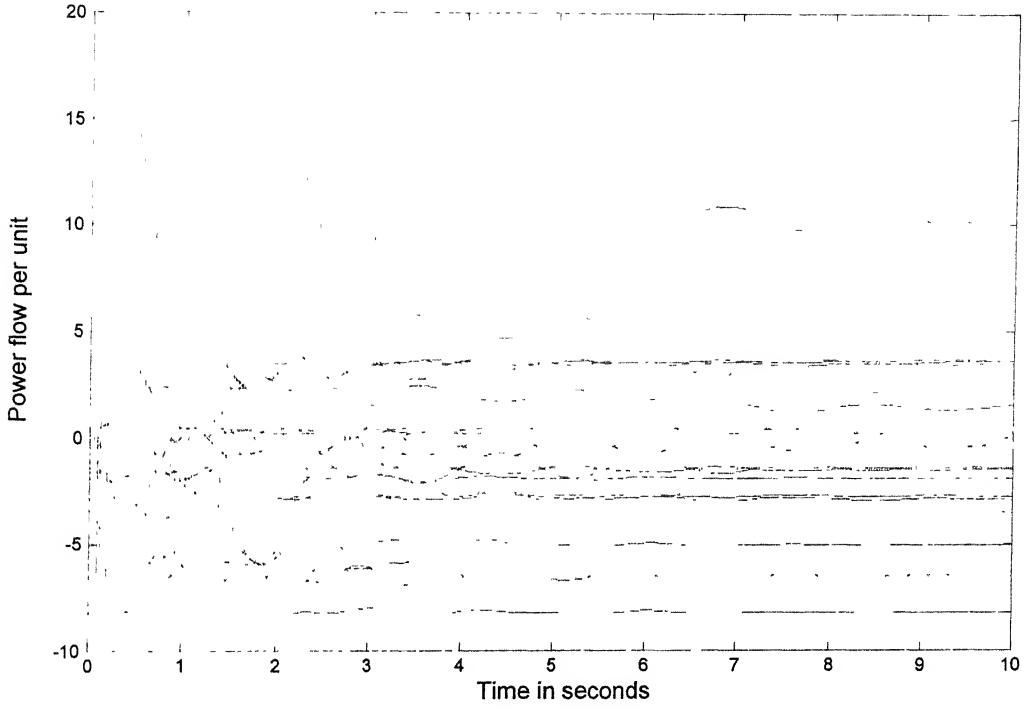

Fig 2.37: Line flows with coordinated PSS (39-bus system)

2.5 Conclusions

An optimal control strategy based on pseudo-decentralization approach has been proposed for obtaining coordinated values of PSS parameters. The proposed scheme is implemented on WSCC 9-bus system and New England 39-bus system. Linerazied eigen-value analysis as well as transient analysis has been carried out on the two systems to study the impact of PSS and coordination of its parameters on system stability. A there phase fault was applied in both the systems for 30ms seconds duration, to study the transient response.

The results obtained for both WSCC 9-bus and New England systems reveal the following:

1. In the 9-bus system, all the eigen-values have negative real parts for the cases without PSS, with uncoordinated PSS and with coordinated PSS. However, two modes in the case without PSS are under-damped (damping ratio less than 0.05). With both uncoordinated and coordinated PSS used at two of the generators, the system damping significantly improves. The later case provides slightly better damping.
2. The transient response in 9-bus system shows that the system is oscillatory unstable without PSS and becomes stable with uncoordinated and coordinated PSS.
3. The eigen-values of the 39-bus system have six unstable modes and ten under damped modes in case when no PSS was used. The unstable eigen-values are eliminated but 12 under damped modes remain with the use of uncoordinated PSS. However, system achieves all has stable modes with acceptable damping when coordinated PSS are used in the generator excitation loop.
4. The transient response in the case of the 39-bus system shows that the system remains unstable both without PSS and also with uncoordinated PSS cases. The system shows stable response with the coordinated PSS.

Chapter 3.

Coordination of Power system stabilizer and static VAR compensator stabilizer control parameters

3.1 Introduction

Flexible AC Transmission systems (FACTS) are popularly being used in the network to improve the system power transfer capability, provide effective voltage control, offer damping to the power system oscillations and, thus, improving the system transient and small signal stability. Among various FACTS controllers, static VAR compensator (SVC) has been extensively used by the power utilities in their network, which employ a supplementary control loop for damping the oscillations. Design of the damping control loop of the FACTS controllers is not as straightforward as that of the power system stabilizer. It is particularly difficult to attain robustness to large changes in operating conditions, as the position of poles and zeros of the transfer function of these FACTS controllers varies by large amount, when the operating condition of the system changes.

Stabilizing controls have been designed for FACTS controllers for the purpose of damping inter-area modes of oscillations [6]. The stabilizer loop placed into a properly designed static VAR compensator can be robust and more effective in damping the inter-area modes than the PSS placed at generators. The controllers have been designed using modal analysis as described in [3]. Only a limited research works are available in the literature, with respect to the coordination of control parameters of PSS and FACTS controllers [8,22]. These methods are based on calculating the impact of damping control loop of FACTS controller on the generator shaft. In this chapter, the optimal control strategy based on pseudo-decentralization, utilized for coordination of PSS in chapter-2, has been extended to SVC stabilizer loop and power system stabilizer parameters coordination.

The proposed method has been implemented on WSCC 9-bus and New England 39-bus systems. To verify the small signal stability of the system with SVC stabilizer and power

system stabilizer, a post fault condition is created by removing one of the lines and then a step change has been applied to all the inputs to observe the small signal stability.

3.2 Static Var Compensator

Static VAR Compensator (SVC) is a shunt-connected static Var generator or absorber, whose output is adjusted to exchange capacitive or inductive current as to maintain or control specific parameters of the power system (typically bus voltage).

SVC, thus, regulates the system voltage by injecting required amount of reactive power (Var) in the system. It includes separate equipments for supplying leading and lagging Vars. A typical scheme consists of thyristor-controlled reactors (TCR) for absorbing reactive power and thyristor switched capacitor (TSC) banks for supplying the reactive VAR as shown in fig. 3.1. Depending upon the size and requirement of VAR support, it may also include fixed or mechanically switched capacitors and reactors. For smooth voltage control, the rating of the TCR is slightly higher than that of a discrete TSC or fixed Capacitor – (FC) block. The harmonic filters employed in the SVC are capacitive at fundamental frequency, supplying reactive power of the order of 10-30% of the TCR rating.

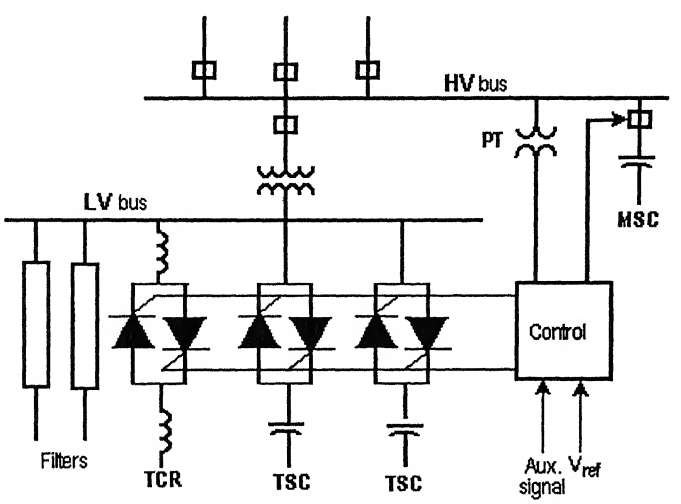

Fig 3.1 A Typical SVC Scheme

When a bus voltage drops below a desired value, the value of required capacitive current is determined. Assuming that the TCR is at minimum (zero) conductance level, the

capacitor has to be switched for Var generation. Transient free switching of the TSC is achieved if it is switched at certain instants. When the residual voltage across the capacitor is lower than the system peak voltage, it should be switched at the instant when the system voltage equals the capacitor voltage. When the residual capacitor voltage is larger than the system peak voltage, it should be switched at the instant of occurrence of the peak voltage. In both the cases, the voltage appearing across the thyristor at the instant of firing is minimum. If the voltage starts rising, the TCR conduction period is increased so that it results in an increase in Var consumption and voltage rise is controlled.

In the active control range, the susceptance (B_{svc}), and hence the reactive current, is varied according to the voltage regulation slope characteristics (Fig. 3.2). The slope value depends upon the desired voltage regulation, the desired sharing of reactive power among various sources and other needs in the system. Typically, it varies between 1-5%. It behaves like a shunt capacitor of maximum value (B_{Csvc}) at the capacitive limit, and as fixed shunt reactor at minimum value ($-B_{Lsvc}$) corresponding to the inductive limit. The limits are reached when there are large variations in the bus voltage. Inductive limit is reached when the bus voltage exceeds the upper limit, and the capacitive limit when it falls below the lower limit.

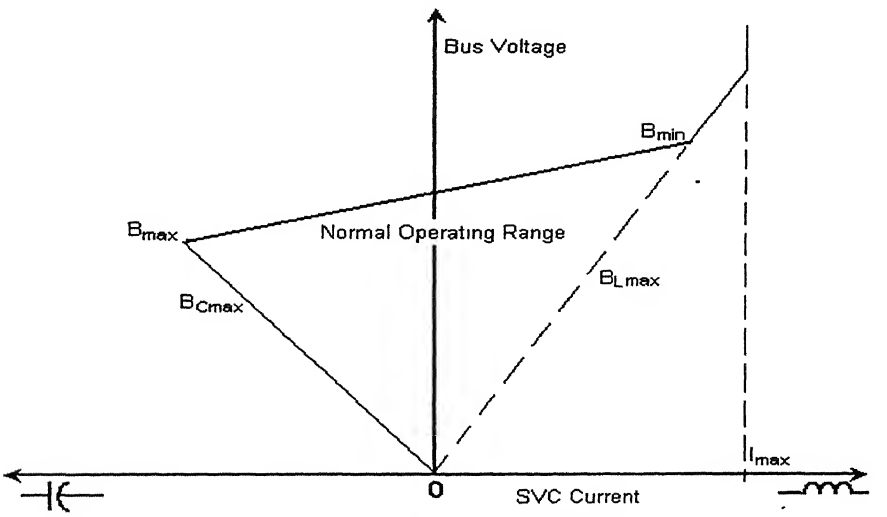

Fig. 3.2 SVC Output characterics

3.3 Dynamic Model of SVC

Fig. 3.3 gives a block diagram representation of IEEE Type-1 benchmark model of the SVC, taken from refs [12-14]. The measurement module for sensing the voltage and converting it into dc feedback signal has been ignored as it has small time constant. Further, in this work, the upper and lower limits of the SVC have been ignored. The gain, K_R, is the reciprocal of the slope setting. K_R is usually between 20 per unit (5% slope) and 100 per unit (1% slope) at the SVC base. The regulator time constant, T_r is usually between 20 and 150 milliseconds.

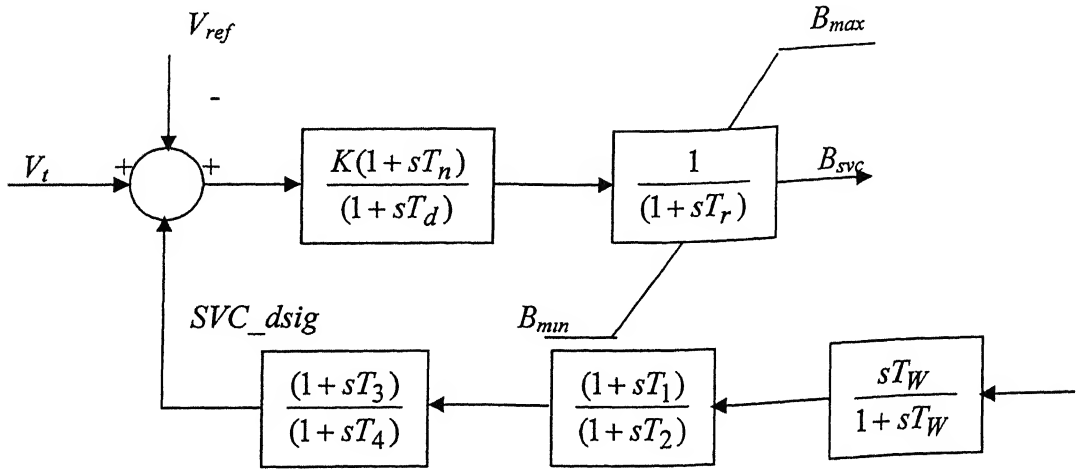

Fig 3.3: Block diagram of SVC with supplementary controller

The time constant T_n is due to the time lag in the application of firing pulses corresponding to the new value of B_{svc}. T_d is the firing circuit time constant representing the effect of firing sequence and is typically of the order of 3 – 6 ms. The limits B_{max} and B_{min} correspond to the upper and lower limits of the SVC. The SVC dynamics can be described by the following equations:

$$T_r \dot{B}_{SVC} = K(V_{ref} - V_t + V_{SVC\_dsig}) - B_{svc} \cdot \tag{3.1}$$

Reactive power balance equation at a SVC bus '*m*' can be written in a modified form as follows:

$$Q_m = V_m \sum_{k=1}^{n} Y_{mk} V_k \sin(\theta_m - \theta_k - \alpha_{mk}) - V_m^2 \cdot B_{svc} \qquad \text{....(3.2)}$$

To include the power balance equations at SVC node in the static load-flow, the elements of the corresponding diagonal elements of the sub-matrix J_4 of Newton-Raphson loadflow Jacobian, $[J]=\begin{bmatrix} J1 & J2 \\ J3 & J4 \end{bmatrix}$ can be modified as:

$$J4(m,m) = J4(m,m) - 2 \cdot V_m K_R \left(V_{ref} - \tfrac{3}{2} V_m\right) \qquad \text{.....(3.3)}$$

$$\text{where, } [J4] = \frac{\partial Q_m}{\partial V_m} . V_m \Big|_{(V,\theta)}$$

The eigen value analysis of the complete system Jacobian derived from the differential algebraic equations has been used for the optimal placement of SVC. The critical eigen-value, i.e. the one closest to the imaginary axis on the negative half of the complex plane, was determined and the corresponding participation factors were computed. The participation factors corresponding to only the bus voltage variables were selected and the bus having the maximum participation factor in most of the cases was selected for the placement of SVC.

A block diagram of SVC supplementary control loop (SVC_stab) for damping the oscillations is shown in fig. 3.4. The output of this stabilizer loop is the *SVC_dsig* signal, also shown in fig. 3.3.

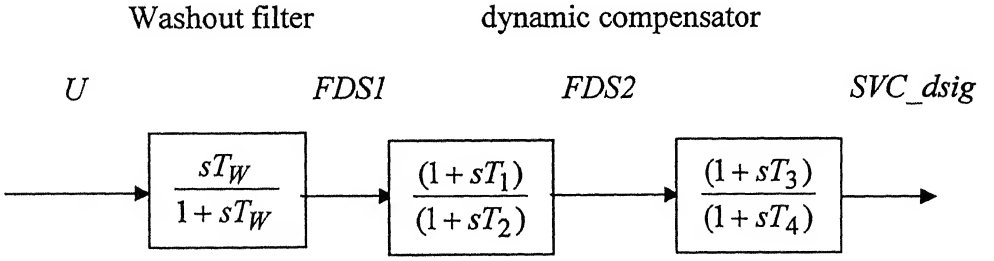

Fig 3.4: The block diagram of SVC_stab

The SVC stabilizer has the same structure as a power system stabilizer. They must respond only to the transient variations and not to the DC offset. For this purpose, a washout filter has been used. A dynamic compensator (lead network compensator) has been used, similar to the power system stabilizer. The dynamic equations of the SVC stabilizer with U as the input signal are:

$$\Delta\dot{FDS}1 = \Delta\dot{U}_t - \frac{1}{T_w}\Delta FDS1$$

$$\Delta\dot{FDS}2 = \frac{1}{T_2}\Delta\dot{U}_t - \frac{1}{T_2}\left(1-\frac{T_1}{T_w}\right)\Delta FDS1 - \frac{1}{T_2}\Delta FDS2$$

$$\Delta\dot{SVC}\_dsig = \frac{T_3}{T_4}\frac{1}{T_2}\Delta\dot{U}_t - \frac{T_3}{T_4}\frac{1}{T_2}\left(1-\frac{T_1}{T_w}\right)\Delta FDS - \frac{T_3}{T_4}\frac{1}{T_2}\Delta FDS2 - \frac{1}{T_4}\Delta SVC\_dsig \qquad (3.4)$$

3.4 Tuning of the PSS and SVC stabilizer parameters

The parameters of the dynamic compensator block of the SVC stabilizer must be tuned. For this purpose, an input signal to the SVC stabilizer loop is to be selected. The procedure for selecting the input signal and the time constants of dynamic compensator [6] is given below.

Taking a simple structure for the J^{th} stabilizer of the form

$$M_J(S) = K_J(S)Q_J(s) = K_J\left(\frac{1+ST_{1J}}{1+ST_{2J}}\right)^{PJ} \qquad (3.5)$$

A locally variable signal is supplied to stabilizer J_i its output signal is fed to the summing point of the SVC modal (Fig 3.3). Assuming that these signals correspond to the m^{th} output and q^{th} input of the state-space model, it may be shown [3] that at the modal frequency λ_h.

$$\frac{\partial\lambda_h}{\partial M_J(\lambda_h)} = r^h_{mq} \qquad (3.6)$$

3.5 Simulation results

The proposed optimal control strategy with pesudo-decentralization for coordination of SVC stabilizer and PSS has been implemented on WSCC-9 bus system and New England 39-bus systems. The line diagram and the system data for the two cases are given in the Appendix A & B. The results obtained on the two systems are as follows.

3.5.1 WSCC 9-bus system

In case of WSCC 9-bus system, a SVC is already present at bus-5. Coordination of the stabilizer loop of the SVC with a PSS at generator-2 was studied. The input signal to the SVC_stab was selected as described in section 3.4 [6]. The residues of different input signals, corresponding to the generator 2, for the SVC stabilizer are given below in table 3.1.

Table 3.1 the residue of different input signals

Internal angle	Terminal voltage	Speed
0.2749	0.0188	0.0074

Since the internal angle of the generator-2 has the highest residue magnitude, it was taken as the input signal to the SVC stabilizer loop. The coordination of the PSS and SVC_stab parameters has been done as described in section 2.3.1 [4,6]. The coordinated parameters of the PSS and SVC_stab are given below in table 3.2.

Table 3.2 Coordinated values of parameters of SVC_stab and PSS:

	Gain	T_W sec	T_1 sec	T_2 sec	T_3 sec	T_4 sec
PSS	3.089	10	0.4	0.03	0.4	0.03
SVC_stab	0.044	10	2.6483	0.2666	2.6483	0.2666

Eigen-value analysis for the base case condition of the 9-bus system shows that there are two under-damped eigen-values (damping ratio less than 0.05) with out considering PSS & SVC_stab. Figure 3.5 gives the plot of the under-damped Eigen-values of the system. The participation factors of the states significantly contributing to the under-damped modes are plotted in Fig 3.6. The normalized participation factors are shown on the Y-axis and the different states on the X-axis. The Eigen-values of the power system without the PSS and SVC_stab (with damping ratio greater than 0.05) are shown in Fig. 3.7. The Eigen-values of the system with the PSS and SVC_stab are shown in fig. 3.8. Fig. 3.8 clearly shows that the eigen-values significantly move towards left half of s-plane when the PSS and SVC_stab with coordinated parameters are placed in the system.

For transient analysis, a post fault condition was simulated by removing a line (line between bus 7-8). A step input of 0.01 p.u. was given to the system to perturb the system. The oscillations of the system without the PSS and SVC_stab are shown in fig. 3.9. The oscillations of the system are damped out in this case. The oscillations with the PSS and SVC_stab are shown in fig: 3.10. Even though, the oscillations are damped out without the PSS and FDS, the magnitude and time of settling of the oscillations are more as compared to that with coordinated parameters of PSS and SVC_stab.

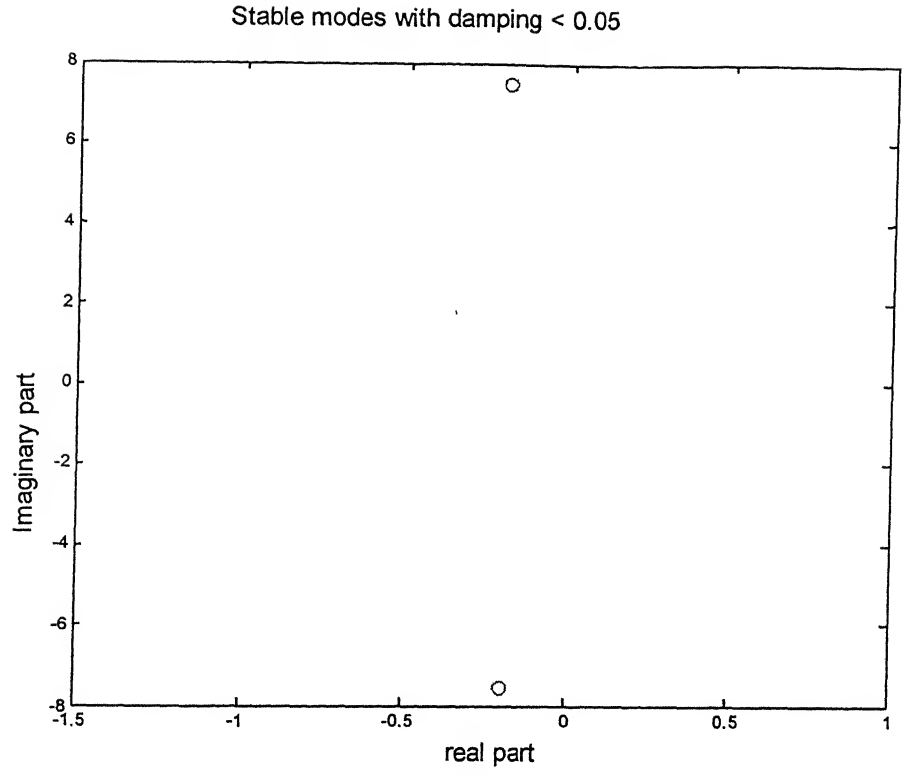

Fig 3.5 Plot of the under-damped Eigen values (9-bus system)

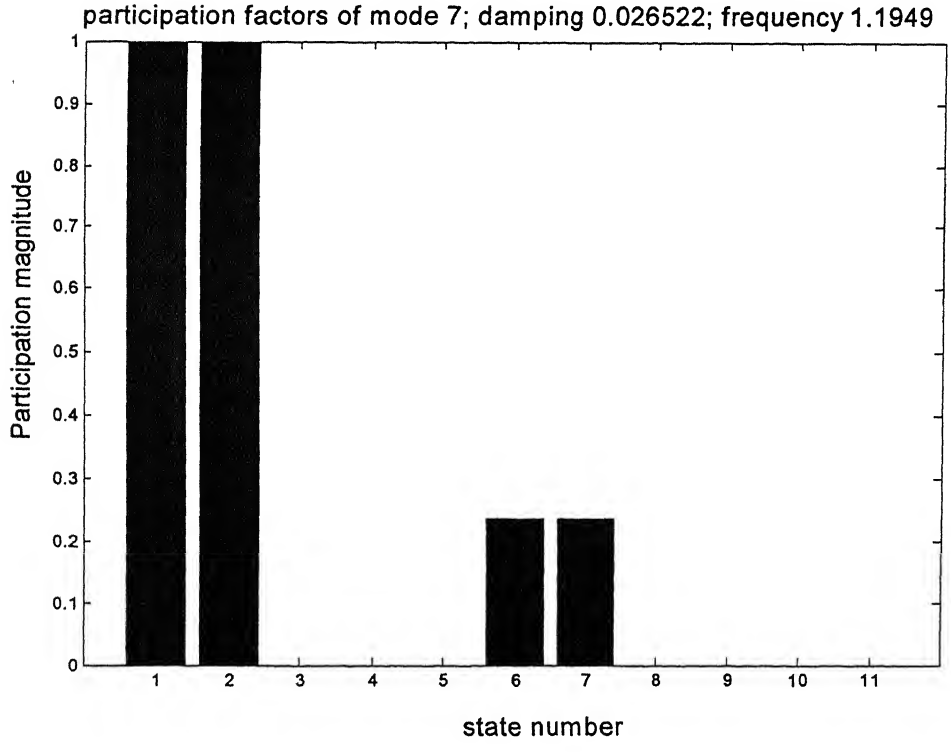

Fig 3.6 participation factors for the under damped Eigen values (9-bus system)

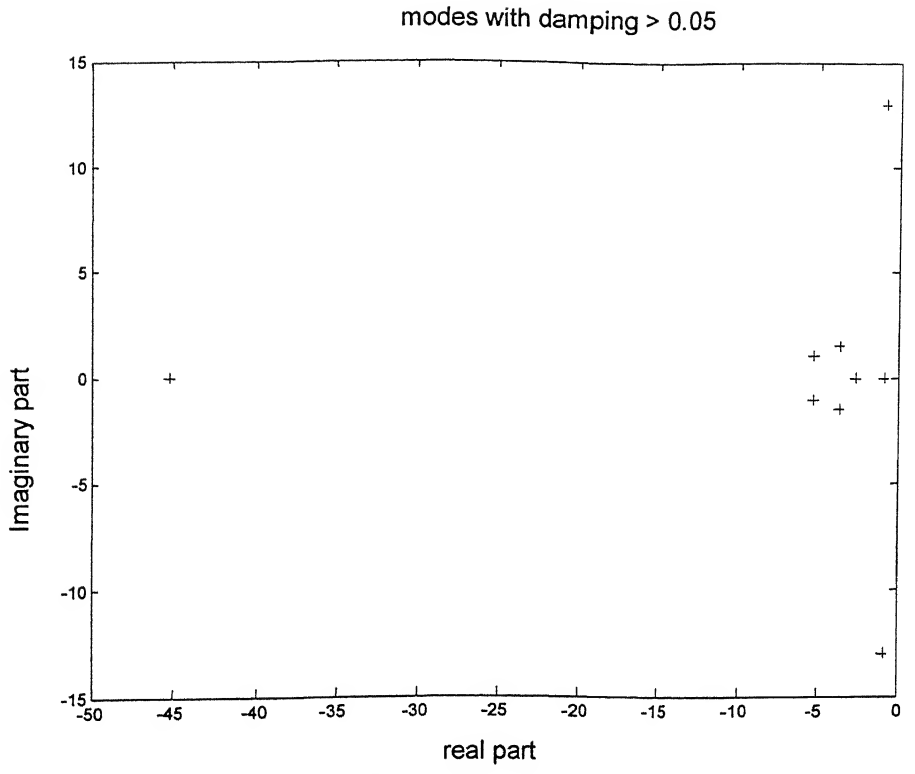

Fig 3.7 Eigen values of the system with out PSS & SVC_stab (9-bus system)

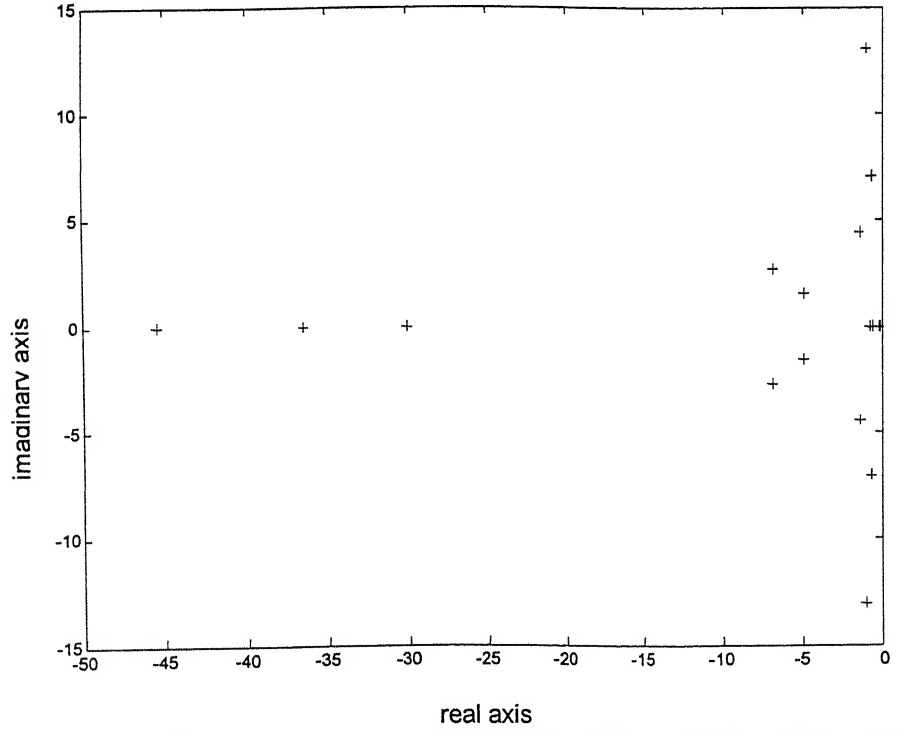

Fig 3.8 the Eigen values of the system with PSS and SVC_stab (9-bus system)

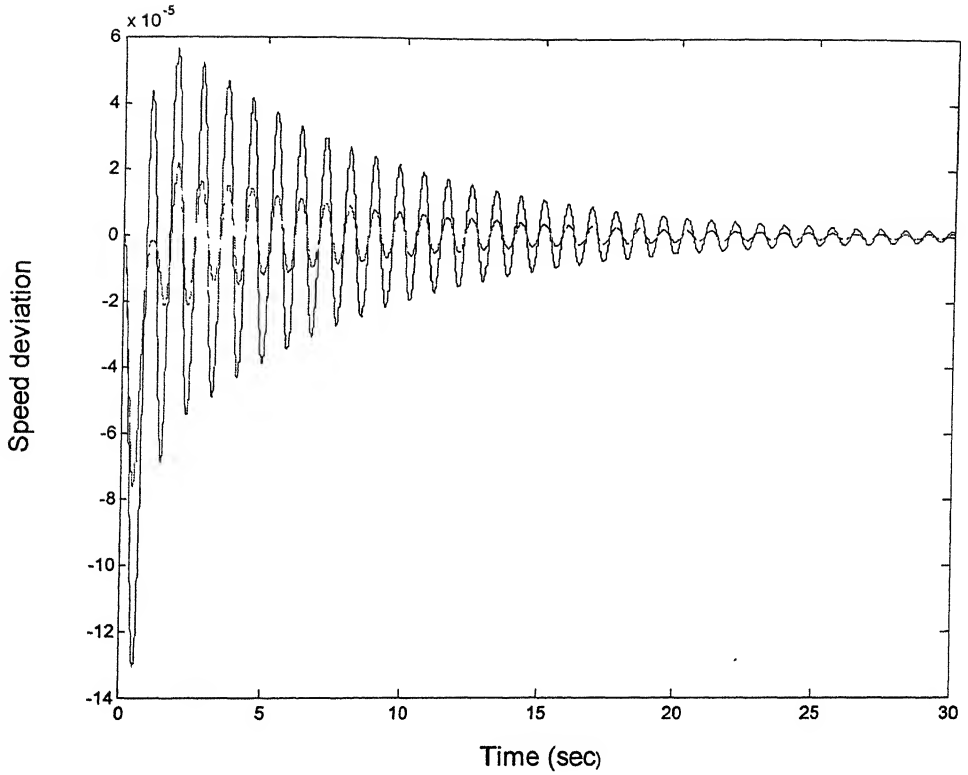

Fig 3.9 Speed deviation oscillations with step input, with out PSS & SVC_stab (9-bus system)

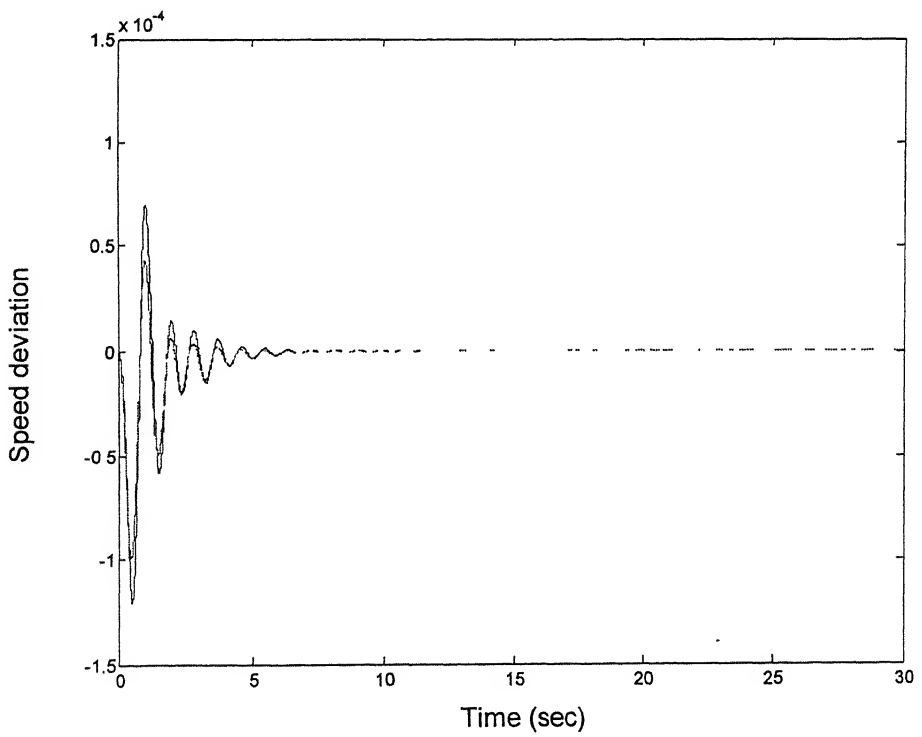

Fig 3.10 Speed deviation oscillations of the system with step input, with PSS&SVC_stab (9-bus system)

3.5.2 New England 39-bus system

This system, in the base case, does not have any SVC. For optimal placement of SVC, participation analysis corresponding to the most critical eigen value was carried out. The voltage participation factors corresponding to the critical eigen value are given in the table 3.3. It is observed that bus 19 has the maximum participation in the critical mode and hence, it was selected for the placement of SVC.

Table 3.3 Voltage Participation factors

Bus	21	15	16	11	17	18	19
PF	0.0190	0.0216	0.0220	0.0229	0.0231	0.0235	0.0257

The input signal to the SVC_stab selected as described in section 3.4 [6]. The residues of the different input signals, corresponding to the generator 10, for the SVC_stab are given below in table 3.4.

Table 3.4 the residues of different input signals

Internal angle	Terminal voltage	Speed
0.029	0.0012	0.00439

Since the internal angle has the highest residue magnitude, it is taken as the input signal to the SVC stabilizer. Hence, the internal angle of the generator of machine 10 is considered as the input signal. The coordination of the PSS and FDS is done as described in section 2.3.1 [4,6]. The coordinated parameters of the PSS and FDS are given below in table 3.5.

Table 3.5 the coordinated parameters of the PSS and SVC_stab

	Gain	T_W sec	T_1 sec	T_2 sec	T_3 sec	T_4 sec
PSS	58.9	10	0.2	0.025	0.2	0.025
FDS	0.044	10	3.870	0.625	3.870	0.625

The Eigen-value analysis at the base case of the 39-bus shows that there are 6 unstable modes. The unstable modes have eigen-values with positive real part and they make the system unstable. Figure 3.11 shows the unstable Eigen-values of the system with out the PSS and SVC_stab. There are 10 under-damped modes (damping ratio less than 0.05). Fig. 3.12 shows the under-damped eigen-values. The participation factors of the states significantly contributing to the unstable modes are shown in figs. 3.13 to 3.15. The participation factors of the states significantly contributing to the under-damped modes are shown in the fig. 3.16 to 3.20. The eigen values of the system without the PSS and SVC_stab are shown in fig. 3.23 and the eigen-values with the PSS and SVC_stab are shown in fig. 3.24. It can be observed that the eigen values of the system with coordinated parameter of PSS and SVC_stab have moved to the left half of the s-plane significantly, as compared to the eigen-values without PSS and SVC_stab.

A post fault condition was simulated by removing a line (in this case line between bus 7-8). A step input of 0.01 p.u. was given to the system to perturb the system. The oscillations of the system without the PSS and SVC_stab are shown in fig. 3.21. The oscillations of the system do not damp out in this case and the magnitude of oscillations increases with time. The fig 3.22 clearly shows that the oscillations damp out rapidly with the coordinated parameters of PSS and SVC_stab.

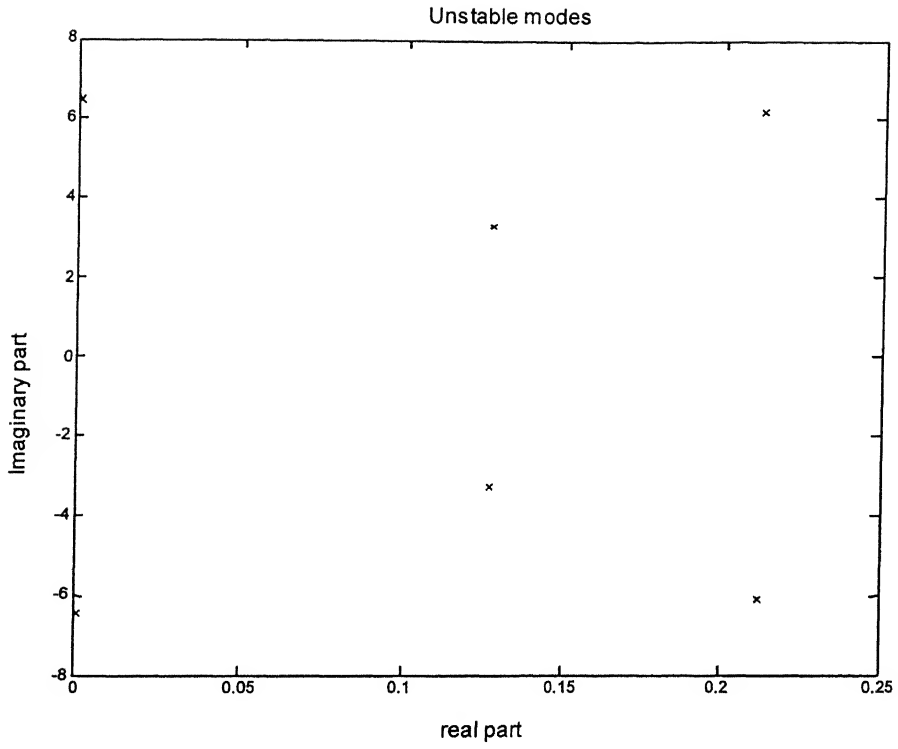

Fig 3.11 Unstable modes of the 39-bus system

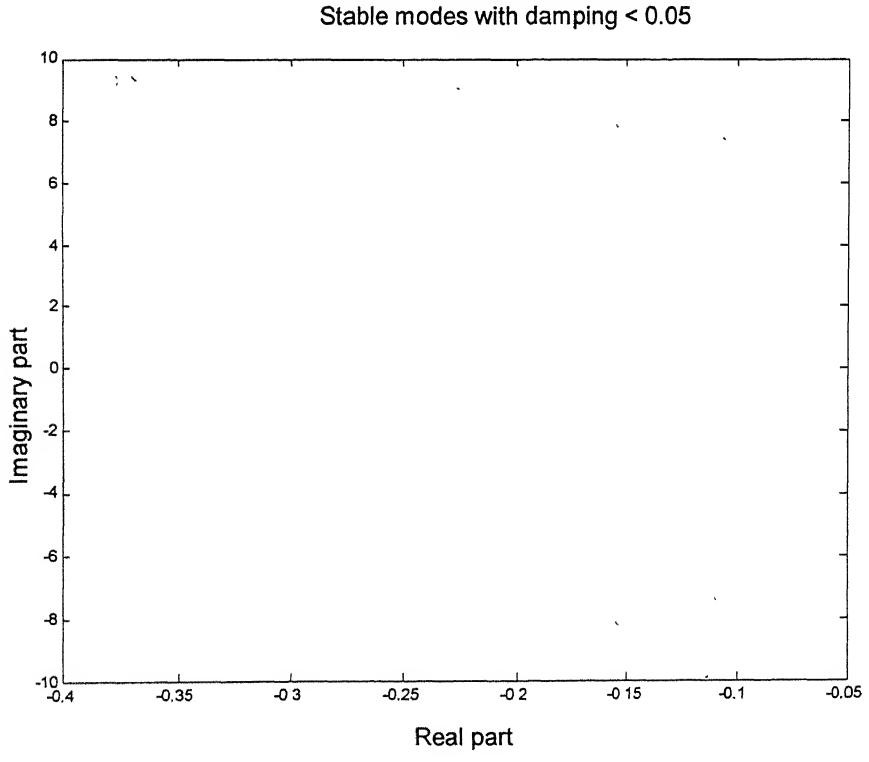

Fig 3.12 Under damped Eigen values of the system (39-bus system)

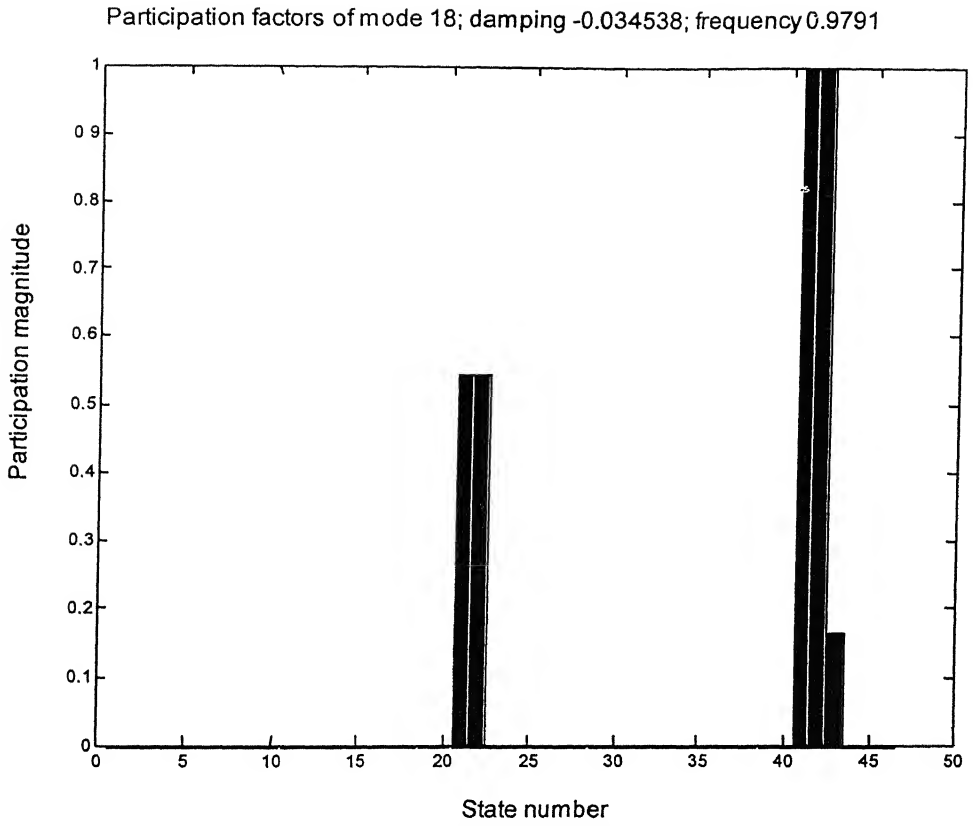

Fig 3.13 Participation factor of the mode 18 & 19 (Unstable modes) (39-bus system)

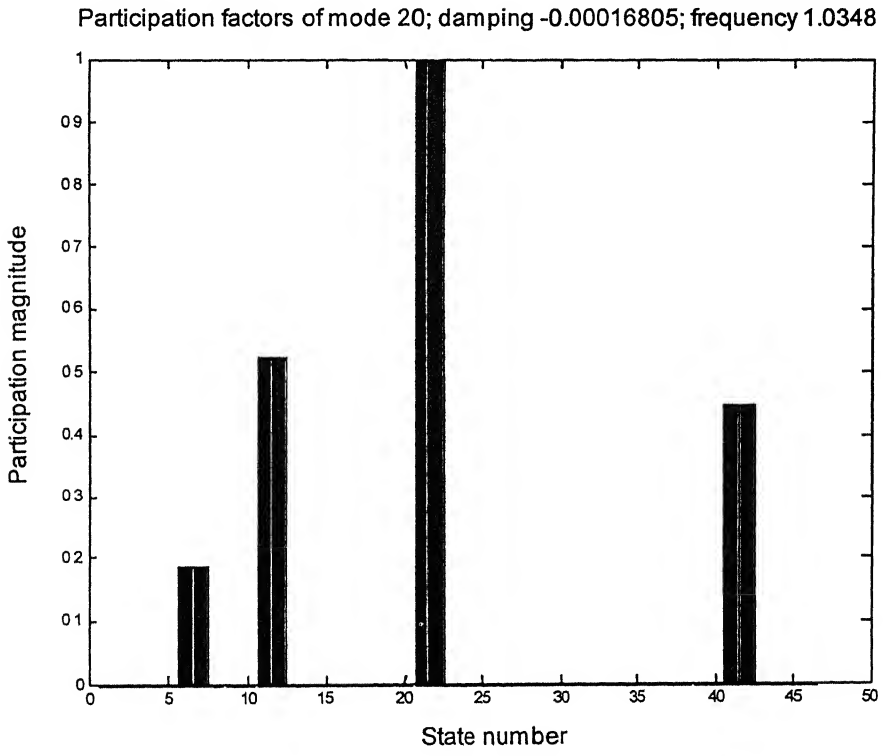

Fig 3.14 Participation factor of the mode 20 & 21 (unstable modes) (39-bus system)

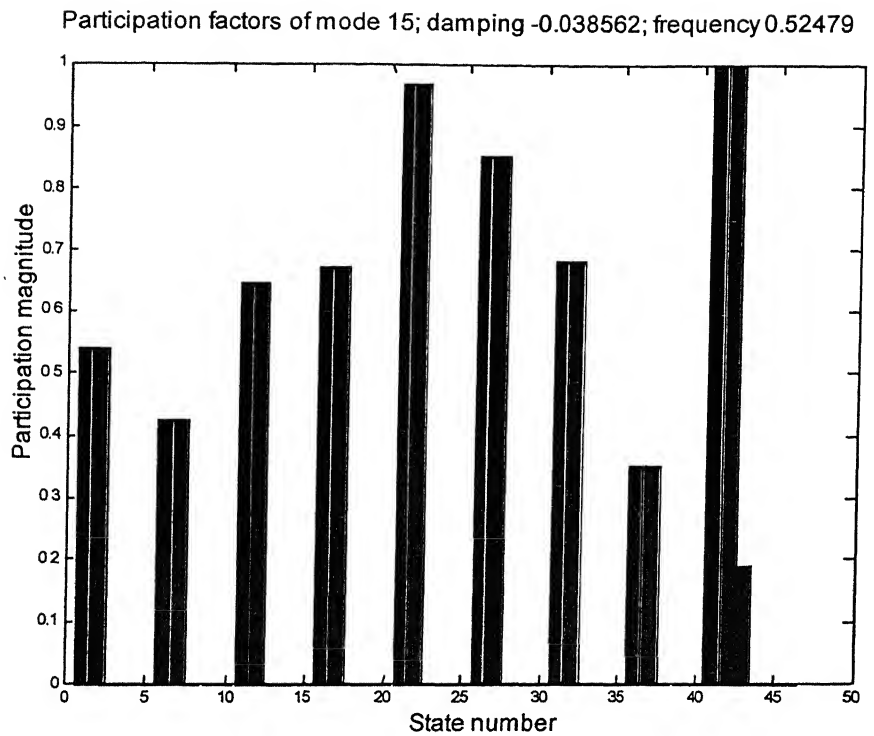

Fig 3.15 Participation factor for modes 15 & 16 (unstable modes) (39-bus system)

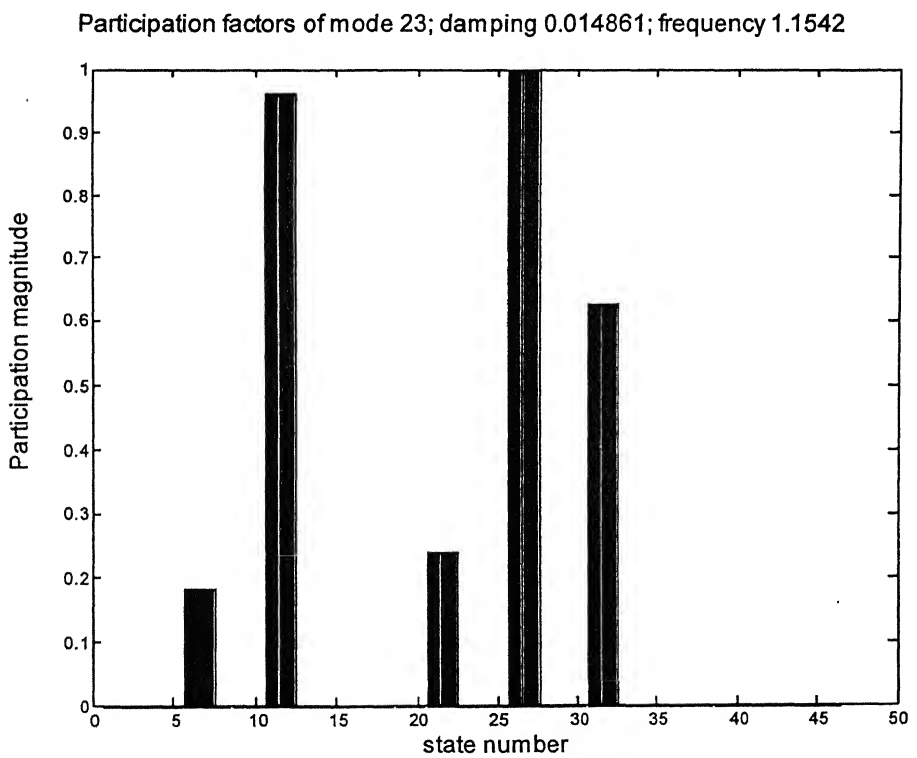

Fig 3.16 Participation factor of the modes 23 & 24 (under damped modes) (39-bus system)

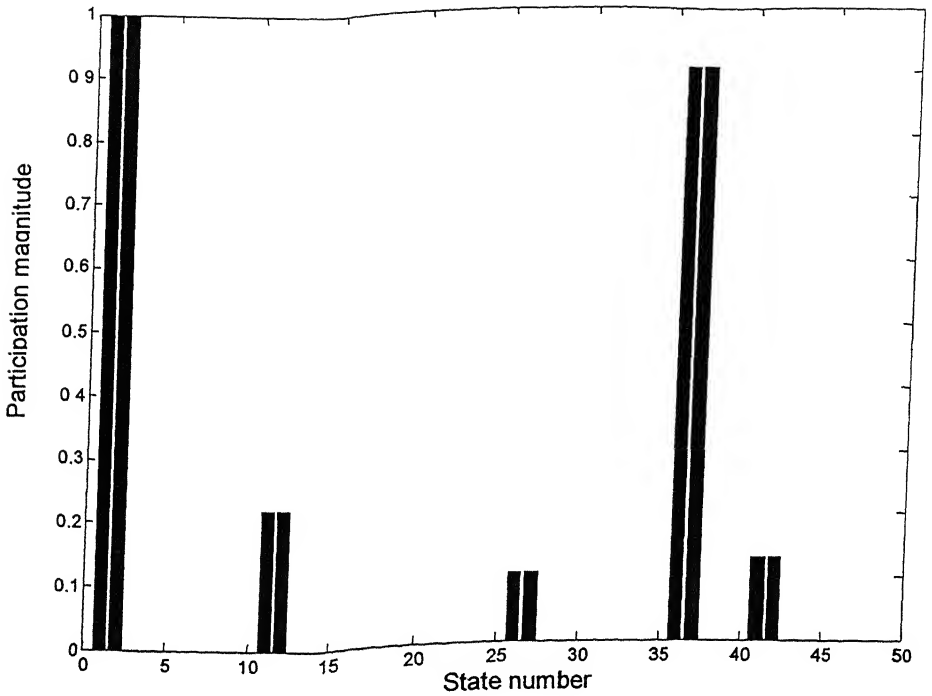

Fig 3.17 Participation factor of the modes 26 & 27 (Under damped modes) (39-bus system)

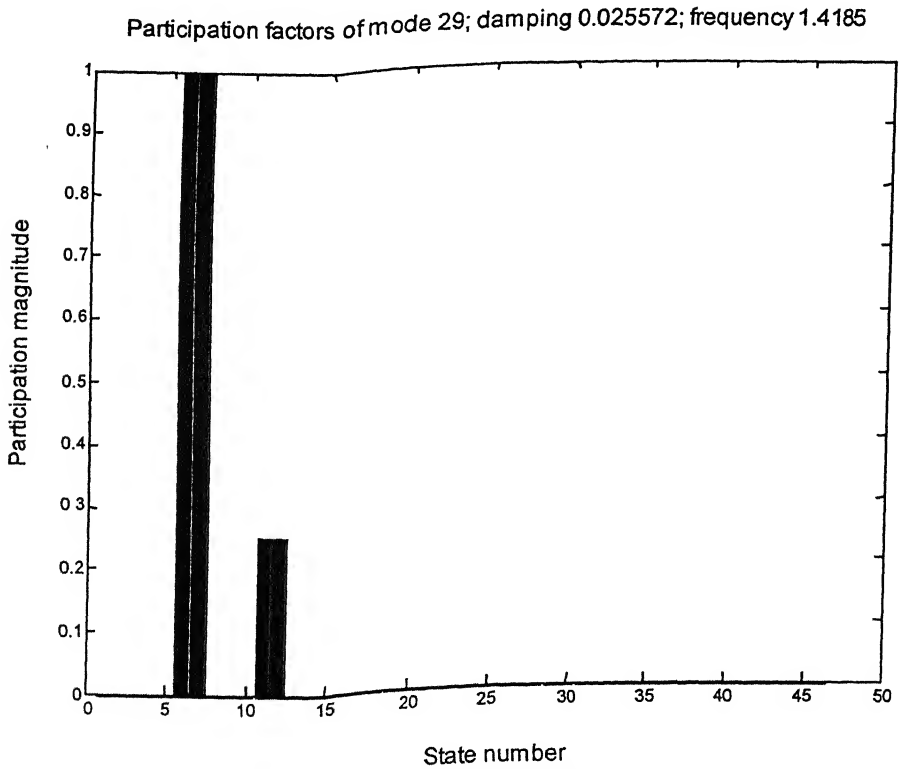

Fig 3.18 Participation factor of the mode 29 & 31 (under damped modes) (39-bus system)

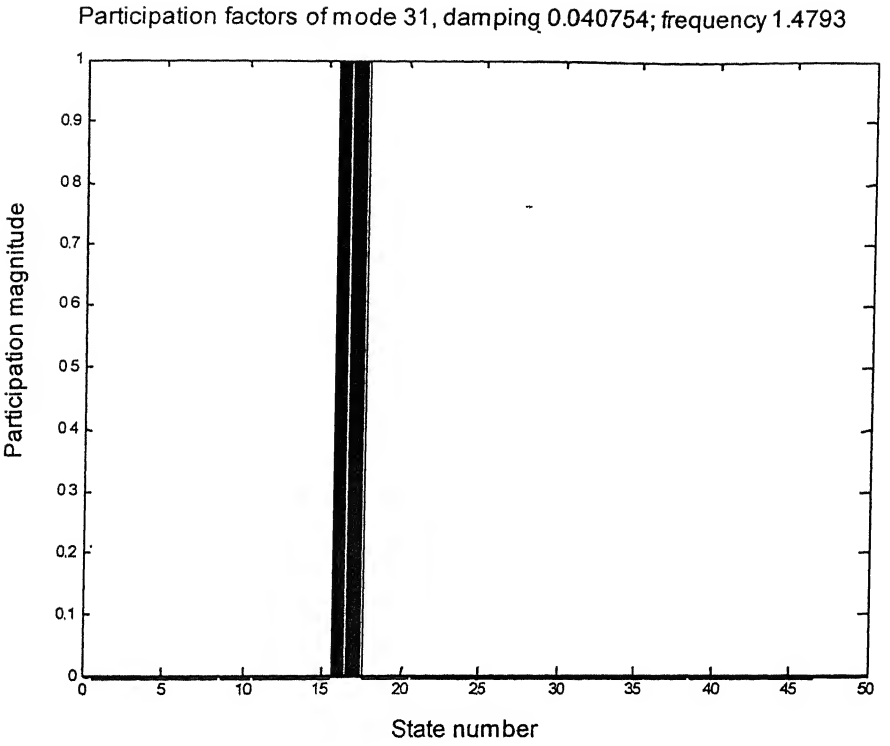

Fig 3.19 Participation factor of the mode 31 & 32 (under damped modes) (39-bus system)

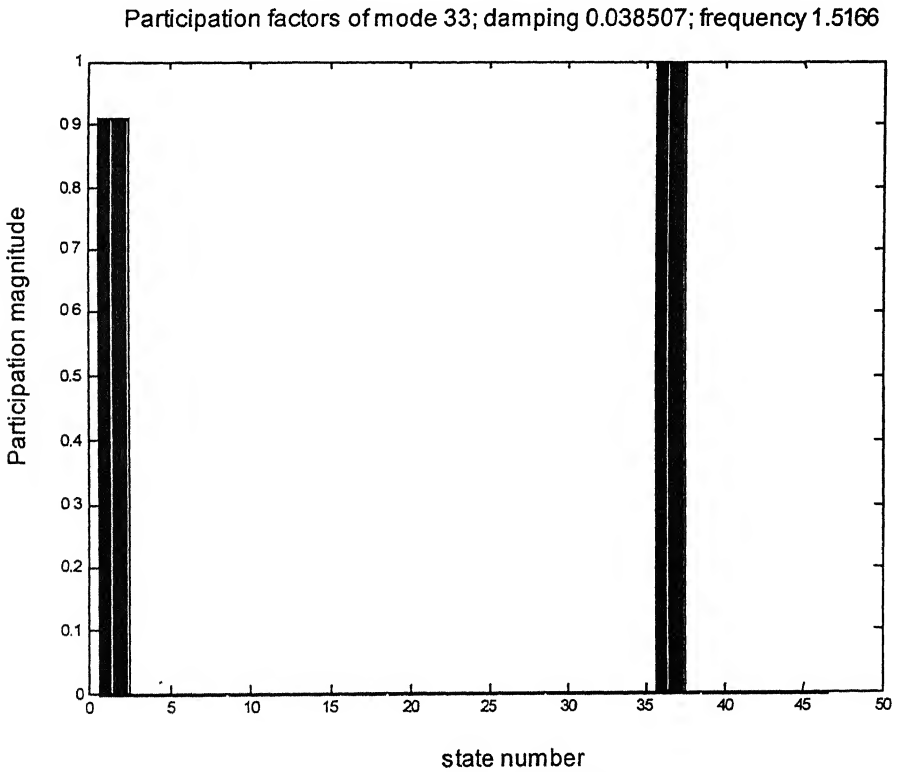

Fig 3.20 Participation factor of the modes 33 & 35 (under damped modes) (39-bus system)

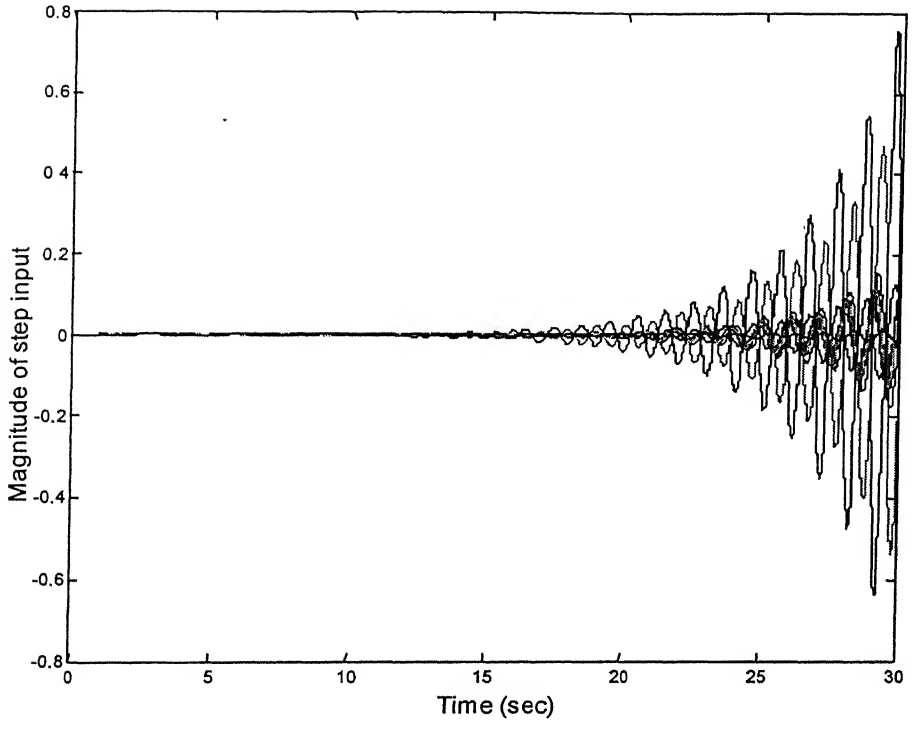

Fig 3.21 Step input response of the system with out PSS-SVC_stab (39-bus system)

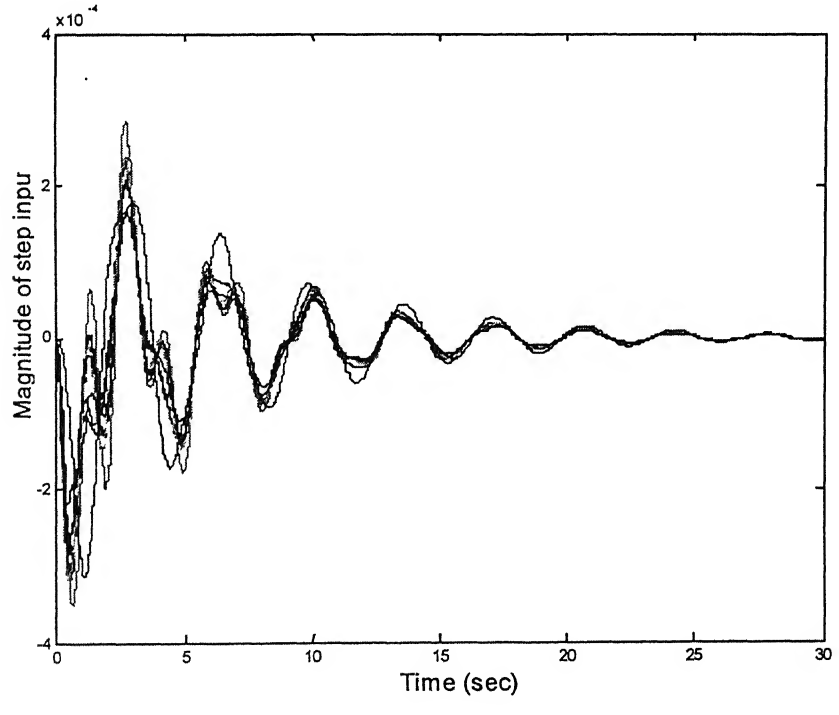

Fig 3.22 the step input response of the system with PSS-SVC_stab (39-bus system)

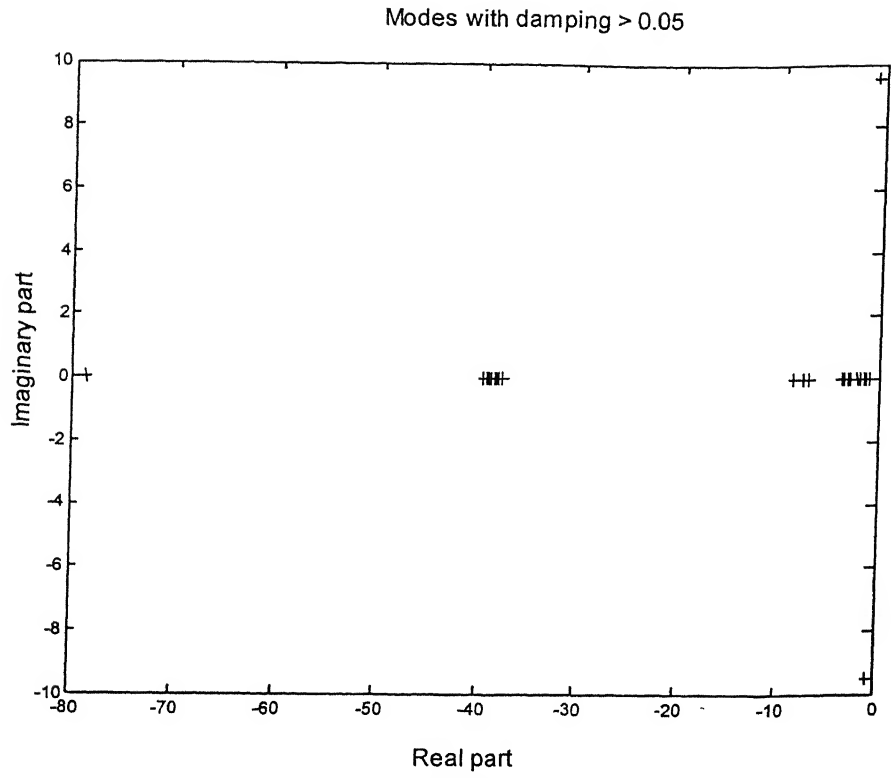

Fig 3.23 Eigen-values of the system with out the PSS and SVC_stab (39-bus system)

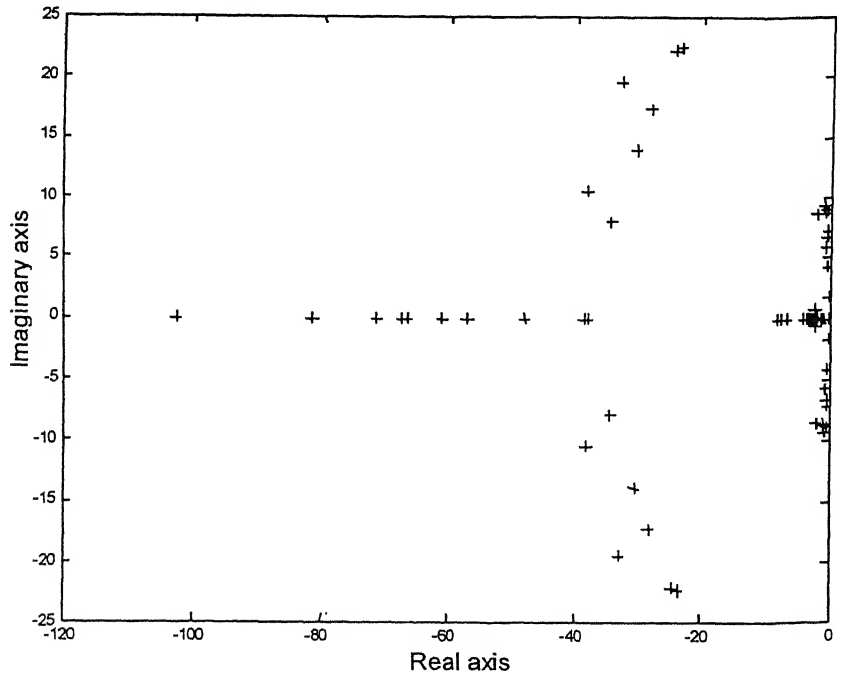

Fig 3.24 Eigen-values of the system with the PSS and the SVC_stab (39-bus system)

3.6. Conclusions

Supplementary damping control loop can be used with FACTS controllers to enhance system damping. In this chapter, a procedure for coordination of parameters of SVC stabilizer control loop (SVC_stab) and power system stabilizer (PSS) has been proposed. The residues of the modes of the system for different possible inputs and outputs are found out. The input signal whose residue is maximum out of all possible signals has been considered as the input signal to the SVC stabilizer. With the input signal selected, the time constants of dynamic compensators are obtained using modal analysis as described in [6].

The gains of the SVC stabilizer and the power system stabilizers have been coordinated using the optimal control strategy with pseudo-decentralization. The results obtained on WSCC 9-bus system and the New England 39-bus system provides the following main conclusions.

1. In the 9-bus system all the eigen-values have negative real part with out PSS & SVC_stab and hence, the system is stable. There are two under-damped eigen-values having damping ratio less than 0.05. The two under-damped eigen values move to the left half of the s-plane and there by increasing the system damping, with the use of coordinated PSS and SVC_stab.
2. The system oscillations, with the coordinated PSS and SVC_stab to a step input, are damp out with overshoot and settling time less than those as compared to the oscillations without PSS and SVC_stab.
3. In the 39-bus case, there are six unstable-eigen values in the base case without PSS and SVC_stab. There are 10 under-damped modes (having damping ratio less than 0.05) without the PSS and SVC_stab. The unstable eigen-values moved from right half to the left half of s-plane and the system damping ratio becomes more than 0.05, with coordinated PSS and SVC_stab present in the system. The under-damped eigen-values also move towards left and attain damping ratio more than 0.05.

4. The system oscillations grow and it becomes unstable with out the PSS and SVC_stab. The oscillations of the system are damped out and system becomes stable with coordinated PSS and SVC_stab.

Chapter 4

Conclusions

The present day practical interconnected power system networks are facing problem of small-signal instability, induced due to insufficient system damping. For high values of external system reactance and generator outputs, the automatic voltage regulator operates at high gain values. Although this introduces a positive synchronizing torque, however it may produce a negative damping torque component. This effect is more pronounced as the exciter response increases. An effective way to meet the conflicting exciter performance with regard to system stability is to provide a power system stabilizer (PSS). The PSS transfer function should have appropriate phase compensation circuit to compensate for the phase lag between the exciter input and the electrical torque. In an ideal case, with the phase characteristics of PSS being an exact inverse of the exciter and generator phase characteristics to be compensated, it would result in a pure damping torque at all oscillating frequencies.

There may be negative interactions of PSS provided at different generators, which may decrease the damping or even make the system unstable. To avoid interactions, the PSS of different generators must be coordinated. Static VAR compensators, which are basically provided in the system for voltage control, can also be used for providing damping to oscillatory modes. A supplementary controller, having similar structure as that of the PSS, can be utilized for this purpose. Supplementary controller of SVC and PSS must also be coordinated to avoid any counter interactions of the two.

This thesis had made an attempt to develop a method to coordinate the power system stabilizers and static VAR compensators supplementary controllers. In chapter 2 an optimal control strategy with pseudo-decentralization method has proposed for the coordination of the PSS parameters. The method was implemented on WSCC 9-bus system and New England 39-bus. The main findings of the studies carried out in this chapter are as follows:

1. In the 9-bus system, all the eigen values had negative real parts for the cases without PSS, with uncoordinated PSS and with coordinated PSS. With both uncoordinated and coordinated PSS, the system damping significantly improved. The later case however, provides better damping.
2. The transient response in 9-bus system had shown that the system was unstable without PSS and became stable with uncoordinated and coordinated PSS.
3. The eigen-values of the 39-bus system consisted both unstable and under damped modes in case when no PSS was used. With the use of uncoordinated PSS, although the unstable eigen-values are eliminated but few under-damped modes were observed. However, system attained stable modes with acceptable damping, when coordinated PSS were used in the generator excitation loop.
4. It was found from the transient response of the 39-bus system that the system remains unstable without PSS as well as with uncoordinated PSS. The system became stable with coordinated PSS.

In chapter 3, the optimal control strategy with pseudo-decentralization, was extended to the coordination of SVC supplementary controller (SVC_stab) and PSS parameters. The main conclusions are as follows:

5. In the 9-bus system all the eigen-values had negative real part and hence the system was stable without PSS & SVC_stab. However, there were two under damped eigen values having damping ratio less than 0.05. These moved to the left in the s-plane and there by increasing the system damping, with the use of PSS and SVC_stab.
6. The system oscillations, with the coordinated PSS and SVC_stab, are damped out with overshoot and settling time less than those compared to the oscillations without PSS and SVC_stab.
7. In the 39-bus system, there were eigen values with positive real part in the base case with out PSS and SVC_stab in addition to this there are also under damped modes. Eigen values moved from right half to left half of s-plane and the system

damping ratio of the modes became more than 0.05, with coordinated PSS and SVC_stab considered in the system.

8. The system oscillations grew and it became unstable without the PSS and SVC_stab. The oscillations of the system were damped out and system became stable with coordinated PSS and SVC_stab.

During the course of the research work carried out in this thesis, the following areas of further research were identified which can be developed for effective coordination of controllers:

- In this thesis the system model, which is nonlinear, is linearized and then analyses was carried out. More research efforts and studies are required for developing the concept of coordination of the controllers utilizing nonlinear model of the system.
- Only SVC supplementary controller was considered in the present study. This can be extended to other FACTS controllers like TCSC, UPFC etc. The coordination of parameters of supplementary controllers of other FACTS devices with PSS can also be studied.
- Research is needed to define a generalized but realistic load models, which incorporates the dynamics of the load. Dynamic load models have not been considered in this work.

References

[1] Francisco P. Demello and Charles Concordia, "Concepts of Synchronous Machine Stability as Affected by Excitation Control", *IEEE Transaction on Power System Apparatus and Systems*, Vol. PAS-88, No. 4, April 1969, PP 316-328.

[2] E.V.Larsen and D.A.Swann, "Applying Power System Stabilizer",*IEEE Transaction on Power Apparatus and System*, Vol. PAS-100, No.6, June 1981, PP 3017-3045.

[3] F.Luis Pagola and George C.Verghese, "On Sensitivities, Residues and Participations Applications to Oscillatory Stability Analysis and Control", *IEEE Transactions on Power Systems*, Vol. 4, No. 1, February 1989, pp. 278-285.

[4] A.J.A. Simoes Costa, F.D. Freitas and H.E. Pena, "Power System Stability design via Structurally Constrained Optimal Control", *Electrical Power Systems Research*, 1995, pp. 33-40.

[5] A.S. Bazanella, A. Fischman, A.S. e Silva, J.M. Dion and L. Dugard, "Coordinating Robust Controllers in Power System", *Proceedings of the IEEE Stockholm Power Tech conference, Stockholm, Sweden*, 1995, pp. 256-261.

[6] Pouyan Pourbeik and Michael J. Gibbard, "Damping and Synchronizing Torques Induced on Generators by FACTS Stabilizer in Multimachine Power Systems", *IEEE transactions on Power Systems*, Vol. 11, No. 4, November 1996, pp. 1920-1925.

[7] Kei Ohisuka and Yasuo Morioka, "A Decentralized Control System for Stabilizing a Longitudinal Power System using Tie line Power flow

Measurement", *IEEE Transaction on Power System*, Vol. 12, No. 3, August 1997, pp. 1202-1209.

[8] Pouyan Pourbeik and Michael J. Gibbard, "Simultaneous Coordination of Power System Stabilizer and FACTS Devices Stabilizer in a Multimachine Power System for Enhancing Dynamic Performance", *IEEE Transactions on Power Systems,* Vol 13, No. 2, May 1998, pp. 473-478.

[9] Alenxandre Sanfelice Bazanella and Cristiane Correa Paim, "Robust Design of Damping Controllers in Power Systems", *IEEE Power Tech 99 conference, Budapest, Hungary, August 29, September 02*, 1999.

[10] P.Kundur, *Power System Stability and Control*, McGraw-Hill, New York, U.S.A., 1994

[11] P.M.Anderson and A.A. Fouad, *Power System Control and Stability*, The Iowa state University Press, 1977.

[12] Graham Rogers, *Power System Oscillations*, Kulwer's Power Electronics and Power System series, 2000.

[13] K.R. Padiyar, *Power System Dynamics Stability and Control*, John Wiley & Sons (Asia) Pte Ltd.

[14] Young Hua Song and Allan T Johns, *Flexible A.C. Transmission Systems*, IEE Power and Energy Series, 1999.

[15] R.J. Fleming, M.A. Mohan and K. Parvatisam, "Selection of Parameters of stabilizers in Multimachine systems", *IEEE Transactions on Power Apparatus and Systems*, vol-100, 1981, pp.2329-2333.

[16] P.Kundur, M Klein, G.J. Rogers and M.S. Zywno, "Application of Power System Stabilizer for Enhancement of Overall System Stability", *IEEE Transaction on Power System*, Vol 4, 1989, pp. 614-629.

[17] N. Martins, "Efficient Eigen-value and Frequency Response Methods Applied to Power System Small-Signal Stability Studies", *IEEE Transaction on Power systems*, Vol-1, 1986, pp. 217-226.

[18] F.P. De Mello, L.N. Hannett and J.M. Undrill, "Practical Approach to Supplementary Stabilizing from Accelerating Power", *IEEE Transactions on Power Apparatus and Systems*, PAS-97, 1978, pp. 1515-1522.

[19] S. Hyrano, "Functional Design for a System-Wide Multivariable Damping Controller", *IEEE Transactions on Power System*, 5, 1990, pp. 1127-1136.

[20] C.E. Fosha and O.I. Elgerd, "The Megawatt-frequency control problem: A New Approach via Optimal Control Theory", *IEEE Transaction on Power Apparatus and Systems*, Vol-89, 1970, pp. 563-577.

[21] M.J. Gibbard, "Robust Design of Fixed-Parameter Power System Stabilizers over a Wide Range of Operating Conditions", *IEEE Transactions on Power Systems*, 1991, pp. 794-800.

[22] E.V. Larsen, J.J. Sanchez-Gasca and J.H. Chow, "Concept for design of FACTS controllers to damp power swings", *IEEE Transactions on Power Systems*, 1995, Pg 948-956.

[23] G.J. Rogers, S. Farrokhpay and M. Klein, L.X. Lee, N.J. Balu, "H_∞ Damping Controller Design in large Power Systems", *IEEE PES winter Meeting*, 1993.

[24] G.E. Bockarim, Shaopeng Wang, J.H. Chow, G.N. Tranto and N. Martins, "A Comparison of Classical, Robust and Decentralized Control Design for Multiple Power System Stabilizer", *IEEE Transactions on Power Systems*, Vol 15, Issue: 4, November 2000, pp. 1287-1292.

[25] M.A. Abido and Y.L. Abdel-Magid, "A Hybrid Neuro-Fuzzy Power System Stabilizer for Multimachine Power Systems", *IEEE Transactions on Power Systems*, Vol 13, Issue: 4, November 1998, pp.1323-1330.

[26] A. Heniche and Karnwai, "Control Loops Selection to Damp Inter-area Oscillations of Electrical Networks", *IEEE Transactions on Power Systems*, Vol 17, Issue: 2, May 2002, pp. 378-384.

[27] S.S. Choi and X.M. Jia, "Coordinated Design of Under-Excitation Limiters and Power System Stabilizers", *IEEE Transactions on Power Systems*, Vol 15, Issue: 3, August 2000, pp. 937-944.

[28] P. Zhang and A.H. Coonick, "Coordinated Synthesis of PSS Parameters in a Multimachine System Using the Method of Inequalities Applied to Genetic Algorithms", *IEEE Transactions on Power Systems*, Vol 15, Issue: 2, May 2000, pp. 811-816.

[29] M.A. Abido and Y.L. Abdel-Magid, "Hybridizing Rule-Based Power System Stabilizer with Genetic Algorithms", *IEEE Transactions on Power Systems*, Vol 14, Issue: 2, May 1999, pp. 600-607.

[30] M.J. Gibard and D.J. Pourbeik, "Interactions Between, and Effectiveness of Power System Stabilizer and FACTS Devices Stabilizer in Multimachie System", *IEEE Transactions on Power systems*, Vol 15, Issue: 2, May 2000, pp. 748-755.

APPENDIX A

WSSC 3-Machine, 9-Bus System

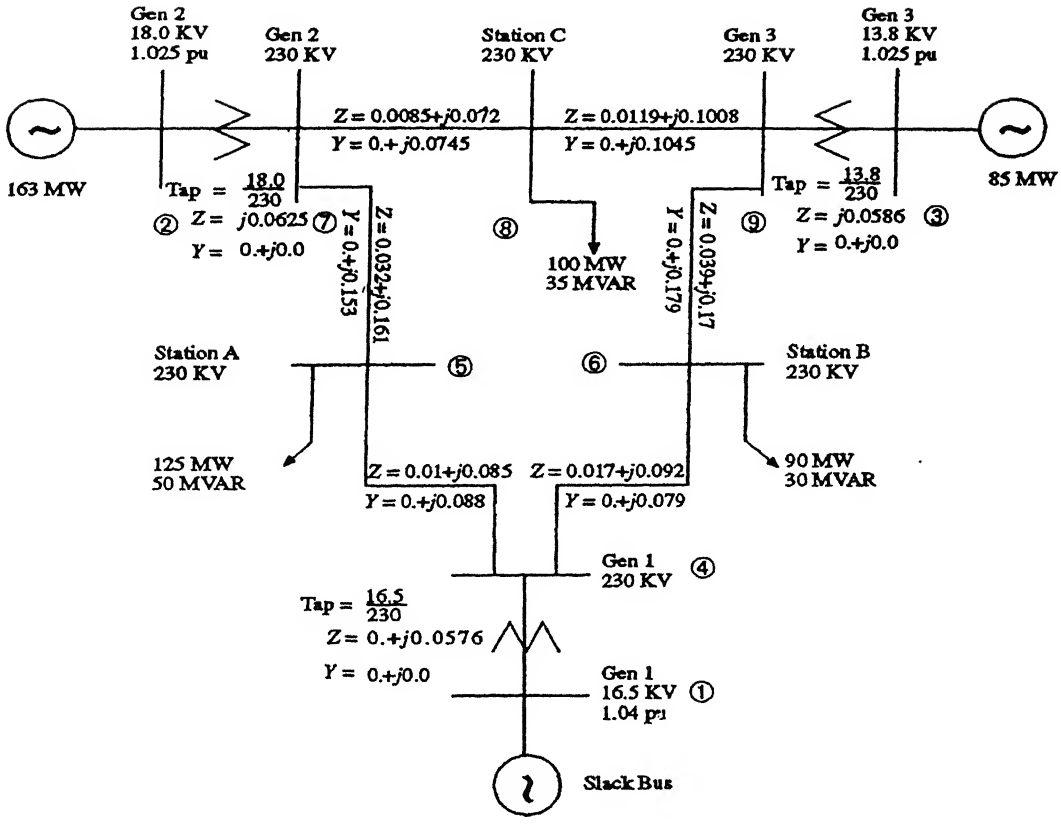

Fig A-1 One line diagram of WSCC 9-bus system.

Table A-1: Base case load flow results

Bus	Voltage	Phase (deg)	Pgen	Qgen	Pload	Qload
1	1.040	0.00	0.7164	0.2705	0.0000	0.0000
2	1.025	9.28	1.6300	0.0665	0.0000	0.0000
3	1.025	4.66	0.8500	-0.1086	0.0000	0.0000
4	1.026	-2.22	0.0000	0.0000	0.0000	0.0000
5	0.996	-3.99	0.0000	0.0000	1.2500	0.5000
6	1.026	3.72	0.0000	0.0000	0.9000	0.3000
7	1.026	3.72	0.0000	0.0000	0.0000	0.0000
8	1.016	0.73	0.0000	0.0000	1.0000	0.3500
9	1.032	1.97	0.0000	0.0000	0.0000	0.0000

Table A-2: Line data

From	To	R_line	X_line	Y_charging	Tapping
4	1	0.0000	0.0576	0.0000	1
7	2	0.0000	0.0625	0.0000	1
9	3	0.0000	0.0586	0.0000	1
4	6	0.0170	0.0920	0.1580	0
4	5	0.0100	0.0850	0.1760	0
5	7	0.0320	0.1610	0.3060	0
6	9	0.0390	0.1700	0.3580	0
7	8	0.0085	0.0720	0.1490	0
8	9	0.0119	0.1008	0.2090	0

Table A-3: Machine data

Gen	H	X_d	X_d'	X_q	X_q'	T_{do}'	T_{qo}'
1	23.6	0.1460	0.0608	0.0969	0.0969	8.96	0.31
2	6.4	0.8958	0.1198	0.8645	0.1969	6.00	0.54
3	3.0	1.3125	0.1813	1.2578	0.2500	5.89	0.60

Table A-4: Exciter data

The IEEE type-1 exciter having identical parameters has been used in all the three generators. The exciter data is given below:

$K_A = 20.00$
$T_A = 0.2$ sec
$K_E = 0$
$T_E = 0$ sec
$K_F = 0$
$T_F = 0$ sec

Appendix B.

New England 39 Bus, 10 Machine System

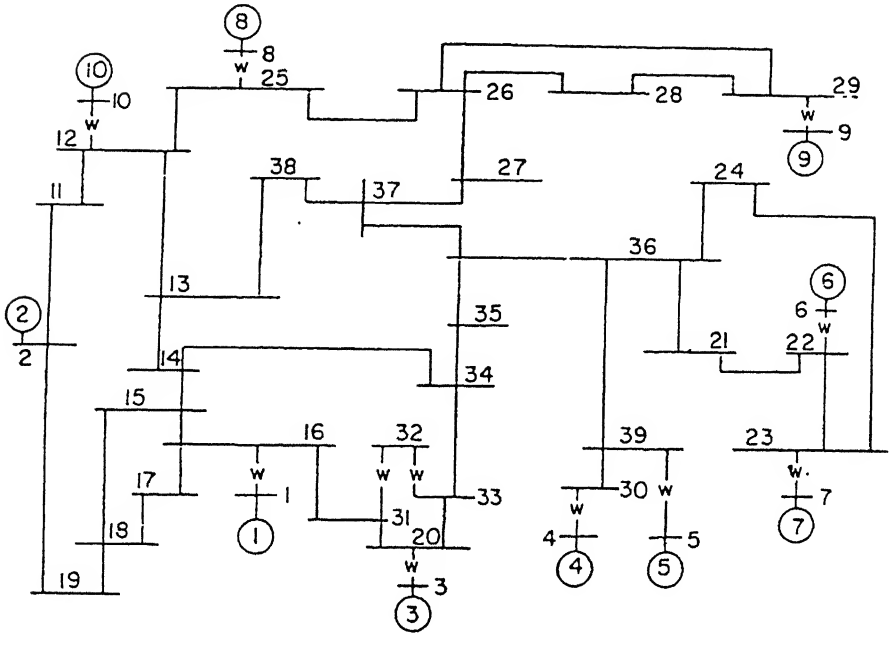

Fig B-1: One line diagram of New England 39-bus system.

Table B-1: Base case load flow results

Bus	Voltage	Phase (deg)	Pgen	Qgen	Pload	Qload
1	0.980	0.00	5.527	1.687	0.092	0.046
2	1.03	-11.06	10.000	2.425	11.040	2.500
3	0.980	2.36	6.500	1.705	0.000	0.000
4	1.010	3.22	5.080	1.673	0.000	0.000
5	0.990	4.30	6.32	0.760	0.000	0.000
6	1.040	5.35	6.500	2.669	0.000	0.000
7	1.060	8.13	5.600	2.415	0.000	0.000
8	1.020	1.95	5.400	0.239	0.000	0.000
9	1.020	7.71	8.300	0.631	0.000	0.000
10	1.040	-4.01	2.500	1.767	0.000	0.000
11	1.033	-9.40	0.000	0.000	0.000	0.000
12	1.010	-6.48	0.000	0.000	0.000	0.000
13	0.979	-9.51	0.000	0.000	3.220	0.024
14	0.945	-10.45	0.000	0.000	5.000	1.840

15	0.947	-9.19	0.000	0.000	0.000	0.000
16	0.948	-8.41	0.000	0.000	0.000	0.000
17	0.940	-10.88	0.000	0.000	2.338	0.840
18	0.941	-11.45	0.000	0.000	5.220	1.760
19	1.006	-11.27	0.000	0.000	0.000	0.000
20	0954	-563	0.000	0.000	0.000	0.000
21	0.978	-4.34	0.000	0.000	2740	1.150
22	1.007	0.26	0.000	0.000	0.000	0.000
23	1.006	-0.02	0.000	0.000	2.745	0.840
24	0.967	-6.83	0.000	0.000	3.086	0.922
25	1.019	-4.97	0.000	0.000	2.240	0.472
26	1.005	-6.23	0.000	0.000	1.390	0.170
27	0.985	-8.38	0.000	0.000	2.810	0.755
28	1.009	-243	0.000	0.000	2.060	0.276
29	1.012	0.53	0.000	0.000	2835	0.269
30	0980	-1.99	0.000	0.000	6.28	1.030
31	0.951	-6.57	0.000	0.000	0.000	0.000
32	0.931	-6.56	0.000	0.000	0.075	0.880
33	0.952	-6.42	0.000	0.000	0.000	0.000
34	0.950	-827	0.000	0.000	0.000	0.000
35	0.951	-859	0.000	0.000	3.200	1.530
36	0.967	-6.93	0.000	0.000	3.294	0.323
37	0.975	-8.15	0.000	0.000	0.000	0.000
38	0.975	-9.15	0.000	0.000	1.580	0.300
39	0.979	-0.98	0.000	0.000	0.000	0.000

Table B-2: Line data

From	To	R_line	X_line	Y_charging	Tapping
39	30	0.0007	0.0138	0.0000	1
39	5	0.0007	0.0142	0.0000	1
32	33	0.0016	0.0435	0.0000	1
32	31	0.0016	0.0435	0.0000	1
30	4	0.0009	0.0180	0.0000	1
29	9	0.0008	0.0156	0.0000	1
25	8	0.0006	0.0232	0.0000	1
23	7	0.0005	0.0272	0.0000	1
22	6	0.0000	0.0143	0.0000	1
20	3	0.0000	0.0200	0.0000	1
16	1	0.0000	0.0250	0.0000	1
37	27	0.0013	0.0173	0.3216	0
37	38	0.0007	0.0082	0.1319	0

36	24	0.0003	0.0059	0.0680	0
36	21	0.0008	0.0135	0.2548	0
36	39	0.0016	0.0195	0.3040	0
36	37	0.0007	0.0089	0.1342	0
35	36	0.0009	0.0094	0.1710	0
34	35	0.0018	0.0217	0.3660	0
33	34	0.0009	0.0101	0.1723	0
28	29	0.0057	0.0625	1.0290	0
26	29	0.0057	0.0625	1.0290	0
26	28	0.0043	0.0474	0.7802	0
26	27	0.0014	0.0147	0.2396	0
25	26	0.0032	0.0323	0.5130	0
23	24	0.0022	0.0350	0.3610	0
22	23	0.0006	0.0096	0.1846	0
21	22	0.0008	0.0135	0.2548	0
20	33	0.0004	0.0043	0.0729	0
20	31	0.0004	0.0043	0.0729	0
19	2	0.0010	0.0250	1.2000	0
18	19	0.0023	0.0363	0.3804	0
17	18	0.0004	0.0046	0.0780	0
16	31	0.0007	0.0082	0.1389	0
16	17	0.0006	0.0092	0.1130	0
15	18	0.0008	0.0112	0.1476	0
15	16	0.0002	0.0026	0.0434	0
14	34	0.0008	0.0129	0.1342	0
14	15	0.0008	0.0129	0.1382	0
13	38	0.0011	0.0133	0.2138	0
13	14	0.0013	0.0213	0.2214	0
12	25	0.0070	0.0086	0.1460	0
12	13	0.0013	0.0151	0.2572	0
11	12	0.0035	0.0411	0.6987	0
11	2	0.0010	0.0250	0.7500	0

Table B-3: Machine data

Gen	H	X_d	X_d'	X_q	X_q'	T_{do}'	T_{qo}'
1	30.3	0.2950	0.0647	0.2820	0.0647	6.56	1.50
2	500.0	0.0200	0.0060	0.0190	0.0060	6.00	0.70
3	35.8	0.2495	0.0531	0.2370	0.0531	5.77	1.5
4	26.0	0.3300	0.0660	0.3100	0.0660	5.40	0.44
5	28.6	0.2620	0.0436	0.2580	0.0436	5.69	1.50
6	34.8	0.2540	0.0500	0.2410	0.0500	7.30	0.40
7	26.4	0.2950	0.0490	0.2920	0.0490	5.66	1.50

8	24.3	0.2900	0.0570	0.2800	0.0570	6.70	0.41
9	34.5	0.2106	0.0570	0.2050	0.0570	4.79	1.96
10	420	0.2000	0.0040	0.1960	0.0040	5.70	0.05

For all machines $R_a = 0$

Table B-4: AVR data (similar for all the generators)

K_A=25, T_A=0.025.